Coordination Chemistry Reviews, 38 (1981) 139–275
Elsevier Scientific Publishing Company, Amsterdam—Printed in The Netherlands

CALCULATIONS OF THE ELECTRONIC STRUCTURES OF ORGANOMETALLIC COMPOUNDS AND HOMOGENEOUS CATALYTIC PROCESSES. PART I. MAIN GROUP ORGANOMETALLIC COMPOUNDS

D.R. ARMSTRONG and P.G. PERKINS

Department of Pure and Applied Chemistry, University of Strathclyde, Glasgow G1 1XL (Gt. Britain)

(Received 7 June 1980)

CONTENTS

A. INTRODUCTION

This is the first part of a general review covering the electronic structures of organometallic compounds. It is completely theoretically biased and

0010-8545/81/0000–0000/$34.25

reviews experimental work only in the context of associated computations. It will be divided into three parts, the first of which is presented here and is concerned with the main-group elements.

Since the discovery of ferrocene nearly 3 decades ago, the area of organotransition-metal chemistry has been one of frenetic activity: a vast number of compounds and amount of chemical knowledge have accumulated. Organometallic compounds of main-group elements were, of course, well known before 1950 but the impetus to the newer research came mostly, perhaps, from the novel structures and the types of reaction which the compounds could undergo. The challenge to bonding theory of the 1950's was stark and formidable, and asked such questions as, how can two neutral benzene molecules bond to a formally 'zerovalent' chromium atom to give dibenzene chromium? It was, moreover, clearly of some considerable interest and importance to know whether organic groups bonded to transition elements would exhibit the same sort of reactivity, both in degree and kind, to that manifest in the non-coordinated ligand. In addition, the great thermal stability attainable by such materials (e.g., ferrocene), their colours and those of their derivative ions, led to many fundamental questions on the origins of these properties. Finally, it rapidly became clear that there was a link between this type of stable system and those intermediates which appear to take part in catalytic processes and recognition of the fact of transition metal–carbon bonds was a major breakthrough in starting to understand this type of catalysis.

As aforestated, the mere existence of compounds typified by ferrocene is a major challenge to the theoretical inorganic chemist and much effort has been expended in attempting to gain an understanding of bonding patterns. Possibly it can be said that this has been achieved in a semiquantitative, though fairly satisfying, manner for a few systems. But the more elusive properties, such as excited states, remain largely unknown and, for metallocenes other than ferrocene, calculated data are sparse. Further, theoretical studies of reactions of the systems or catalytic processes involving metal–carbon bonds is a largely untouched area. The latter is not surprising, since it is hardly feasible at present to apply the most sophisticated techniques of quantum chemistry, i.e. ab initio calculations, to the problem. The computational exigencies of such molecules are very great indeed, particularly if one were to try to abstract fully quantitative data. Hence, such work as there is has been forced to progress along lines which attempt only to be the next step beyond the chemist's intuition (though better-quality information can be gleaned in favourable cases). When one considers the multi-dimensional problem of a reaction coordinate then, for a system of real interest, calculation by any method leading to a multiple minimum on the energy hypersurface would be a tour de force. Add to this the possibility that the wrong

basic model for the reaction may be taken and one can easily see that, far from his having a magical illuminating technique, the area could be a veritable graveyard for the theoretician. In this context the present authors' view is that the definition of a reaction path purely by theoretical methods for such systems as complex as those under discussion is likely to be a time- and resource-wasting procedure and a pragmatic approach must necessarily involve a dialogue between interested theoretician and experimentalist. In this fashion, intuitive and experimentally supported models can be tested theoretically, the strengths and weaknesses of the theoretical approach and of the experimental model can be evaluated in a synergic manner and action taken to improve their predictive capacity. A series of investigations of different systems in which this philosophy has been adopted will be discussed in Part II of this general review.

Organometallic compounds of main-group elements were well recognised long before those formed by transition elements and some elements, e.g. As, give rise to an extensive chemistry. Despite this experimental strength, theoretical investigation has been relatively limited, although a number of compounds are known where the bonding is 'non-classical'. The dimer of trimethylaluminium has long excited interest and similar compounds, hexavinyldigallium and hexaphenyldialuminium, have been synthesised. The tetramer $(LiMe)_4$ is also well authenticated. These systems will be discussed further in context. In this review we do not consider the organo-derivatives of recognised non-metals, hence those of nitrogen, phosphorus, oxygen, sulphur and the halogens are not included. We also decided to stick strictly to calculations on organometallic compounds, so investigations on related molecules such as the hydrides and halides of the main-group metals (e.g. LiH, BF_3 and Al_2Cl_6) have not been included in this review.

B. PERIODIC GROUP I

(i) Organolithium compounds

Organolithium compounds have properties which are typical of 'covalent' substances. They are soluble in hydrocarbon solvents, usually forming tetrameric or hexameric species, whilst in donor solvents such as ethers, solvated complexes are usually formed. Their use in synthetic organic chemistry and their role as catalytic reagents has gained for them a position of commercial importance.

The electronic structures of several organolithium compounds have been reported [1–88]. The position of lithium in the Periodic Table has enabled non-empirical as well as semi-empirical calculational techniques to be employed in investigations. The principal gain in our understanding of organo-

lithium chemistry by this additional mode of attack has been in the calculation of geometry-optimised structures.

Calculations performed on the simplest organometallic system of lithium, i.e. CH_2Li^- [1] involving a geometry search yielded the following: HCH = 105°, C–H = 1.09 Å and C–Li = 1.80 Å, the molecule adopting a planar configuration. The energy differences between the ground state of CH_2Li^- and some types of dissociation product indicated that it is less stable with respect to $[CH_2 + Li + e^-]$ and to $[CH_2 + Li^-]$ but lower in energy than $[CH_2^- + Li]$. Thus, CH_2Li^- is not stable with respect to the most probable mode of dissociation.

The electron distribution of methyllithium has been thoroughly examined [2–11]. Four geometry optimisations by ab initio techniques yielded a Li–C bond length in the monomer of 2.05 Å [2], 2.026 Å [3], 2.021 Å [4] and 1.989 Å [5]. From calculations on Li_2 and C_2H_6, a bond length of 2.12 Å is expected [3] for a covalent bond and there appears to be an appreciable ionic contribution. This is also reflected in the atomic charges on lithium in $LiCH_3$ produced from various calculations; thus, from ab initio we have +0.37 [2], +0.14 [3], +0.35 [6], from CNDO +0.37 [7] and from an Extended Hückel calculation, +0.45 [8]. Hinchliffe and Saunders [9] have analysed the wavefunction of methyllithium in terms of the Löwdin–Daudel [10] technique which partitions the overlap population according to the projection of the bond dipole along the bond. The C–Li bond is covalent in character, since the overlap density is fairly equally shared by C and Li. The atoms, however, carry substantial charges corresponding to $C^{-0.215}(H^{-0.141})_3Li^{+0.638}$. By contrast, Streitweiser et al. [4] showed, with the help of electron density and projection plots, that the bonding is largely ionic, with about 0.8 electrons transferred from Li to CH_3. Of special interest is the extent of the hyperconjugation of the π electrons of the methyl group. The orbital occupancy of the $2p_\pi$ orbital is low (0.054 [2], 0.056 [5]), while a determination of the hyperconjugation energy yielded a value of 2.8 kcal mole^{-1} [2]. A simple FSGO model [11] has been used to study the electronic structure of $LiCH_3$. The electron momentum distribution and Compton profiles are also recorded.

The geometry of the methyllithium dimer was partially optimised [2], yielding Li–C and Li–Li bond lengths of 2.31 and 2.15 Å, respectively. The dimerisation energy was 34.9 kcal mole^{-1}. This arises from an increase in the total bond overlap populations. The individual Li–C bond populations are almost halved in value but this is compensated by the twofold increase in the number of bonds. The stability of this species, perhaps surprisingly, depends on the Li–Li interactions, which have a large bond population (0.278).

The inversion barriers in primary alkyllithiums are known experimentally

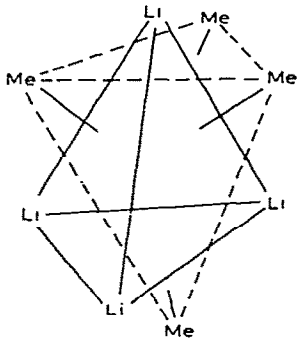

Fig. 1. The structure of tetrameric methyllithium.

to be ca. 63 kJ mol^{-1} [12,13]. The inversion of monomeric MeLi and EtLi, calculated as the planar–tetrahedral energy difference at the carbon bonded to lithium, are 219 kJ mol^{-1} and 200 kJ mol^{-1}, respectively, for the split valence 4–31G basis set [14]. The calculated [15] inversion energy of dimeric methyllithium is 97.3 kJ mol^{-1}. This is defined as the difference in energy between the most stable structure (C_{2h}) and the transition state (C_s) which has a methyl group constrained to lie in a plane bisecting the Li–C–Li angle. The reduction of the inversion energy due to association arises from a stabilisation of the planar methyl group in the dimeric structure. A carbon *p* orbital of the planar methyl group interacts with an antisymmetric combination of lithium *s* orbitals. The resulting molecular orbital is favoured by a planar methyl group, as the overlap of the carbon *p* orbital is more effective than that of a π CH_3 orbital of a pyramidal methyl group. Hence, the planar methyl group is preferentially stabilised in an alkyllithium inversion by association with a Li–Li edge rather than a Li_3 triangular face.

The normal form of methyllithium is a tetramer in which the four lithium atoms adopt a tetrahedral arrangement and the methyl groups are positioned symmetrically above each face of the tetrahedron (Fig. 1). This is lower in energy (by 4.8 eV) than four isolated CH_3Li molecules [6]. The gain in stability can be correlated with an increase in the number of Li–C bonds whilst the presence of Li–Li bonds (overlap population = 0.057) more than compensates for the decrease in the overlap population of individual Li–C bonds. A localised bonding picture [6] of the monomer and tetramer produces a single C–Li bond orbital polarised towards the carbon for $LiCH_3$, while for $(LiCH_3)_4$ there is a four-centre CLi_3 bond orbital with the three equivalent Li atoms bonding to a single carbon atom and being strongly polarised towards the latter. Following his work on methyllithium [4], Streitweiser proposed an electrostatic model of the methyllithium tetramer [16]. This consisted of a collection of 4 positive and 4 negative point

charges arranged as two interpenetrating tetrahedra. The resulting Coulombic forces have a minimum electrostatic energy when the ratio of the sides of the two tetrahedra is 0.783. This can be compared with the ratio 0.73 for the observed Li–Li to C–C distance in the crystal structure [17]. Thus, the methyllithium tetramer can be interpreted as an aggregate of ion pairs without involvement of non-classical character.

Baird et al. [2] propose that:

(i) The bonding between the lithium atoms and the alkyl radicals in all Li–R aggregate systems is sufficiently ionic in character that the total bonding energy of the aggregate is equal to the total number of nearest neighbour Li^+-R^- interactions multiplied by a constant ϵ (ϵ for R = Me, and Et is 17 kcal $mole^{-1}$).

(ii) Although Li–R bonding is predominantly ionic, sufficient covalent character is present so that the number of nearest neighbours to each lithium atom does not exceed six.

(iii) Excitation or ionisation of a valence electron in an alkyllithium aggregate is a localised event.

Predictions from the above are in semiquantitative agreement with the known properties of the alkyllithium compounds.

The energies of electronic transitions in methyllithium aggregates have been obtained using SCC [8], CNDO [8,18] and ab initio [4] methods. The first singlet-to-singlet transition energy for methyllithium, corresponding to an excitation from σ (C–Li localised about C) to σ^* (C–Li localised about Li), is calculated to be 2.8 eV [4]. The low electron affinity of the methyl radical dictates that the energy required for the electron transfer from CH_3 to Li in the excitation process is low. Fair agreement between the calculated and observed transitions for tetrameric and hexameric methyllithium was afforded by a CNDO calculation [18]. For the tetramer, the lowest energy transition originates from a MO centred on the carbon atoms and terminates on a MO which is localised about the lithium atoms. By contrast, the lowest energy symmetry-allowed transitions of the hexameric species do not exhibit this charge-transfer character. However, two of the low-energy transitions which are symmetry forbidden for the methyllithium hexamer do display this character. It is predicted that the photochemical reactions of alkyllithiums will involve formation of radicals by the charge-transfer process.

Related to the above work on methyllithium is an ab initio investigation [19] of clusters containing 4 and 10 atoms of lithium and their interactions with a methyl group. The geometrical arrangement of the methyl group with respect to the cluster sites has been optimised starting from a C_{3v} site symmetry. Two sites which are prevalent on the (1,1,1) surface of Li are identified as possibilities for the binding of methyl to lithium surfaces. These sites occur at positions above subsurface lithium atoms located below a

surface triad of lithiums. Binding of methyl at a site with a first subsurface lithium atom is more favorable by 42 kcal mole^{-1} than at a site on a second subsurface plane. Qualitatively, the binding is between the methyl and an axial lithium, with a triad encirclement of lithium to satisfy electron deficiency. This type of binding should be possible in many locations, not just on Li(1,1,1) crystal faces. A potential surface for motion of CH_3 on Li(1,1,1) suggested an activation energy of 35–40 kcal for the process of associative desorption of methyl, giving ethane. Quantitatively, the strengths of binding of methyl to the lithium clusters appear to depend on second and third nearest neighbour substrate atoms.

The molecular complexes of methyllithium with Lewis bases (amines) have been investigated by Ratajczak and co-workers [20]. Certain molecular properties, i.e. interaction energy, equilibrium distance, charge transferred, and enhancement of dipole moment, are inversely correlatable with the ionisation potential of the amines. The possibility of a 'lithium bond' analogous to the hydrogen bond has been considered. The lithium bond in $CH_3Li \cdot NH_3$ is considerably stronger than the hydrogen bond in $CH_3H \cdot NH_3$. Formation of a lithium bond produces a decrease of charge density at the nitrogen and hydrogen atoms of ammonia, a slight decrease at the carbon and hydrogen atoms of methyllithium and a marked increase (the positive charge drops from +0.29 to +0.03) at the lithium atom. In the hydrogen-bonded system there is considerable loss of electron density at the bridged hydrogen as this provides a path for electron flow from ammonia to the methyl group.

Organolithium compounds are initiators in the copolymerisation of acrylonitrile with methylacrylate. This has prompted a theoretical investigation (CNDO) into the complexes of acrylonitrile and methylacrylate with methyllithium [21]. Complexation with CH_3Li sharply enhances the anionic polymerisation of these compounds by increasing the electropositive nature of their β carbon atom. The coordination energies of $LiCH_3$ with methylacrylate and acrylonitrile are computed to be 140 kcal mole^{-1} and 180 kcal mole^{-1}, respectively. These values correlate with the higher activity of the latter in anionic polymerisation and with the lower activity of acrylonitrile, if the two compounds are compared in the same system in the presence of a small amount of Lewis base. The electronic structures of methyllithium complexes with acrolein, vinylformate and formaldehyde are also reported.

The symmetrical bridging complex between methane and lithium hydride has been examined [22]. There is a weak interaction between the molecules, yielding $H_2C---(H_2$ bridging$)---LiH$. The $C-H_{br}$ distances (1.094 Å) and ($H_{br}CH_{br}$) angles (110.6°) indicate little distortion from the original CH_4 structure. The Li–C and $Li-H_{br}$ bonds span 2.486 Å and 2.093 Å, respectively.

Ethyllithium posseses essentially the same electronic features as methyllithium. The Mulliken population analysis yields a charge on lithium of +0.572 [4], whilst the corresponding value for methyllithium is +0.559. The calculated C–Li bond length is 2.02 Å [5], with the staggered conformation possessing a lower energy (by 3.29 kcal mol^{-1}) than the eclipsed conformation [22]. The barrier to internal rotation in ethane calculated with the same basis set is 3.26 kcal mol^{-1} [22]. The nuclear spin coupling constants, $^1J_{C-C}$, $^1J_{C-Li}$ and $^1J_{C-H}$, of ethyllithium have been calculated [23] and are 6.5 Hz, 20.7 Hz and 70.4 Hz, respectively. A conformation incorporating a C–C–Li angle of 90° gives better agreement with the experimental J_{Li-C} than that with a C–C–Li angle of 109°47′. A comparison of the total energy also favours the former geometry [23].

Electron densities on the hydrogen atoms of EtLi and LiCHMeEt in various conformations were determined [24] using an STO-3G basis set. The hydride donor property of these compounds is explained by frontier orbital consideration of calculated electron densities.

Radom et al. [25] have carried out ab initio calculations on 1-fluoro-2-lithioethane. They find that the rotational energy exhibits minima for *cis*(eclipsed) and *trans*(staggered) conformations. This is in accord with their prediction for 1,2-disubstituted ethane with the properties of one electronegative and one electropositive substituent. The *cis* isomer is actually favoured by 19.4 kJ mol^{-1} with a *trans* → *cis* barrier of 26.6 kJ mol^{-1}.

Vinyllithium has been examined in several investigations [4,26,27]. Geometry-optimisation exercises yielded C–Li = 1.89 Å [26] and C–Li = 1.98 Å [4]. A population analysis via the Löwdin–Daudel technique [10] indicates that the C–Li bond is weak and is best visualised as a weak σ interaction between a C^- sp^2 hybrid and a Li^+ ion. There is a negligible π contribution to the C–Li bond. The lithium atom carries a +0.77 charge, while the nearest carbon atom possesses a negative charge of −0.34. The β-carbon, by contrast, is almost neutral (−0.096).

Vinyllithium, butadienyllithium and hexatrienyllithium have been subjected to the CNDO technique [27], so as to gain information about anionic acetylene polymerisation. It was found that the density of charge localised in the reaction centre decreases with increasing chain length and is the probable reason for kinetic deactivation of the centre. Propagation is stopped, however, by the cooperative effect of kinetic and thermodynamic factors. Comparison with the electronic structure of the corresponding anion reveals that the C_α–C_β bond order is essentially unaltered by the presence of Li, but large changes occur in the neighbouring bonds. The lithium atom thus causes a redistribution of bonding electrons in favour of the newly formed C_α–Li bond. The charge on lithium increases along the series from vinyllithium (+0.43) to hexatrienyllithium (+0.46). The charge density on C_α decreases

due to the presence of lithium and this must be considered as one of the possible factors bringing about deactivation of the reaction centre in a nonsolvating reaction medium.

The electronic structure and rotational barriers for the singlet and triplet states of 1,1-dithioethylene have been calculated [28]. The triplet perpendicular configuration is predicted to be more stable than both the triplet planar form and the singlet configurations. The relative stabilities of the two single states is basis-set dependent. The stability of the perpendicular form is due to the special combination of the σ-donor and π-acceptor character of lithium. This allows formation of a cyclopropenium-type system for the Li_2C moiety as well as allowing the stabilising hyperconjugative effect of the Li–C bond with the C_β p orbitals (Fig. 2).

Nagase and Morokuma have analysed [29] the rotational barrier around the double bond for a number of lithioethylenes. They used a UHF ab initio framework and the 4–31G and STO-3G basis sets. The authors decompose and interpret the rotational barrier in terms of five chemically meaningful interaction components; electrostatic (ES), exchange repulsion (EX), polarisation (PL), charge transfer (CT) and their coupling (MIX) terms. The variation of the energy and its components for the rotation of the double bond in ethylene indicates that the contributions of ES, PL and MIX components to the barrier are small and almost constant throughout the rotation. The energy increase for the rotation is thus ascribable to the destabilisation caused by both a decrease in CT stabilisation and an increase in the EX repulsion.

The effect of a substituent on the barrier and the CT and EX components was examined for $CX_2{=}CH_2$ where X = Li, Na, BeH, CH_3, CN and F. Lithium substitution dramatically reduces the CT and EX destabilisation and the perpendicular form is predicted to be more stable than the planar forms. The order of lowering the energy barrier is Li > Na > CN > BeH >

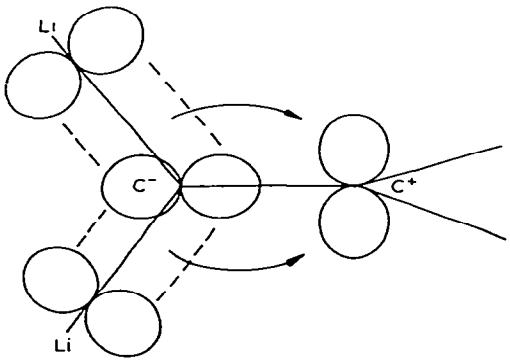

Fig. 2. Hyperconjugative bonding in $Li_2C{=}CH_2$.

$H > CH_3 > F$. $CLi_2{=}CF_2$ and $CLi_2{=}C(CN)_2$ were also studied and the barrier to rotation calculated to be 10.1 and 8.2 kcal mole^{-1}, respectively. This is a significant lowering of the barrier of ethylene which is 46.1 kcal mole^{-1}. As the Li substituent is particularly effective in lowering the energy barrier in ethylene, the multiple substitution of ethylene was of interest and the computed energy barriers (in kcal mole^{-1}) are, $CH_2{=}CH_2$ (46.1), $CHLi{=}CH_2$ (32.4), $CLiH{=}CLiH$ (21.7), $CLi_2{=}CH_2$ (−1.5), $CLi_2{=}CLiH$ (−3.5), and $CLi_2{=}CLi_2$ (11.2). The first and second atom substitution to give $CLi_2{=}CH_2$ provides the most effective lowering of the energy barrier because of the sharp decrease in the EX and CT destabilisation. The inefficiency of the second Li atom in $CHLi{=}CHLi$ is caused by a smaller reduction of CT and especially EX. The mild energy-lowering as seen in $CLi_2{=}CLiH$ and $CLi_2{=}CLi_2$ is due to the behaviour of the CT term which actually increases for the trisubstituted ethylene.

Lithium substituents are unique in making the perpendicular form more stable than the planar form because, not only do they increase the energy of the planar form, as do other substituents, but they lower the energy of the perpendicular form, whereas other substituents raise this energy.

Ethynyllithium (lithioacetylene) has attracted attention [4,30–32]. The calculated geometrical parameters which emerge from optimisation procedures are, C–C = 1.22 Å [30], Li–C = 1.842 Å [30], 1.88 Å [31], and 1.93 Å [4], and C–H = 1.099 Å [30]. The C–Li bond is weak and could be thought of as a weak electrostatic interaction between electron density in a carbon *sp* hybrid and a lithium cation [30]. The atomic charges for Li, C_α, C_β and H are +0.74, −0.40, −0.33 and −0.01 [30] and +0.71, −0.47, −0.41 and +0.17 [31], respectively.

The configuration of monomeric ethynyldilithium (dilithioacetylene) was analysed [33] and the relative energies of a linear and a doubly bridged, i.e. cyclic, structure were obtained using various basis sets. Unfortunately, the relative energies of the two forms are basis-set dependent. However, the larger basis set favours the cyclic structure with bond lengths C–C = 1.260 Å and C–Li = 2.059 Å. By contrast, the linear forms of both $HC{\equiv}CH$ and $HBeC{\equiv}CBeH$ are far more stable.

When a solution of dilithioacetylene in liquid ammonia is irradiated at −45°C for 6 h with a high-pressure mercury lamp, the dimer C_4Li_4 is thought to be produced [34]. Ab initio molecular-orbital calculations were employed to provide information about the species isolated. Three structures were chosen, two based on a tetrahedral structure with (a) the C–Li bonds radiating from the corners of a C_4 tetrahedron and (b) the lithium atoms positioned above the faces of the C_4 tetrahedron. The third structure had a cyclobutadiene framework with each lithium bonded to two carbon atoms. The total energies of these three structures are −180.66590, −180.74831 and

− 180.79084 a.u., respectively. Although the cyclobutadiene structure gives the lowest energy, the observed ^{13}C chemical shift rules out the olefinic structure. Hence, these calculations suggest that the face-centred tetralithiotetrahedrane is the more stable structure of C_4Li_4. The calculated bond lengths of this T*d* structure are C–C = 1.529 Å and C–Li = 1.937 Å.

The energy of the gas-phase reaction

$$LiR \rightarrow Li^+ + R^-$$

has been calculated for R = methyl, vinyl and ethynyl [4,26]. The energy of dissociation progresses as methyl > vinyl > ethynyl and this is the order expected from bonding considerations. The energy of lithiation, defined as the energy of the reaction

$$Li + RH \rightarrow RLi + H$$

has been evaluated for $R = CH_3$, C_2H_3 and C_2H; it is 69, 64 and 53 kcal mole^{-1}, respectively [4]. Moffat [32] examined the electronic structures of LiCCCN, LiCCCCH, LiCCCCLi and LiCCCCCN. He found that the C–C and C≡C internuclear distances depend on the length of the molecule, the position of the particular bond in the molecule and the presence or absence of substituents. All the Li–C distances fall in the region 1.84 ± 0.02 Å. Population analysis indicates that the lithium atom readily transfers electron density along the linear molecule and,with the exception of the neighbouring carbon atom, all carbon atoms possess a more negative charge than those in the corresponding parent hydrocarbon molecule. Increase in the alkyne chain length results in an increase in the σ-electron donation from lithium and a general decrease in the π-electron population on lithium. The average energy of substituting lithium for hydrogen in the parent hydrocarbon for the above series is −6.76 ± 0.01 Hartrees. The deviation from the average is a mere 6 kcal mole^{-1} and so this bond contribution should be quite acceptable for many chemical purposes.

Lithium substituted α-cations, i.e. $LiCH_2^+$, $LiCH^+ \cdot CH_3$ and $LiC^+ = CH_2$, were studied to evaluate the effects of Li on the stabilities of the parent cations [35]. It was found that Li is very effective in stabilising the carbenium ions and, indeed, stabilises the ethyl and vinyl cation even better than the best π donor (the amino group). The stabilisation energy for the reaction

$$LiR^+ + RH_2 \rightarrow RH^+ + RLiH$$

is 79.6 kcal mole^{-1} for $R = CH_2$, 69.4 kcal mole^{-1} for $R = C_2H_4$ and 91.9 kcal mole^{-1} for $R = C_2H_2$.

A related investigation was concerned with the effect of lithium on stabilising β-cations such as β-vinyl and β-ethyl [36]. The stabilisation energy for β-vinyl lithium is 89.0 kcal mole^{-1} and for β-ethyl is 88.9 kcal mole^{-1}. Very high barriers to C–C rotation were obtained for β-lithioethyl

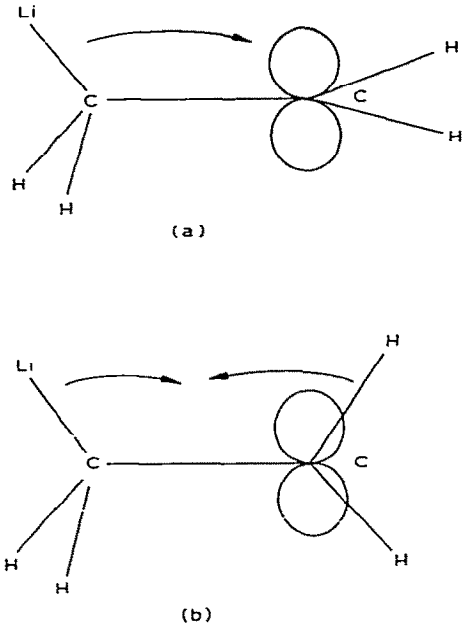

Fig. 3. Hyperconjugative bonding in $LiCH_2CH_2^+$, (a) perpendicular, (b) eclipsed.

cation (49.8 kcal $mole^{-1}$). Hyperconjugation between the Li–C bond and the vacant $2p$ orbital on the β carbon stabilises the perpendicular configuration but destabilises the eclipsed form (Fig. 3).

The geometry of the lithium cation adduct to methylene phosphorane has been examined by a CNDO method [23]. Lithium does not perturb the electron distribution or conformation about the methylene group. The Li–C bond is 2.06 Å long and the P–C–Li angle is 90°. The positive charge is distributed throughout the molecule but is especially located at Li (+0.385) and P (+0.451).

The geometry of the possible structures of CH_2Li_2 has been optimised [37] and the energies compared to see if substitution of two hydrogens by lithium atoms could produce a planar substituted methane molecule. It turns out that the tetrahedral rather than the planar form has the lowest energy. However, the most stable planar structure has a *cis* arrangement of lithium atoms and is only 8.7 kcal mol^{-1} higher in energy than the tetrahedral case. The electron distribution of tetrahedral CH_2Li_2 involves polarisation of electrons towards the CH_2 portion, leaving the lithiums with a +0.365 charge. There is an unusually high negative overlap population for the Li–Li bond, indicating weak repulsion. By contrast, the overlap population of the Li–Li bond of planar CH_2Li_2 is +0.16, indicating a bonding situation. This

arises from a stabilising ring current generated over the C–Li–Li framework.

In a related series of calculations, Pople and his coworkers [14] evaluated the energies of the planar and tetrahedral forms of 52 tetracoordinated molecules, of which 19 contain lithium. It was suggested that the presence of electropositive atoms might stabilise the planar configuration by delocalisation of the lone pair of electrons of the carbon by π conjugation and by provision of more electron density to carbon by σ-donation. The correctness of this reasoning is elegantly illustrated by the planar–tetrahedral energy differences (in parentheses and in kcal mole^{-1}) for the series CH_4 (168), CH_3Li (42), *cis*-CH_2Li_2 (10), *trans*-CH_2Li_2 (47), $CHLi_3$ (7), CLi_4 (6). Furthermore, the planar form of *cis*-CLi_2F_2 is predicted to be more stable than the tetrahedral configuration by 25 kcal mole^{-1}. Reduction of the angle

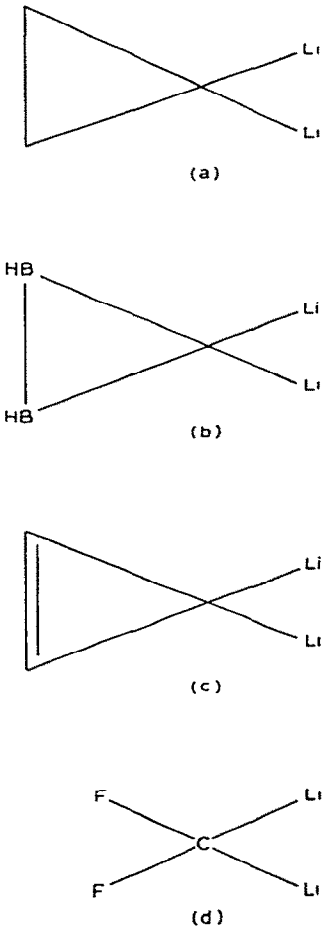

Fig. 4. Lithium compounds predicted to possess stable planar geometry.

around the carbon atom can also be achieved by means of small rings. Electropositive atoms can be incorporated into the ring structure or be present as substituents. Thus, the following are predicted to possess a stable planar geometry: 1,1-dilithiocyclopropane (−7), 3,3-dilithiocyclopropene (−10) and 3,3-dilithio-1,2-diboracyclopropane (−13) (Fig. 4). Laidig and Schaeffer [38] have further investigated the triplet and singlet states of the planar and tetrahedral conformations of CH_2Li_2 by using a double-zeta basis set and including the effects of electron correlation by addition of all single and double excitations. The most stable state is the tetrahedral singlet state, which lies 2.1 kcal mole^{-1} below that of the triplet state. The most surprising result is that the planar triplet state lies only 3.9 kcal mole^{-1} above the most stable state while the planar singlet state lies a mere 8.3 kcal mole^{-1} above the ground state, so both planar states are low-lying states which may be detected. The planar and tetrahedral singlet states have very large dipole moments with polarity C^-Li^+ while the triplet values are much smaller and have a C^+Li^- polarity.

Jemmis et al. have investigated [39] nine possible models for dimeric dilithiomethane $(CH_2Li_2)_2$. The minimal basis (STO-3G) was used for full geometry optimisation and then an extended basis (4-31G) was employed for a single point calculation. Two types of dimer structure were examined. In the first, the lithium atoms of one molecule interact with the hydrogens of the other, and four such configurations of this head-to-tail structure were considered. In the second dimer type the four lithium atoms are adjacent and five models of the head-to-head species were examined. The latter dimer type is considered to be more stable and the most stable structure is of D_{2d} symmetry and consists of two planar CH_2Li_2 species lying perpendicular to each other. The calculated geometrical parameters are C–C = 2.978 Å, C–H = 1.104 Å, C–Li = 2.041 Å and 2.166 Å, angle Li–C–Li = 93.3° and angle H–C–H = 97.3°. This geometry allows lithium to bond to both carbon atoms and this is a dominant feature in association of lithium compounds.

Lehn and Wipff [40] investigated the stereoelectronic and stabilisation effects in the species CH_2LiOH, $CHLi(OH)_2$, CH_2LiSH, $CHLi(SH)_2$ and CH_2LiSCH_3. Two types of conformations were adopted for the five molecules, the equatorial and axial configurations corresponding to the equatorial and axial orientation of Li if the fragments were included in a cyclohexane ring with the given conformation (Fig. 5). In all five compounds, the equatorial configuration gave the lowest energy, with the following energy differences (in kcal mole^{-1}) for the axial configuration CH_2LiOH (1.4), $CHLi(OH)_2$ (4.7), CH_2LiSH (1.6), $CHLi(SH)_2$ (3.4) and CH_3SCH_2Li (2.6). In the LiCXH fragment (where X = S or O), the C–Li bond mixes strongly with the σ^* (X–H) orbital of the antiperiplanar X–H bond in the equatorial configuration. The first interaction is stabilising and the second one is

destabilising. The bond overlap populations indicate a stronger X–H bond and a weaker C–Li bond in the axial configuration than in the equatorial configuration.

Much attention has been directed to the electronic structure of the allyllithium species [41–44]. This species is important because of its involvement in anionic polymerisation reactions. Allyllithium is reactive and requires the presence of a donor solvent such as ethyl ether or a tertiary amine for stability.

The geometry of allyllithium has been determined by ab initio [41] and CNDO [42] methods and general agreement has been reached with respect

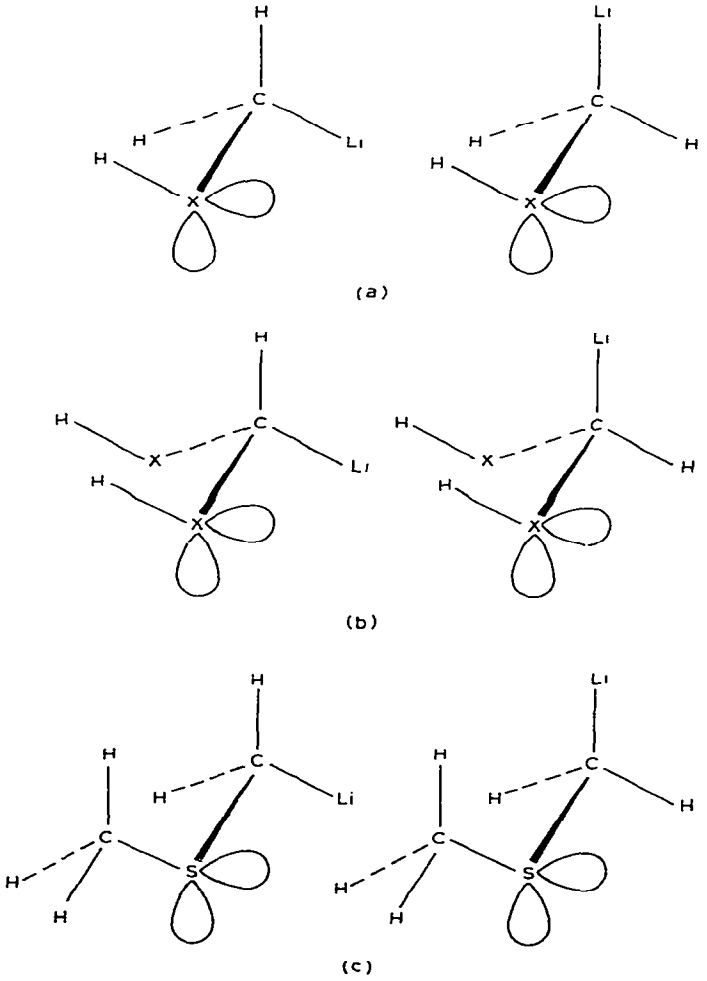

Fig. 5. The conformations of, (a) CH_2LiXH, (b) $CHLi(XH)_2$ and (c) CH_3SCH_2Li, where X = O, S.

to the gross features. The structure consists of a lithium atom symmetrically located at a height of 1.71 Å [41] over the plane of the allyl species; the Li–C_2 distance is 1.89 Å [42]. The bonding between the lithium and the allyl species involves interaction of the lithium $2p$ orbitals with the allyl π electron system. The most important contribution is the bonding of the lithium $2p_x$ orbital with the π orbitals of the outer carbon atoms (i.e. the highest filled π molecular orbital of the allyl radical). This produces the three-centre bonding molecular orbital which is a familiar stabilising influence in lithium chemistry. Both methods yield a relatively low charge on the lithium of +0.12 (CNDO) [42] and +0.159 (ab initio) [41]. The Li $2p$ orbital population (0.674) [41] reflects the extent of involvement in back-bonding.

Pople, Schleyer and their co-workers have completed a recent ab initio investigation [43] of the structure of allyllithium. The classical and non-classical allyllithium geometries have been optimised using a STO-3G basis and single point calculations have been performed with larger basis sets. The non-classical structure, where the lithium is symmetrically situated with respect to the allyl moiety and the C_2Li out-of-plane angle is 46.9°, is found to have the lowest energy for all basis sets used. The *syn* and *anti* classical structures are less stable by 15.7 and 18.5 kcal mole^{-1}, respectively. The Mulliken population analysis for the stable structure indicates that the outer carbons carry a charge of −0.55, while the inner carbon (+0.15) and lithium (+0.44) are both positively charged. The overlap populations show that lithium is clearly bonded to the outer carbon atoms, although the inner carbon atom is the closest carbon atom to the lithium. The allyl fragment is significantly distorted from a planar arrangement in order to enhance bonding between the allyl anion HOMO with the lithium p orbital whose axis is parallel to the carbon framework.

The effect of solvation on the allyllithium species has been investigated by ab initio [41], CNDO [42] and INDO [44] calculations on $RLi(OH_2)_2$, $RLi(NH_3)_2$ and $RLi[O(CH_3)_2]_2$, respectively. The geometry-optimised structures reveal that the coordinating atom of the solvent molecule lies in a plane containing the lithium atom and the central carbon atom of the allyl moiety. The solvent and the outer allyl carbon atoms are arranged tetrahedrally about the lithium atom. The separation of the lithium–allyl species is increased by solvation. The addition of the solvent species, as expected, reverses the charge of the lithium atom and the electron distribution of the allyl fragment now resembles that of an allyl anion due to electron transfer from the solvated lithium species.

Solvent studies on allyllithium have indicated that dimerisation and higher degrees of aggregation can occur and CNDO [42] conformational studies have been concentrated on the stacking of monomeric units. For the dimer,

the *cis* arrangement of the allyl species with respect to the axis between the lithium atoms is more stable than the *trans* structure. Comparison of the energy of solvation (86.9 kcal mole^{-1}) [41] indicates that the formation of polymeric species of allyllithium should take place in hydrocarbon solvents whilst in donor solvents, interaction with the solvent molecules will be preferred.

An ab initio calculation on the lithium fluoride–ethylene complex has been performed by Szcześniak and Ratajczak [45]. A configuration was chosen with the lithium fluoride molecule placed along the C_2 axis perpendicular to the C_2H_4 plane. The minimum energy of the complex occurs when the distance between the ethylene and the lithium atom of LiF is equal to 2.48 Å. This yielded a stabilisation energy of 8.75 kcal mole^{-1}. The

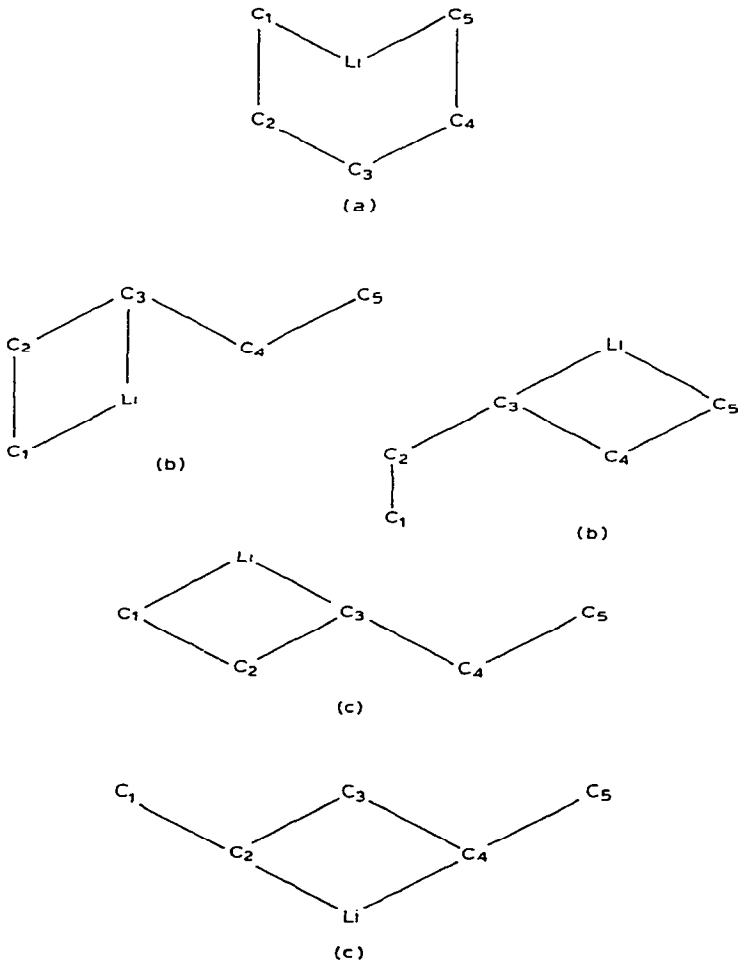

Fig. 6. The conformations of pentadienyllithium.

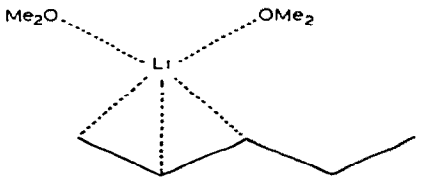

Fig. 7. The structure of *bis*(dimethylether) pentadienyllithium.

Mulliken population analysis indicates a transfer of 0.056 electrons from the ethylene to the lithium fluoride molecule and, in particular, to the lithium (0.050 electrons). The source of these donated electrons is the hydrogen atom.

The optimised geometry of pentadienyllithium was obtained by ab initio techniques [46]. The strong chelating ability of the lithium atom with the π electrons allows a non-planar 'U' conformation to be the most stable structure (Fig. 6). By contrast, the calculated structure [47] of *bis*(dimethylether) pentadienyllithium yields a bridged lithium bonding to an allylic fragment of a pentadienyl anion (Fig. 7). This interaction involves the lithium $2p$ orbitals and the highest occupied π-molecular orbital of the pentadienyl fragment.

A second geometry optimisation [48] by a CNDO technique has been performed on the planar U-, sickle- and W-shaped conformations of pentadienyllithium (Fig. 6). For the latter two configurations, two local minima were found for the position of the lithium ion. For the sickle conformation, the lithium bridges C_1 and C_3 at a height 1.58 Å above the anion plane (site 1) and bridges C_3 and C_5 at a distance 1.60 Å above the organic plane (site 2). In the W-shaped configuration, site 1 consists of a lithium bridge straddling C_1 and C_3 at a distance 1.53 Å above the plane, while for site 2, lithium positioned 1.60 Å above the plane coordinates C_2 and C_4. The U-shaped conformer has only one energy minimum. Here the lithium is centrally placed with respect to the carbon atoms of the anion and occupies a plane 1.42 Å above the organic moiety. In all three conformations of the pentadienyllithium, the central carbon atom bears the large charge and should be more reactive than the other carbon atoms. Bonding is discussed in terms of frontier orbital theory, with the vacant lithium p orbital having the same symmetry as the combination of π orbitals of the highest filled molecular orbital of the anion. The bonding is also discussed in terms of Möbius aromaticity, where pentadienyllithium is seen as the Möbius equivalent of vinylcyclobutadiene.

Mono- and disubstituted alkylidene carbenes, LiHC=C: and Li_2C=C:, have been studied by Apeloig and Schreiber [49]. The stabilities of these carbenes are compared with those of the parent alkylidene carbenes by

means of the isodesmic reactions

$$LiHC{=}C{:} + H_2C{=}CH_2 \rightarrow H_2C{=}C{:} + LiHC{=}CH_2$$

$$Li_2C{=}C{:} + H_2C{=}CH_2 \rightarrow H_2C{=}C{:} + Li_2C{=}CH_2$$

The calculated energies are 37.1 and 89.2 kcal mole^{-1}, respectively and indicate that the electropositive lithium stabilises the carbenes. The importance of hyperconjugation as a stabilising mechanism can be deduced by the 0.25 electron population of the formally empty $2p$ carbenic orbital.

Propyne can be lithiated sequentially to give propynyllithium, $C_3H_3Li(LiC{\equiv}CH_3)$, $C_3H_2Li_2$, C_3HLi_3 and C_3Li_4. Allene behaves similarly except the C_3H_3Li species is allenyllithium $(HCCCH_2)Li$. These species as well as lithiated cyclopropenes have been examined by ab initio calculations [50,51]. For the C_3H_5Li isomers the most stable structure is $LiC{\equiv}CCH_3$ and this is 12.7 kcal mole^{-1} more stable than the allene structure. The optimised geometry of the allenyllithium consists of an angular carbon framework (angle $C_1{-}C_2{-}C_3 = 157°$), with the lithium bridging the carbon skeleton. The bonding is similar to that found in allyllithium, with the $C_1{-}Li$, $C_2{-}Li$ and $C_3{-}Li$ bond overlap populations calculated as 0.48, -0.02 and 0.24, respectively, even though lithium lies closest to C_2. 1-Lithiocyclopropene and 3-lithiocyclopropene are 46.5 and 73.5 kcal mole^{-1} less stable than propynyllithium.

Thirteen structures were considered for $C_3H_2Li_2$ isomers. The most stable geometry again involves a bent allene structure and a bridging lithium atom, i.e. $[H_2CCCLi]Li$. The dilithiated cyclopropenes are considerably less stable, by 46–127 kcal mole^{-1}, than the dilithioallene structure. The 1,2- isomer has the lowest energy of the dilithiocyclopropenes and the double-bridged arrangement of the lithium atoms is preferred over the classical structure. The lowest energy structure of C_3HLi_3 has two bridging lithium atoms in C–Li–C planes roughly at right angles, together with C–Li and C–H bonds.

The energies of the probable geometries of C_3Li_4 have been calculated by Schleyer and co-workers [50] and Pople and co-workers [51]. The most stable structure has two lithium-bridged atoms and two acetylide Li–C bonds (see

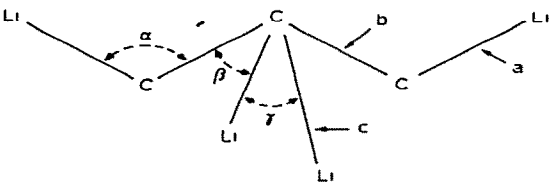

Fig. 8. The structure of Li_4C_3. $a = 1.794$ Å; $b = 1.326$ Å; $c = 1.869$Å; $\alpha = 149.3°$; $\beta = 155.1°$; $\gamma = 93.2°$.

Fig. 8). The terminal lithium atoms form a partially covalent σ bond with the outer carbon atoms of the three carbon chain and are also π acceptors. The central lithium atoms interact with the non-bonding π orbitals of the carbon chain and act primarily as π acceptors. The bonding of the central carbon atom is remarkable in that its four valences extend in one direction.

A CNDO investigation [52] of the dilithio derivatives of propyne was concerned with the relative stabilities of a linear sesquiacetylenic structure compared to a twisted allenic geometry of the carbon framework. The former conformation is predicted to be more stable and it has the two lithium atoms bonded to the central carbon atom with a $Li-C_2-Li$ angle of 90°. The atomic charges are +0.26 (Li), −0.48 (C_1 and C_3), +0.22 (C_2), and +0.11 (H).

Cyclopropyllithium has been geometry optimised [53] using a double-zeta basis set in an ab initio procedure. The important bond lengths are C_1-C_2 = 1.533 Å, C_2-C_3 = 1.501 Å, and C_1-Li = 1.945 Å, the lithium out-of-plane angle is 55.1°. The electron flow is dominated by a drift of electron density into the σ-electron system but there is significant back donation into the *p* orbitals of the metal atom. The atomic charges are +0.64 (Li), −0.56 (C_1) and −0.42 (C_2,C_3). The hydrogens are all positively charged (from +0.13 to +0.17).

Cyclopentadienyllithium has been subjected to a geometry-optimisation procedure [54]. The computed potential energy produced the most stable configuration, with Li lying 1.82 Å above the centre of the ring. The C–H bonds are predicted to lie at an angle of 3.56° out of the cyclopentadienyl plane away from the lithium. The reorganisation from the planar configuration yields a 0.42 kcal $mole^{-1}$ stabilisation. The bending of the C–H bonds is interpreted in terms of the ring–metal bonding in CpLi possessing wholly ionic character. This enhances the coulombic attraction by shifting more of the ring's negative charge to the side facing the lithium cation, and so implies that in those organometallic ring compounds in which hydrogens bend towards a central metal (e.g. Cp_2Cr and Cp_2Fe), bonding is predominantly covalent rather than ionic. In the latter examples, the directional character of orbitals used for ring–metal covalency is improved by the C–H bending.

INDO calculations [55] on PhLi and $2F-C_6H_4Li$ indicate that their physical and chemical behaviour is largely caused by the low value of the singlet-triplet interval and, as a result, the significant contamination of molecules in the low triplet excited state occurs.

The electronic structures and energies of lithium-substituted phenyl cations have been reported by Pople and co-workers [56]. The stability of the possible electronic configurations is in the order *ortho*-triplet > *para*-triplet > *meta*-triplet > *ortho*-singlet > *meta*-singlet > *para*-singlet. The Mulliken population analysis indicates a charge transfer to the phenyl ring of ca. 0.5

electrons to the sigma system. Evaluation of the reaction energy for

$$LiC_6H_4^+ + C_6H_6 \rightarrow C_6H_5^+ + C_6H_5Li$$

gives a measure of the stabilisation energy due to Li. For the singlet states this energy is 56.7, 37.8 and 31.1 kcal mole^{-1} for the *ortho-*, *meta-* and *para*-substitution, respectively. The large value of the *ortho*-substituent is due to strong hyperconjugation leading to 'lithiated' benzene.

Stucky and co-workers have examined the charge distribution in solvated lithium salts of the following carbanions [57–65]: benzyl [57], triphenylmethyl [58], fluorenyl [59], indenyl [61], bifluorenyl [62] anions and complexes with naphthalene [60], *trans*-stilbene [62,64], bifluorenylidene [62], anthracene [63] and acenaphthylene [65]. The position of the solvated lithium atom relative to that of the benzylic-type anion is such that the $2s$ and $2p$ orbitals of the lithium can be used in bonding to the highest filled molecular π orbitals of the particular carbanion. This allows the formation of three-centre C–C–Li bonds involving the π orbitals of an allyl moiety and the lithium $2p$ orbital. In the ethylenic derivatives investigated, the closest approach of the lithium atom is along a perpendicular bisector of the olefinic

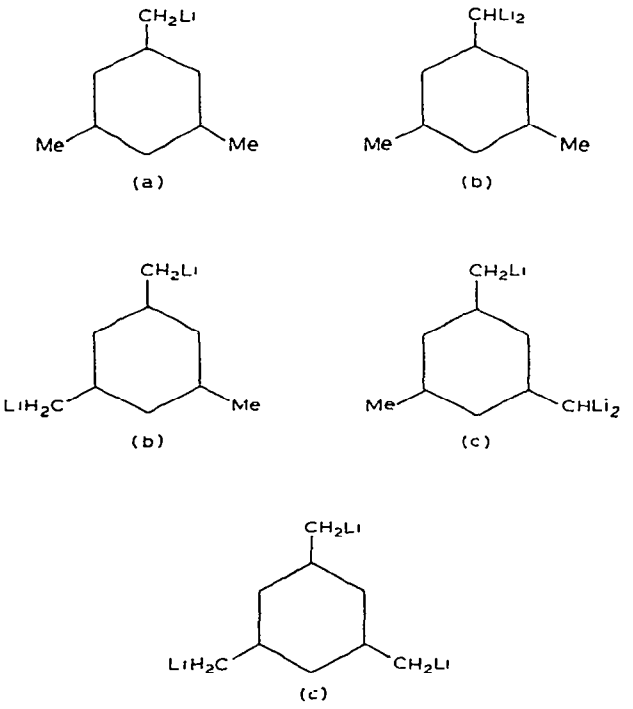

Fig. 9. Polylithiated mesitylenes: (a) monolithio-, (b) dilithio-, (c) trilithio-derivatives.

bond. The highest occupied molecular orbital of the ethylenic dianions are found to be antibonding with respect to the olefin bond. This is of the appropriate symmetry for its interaction with the lithium *p* orbital. This bonding is elegantly described in an excellent review by Stucky [66]. Metalation of mesitylene with butyllithium yields mono-, di- and trilithiated species [67] (Fig. 9). Dilithiation occurs partly at the same, but preferentially at different methyls. The symmetrical *tris*-1,3,5-lithiomethylenebenzene was the main product. Similar metalation occurs with *m*-xylene. *O*-xylene also gives dilithiated products whilst *p*-xylene gives exclusively the *gem* dilithio derivative. CNDO calculations [67] on the organic anions alone were unable to explain the substitution. Inclusion of the lithium atoms in the scheme produced a good correlation between the eexperimental stability and the computed energies. This leads to the conviction that lithium–anion interaction can effect drastic changes in the order of stabilities of various anions, particularly when charge–charge repulsion is involved. In a related manner the electronic energy and distribution of the lithium dihydrobenzenes were calculated (INDO) in order to rationalise the action of alkyllithium on t-butylphenyl sulphone [68].

The pyrazine--lithium system has been the subject of semiempirical [69,70] and nonempirical studies [71]. All three methods show that there is a charge transfer from lithium to the pyrazine species. An early calculation indicated that the Li^+ should be located above the pyrazine ring. Two separate later calculations [70,71] predicted that the Li^+ lies along the C_2 axis of pyrazine at a distance of 1.7 Å [71] or 2.7 Å [70] from the nitrogen atom. The stabilisation of this ion pair is strongly supported by the solvation energy [70].

The ion pair formed by 4-nitropyridine with lithium has been investigated by the INDO and ab initio procedures [72]. It is concluded that the lithium cation is present in the region of the nitro group but at least 2.25 Å over the molecular plane. The potential energy maps present in ref. 72 illustrate the nature of the electrostatic interaction energy for this ion pair.

The lithium–formaldehyde ion pair has been theoretically characterised by Bernardi and Pedulli [73] using an ab initio UHF treatment. A detailed search of the energy surface yields two minima. In the more stable conformation, the Li^+ lies 1.46 Å from the oxygen atom along the C–O bond axis. The cation–anion interaction has a predominant π character. In the second stable site the Li^+ is positioned 1.61 Å over the molecular plane directly above the oxygen atom. Here, the lithium–oxygen bond has mainly σ-character.

Pullman and Schuster [74,75] have made a detailed analysis of both the SCF energies of interaction and the calculated wavefunctions of this system. Both electrostatic and polarisation energies are the driving forces of complex

formation. Closed-shell repulsion as represented by the exchange contribution represents the most important counteracting force and determines thereby the equilibrium distances. Dispersion energy represents a contribution of probably minor importance only. Analysis of the wavefunction demonstrates that charge transfer is not important. Mutual polarisation of the subsystems leads to a complex pattern of charges in electron densities which seems interpreted most easily in terms of polarisation of individual localised MOs.

Several investigations have made a valuable contribution to our understanding of the interactions between the lithium cation and certain organic moieties [76–88]. The electronic structure of the Li^+-CH_2O ion pair [76] has been examined and the stabilisation energy is 51.5 kcal $mole^{-1}$. Dil'mukhambetov and Lygin [77] used an $Li^+-C_2H_4$ system to simulate an ethylene–zeolite system. The changes in the molecular dipole moment of ethylene due to the presence of the cation were evaluated. A related study involved the $Li^+-C_6H_5NO_2$ and $Li^+C_6H_5NH_2$ systems [78]. These were used to rationalise the displacement of the absorption bands of the organic moieties, due to their adsorption on zeolites, in terms of the interaction of the molecular orbitals of the adsorbates with the vacant orbitals of the cations. The electronic structure of the complexes of acetonitrile with Li^+ [79] indicates that the addition of Li^+ causes only small changes in the electron distribution of the acetonitrile. The calculated Li–N bond distance is 2.21 Å. A related series of calculations has been performed by Kollman and Rothenberg [80] and by Pullman and co-workers [81–83] who calculated the Li^+ affinities of some simple organic bases. Rode and co-workers [84–88] have also made valuable contributions to the understanding of the bonding of lithium cation to formamide and its derivatives.

(ii) Organosodium compounds

In contrast with organometallic compounds of lithium, there have been only a limited number of theoretical investigations of the electronic structure of organosodium compounds. Interest has mainly focused on the ion-pair species formed by sodium with various organic molecules.

The sodium derivatives of methane, CH_3Na and CH_2Na_2, have been studied by Pople and co-workers [14]. The optimised geometry for the former molecule has C_{3v} symmetry with a C–Na bond length of 2.087 Å and H–C–Na angles of 114.3°. The planar C_{2v} form of CH_3Na is less stable by 76 kcal $mole^{-1}$. The corresponding tetrahedral – planar configuration energy difference for CH_3Li amounted to 52 kcal $mole^{-1}$.

The optimum geometry of CH_2Na_2 comprises two C–Na bonds of length 2.05 Å separated by an Na–C–Na angle of 123°. The C–H bonds are 1.09 Å

and the H–C–H angle subtends 109.47°. The *cis* planar conformation of CH_2Na_2 is more stable than the *trans* isomer by 51 kcal mole^{-1} and is less stable than the tetrahedral geometry by 59 kcal mole^{-1}. The corresponding tetrahedral – planar configuration energy difference for CH_2Li_2 is 17 kcal mole^{-1} [14]. Compared to lithium, sodium has a much smaller stabilising effect on the planar geometries because of the diffuseness of its *p* orbitals.

The sodium–formaldehyde ion pair species has been subjected to an ab initio MO SCF UHF procedure [89]. The results predict the existence of only one stable species with the Na^+ cation lying above the plane of the molecule at 1.90 Å from the oxygen atom. The bonds involving sodium are found to be mostly ionic with the charge distribution, C(−0.20); H(−0.04); O(−0.46); and Na(+0.74). The corresponding charges for the lithium–formaldehyde ion pair [73] are; +0.25 (Li); and −0.31 (O) illustrating the greater ionic character of the sodium system. The Na–O bond is almost completely a σ-bond while in the Li–O bond there is a significant (35%) π component. The computed barriers to inversion and rotation are 10.4 and 1.22 kcal mole^{-1}, respectively.

The sodium *o*-benzosemiquinone ion pair has been studied [90] and the ^{23}Na hyperfine splitting constant calculated for different positions of the counterion relative to the organic moiety. When the sodium is in the plane of the molecule the only contribution to the splitting is due to the spin-polarisation of the lone pair of electrons of the oxygen atoms. For positions outside the molecular plane, mixing of the π orbitals with the metal *s*-orbital occurs. The calculations explain the variation in the ESR spectrum produced by temperature change and the use of different solvents. Similar calculations have been performed on the *o*-dimesitoylbenzene complex with sodium [91].

A quantum mechanical study of the *N*,*N*-dimethylacetamide and methyl-acetate interactions with Na^+ has been reported [92]. This is related to the work by Pullman [93,94] on the relative affinities of peptide and ester carbonyl groups for Na^+ ions. The binding of alkali cations to crown ethers has also been looked into [83].

Ab initio calculations have been performed on the binding of Na^+ to the purine and pyrimidine bases of nucleic acid [95]. The intrinsic complexing ability of the free bases towards Na^+ as measured by the values of the interaction energy is greater for guanine and cytosine than for uracil and adenine. Comparing the results with those on proton affinities, two principal differences arise; firstly, the increased significance in cation binding of the individual oxygen binding sites in bases containing both oxygen and nitrogen; secondly, the appearance in cytosine and guanine of bridged positions between a nitrogen and a carbonyl oxygen as the preferred binding sites.

CNDO calculations [77] on the ethylene–Na^+ complex concentrates on the changes in the molecular dipole moment of ethylene associated with the

change in its equilibrium configuration. The results were compared with the infrared spectra of ethylene adsorbed on zeolites containing exchangeable Na^+ cations. The intensity of the absorption bands due to the ethylene vibrations depends on the location of the molecule relative to the cation and the symmetry of the adsorption complex of ethylene in zeolites containing Na^+ cations is lower than C_{2v}.

Michel has studied the ^{13}C NMR spectra of 2-butene molecules adsorbed on NaY and NaX zeolites [96]. The results have been rationalised with the aid of CNDO calculations on the interaction between an individual molecule, *cis*-butene and a sodium cation. The most favourable position of the Na^+ ion is at the normal of the plane through the four carbon atoms at a distance 3.3 Å from the centre of the double bond. There is an expected transfer of electrons to the Na^+, with about 30% of these electrons originating from the π orbitals of the *cis*-butene. The electron density at the carbon atoms C_2 and C_3 remains unchanged, since the electron transfer is compensated by electron donation of the hydrogen atoms directly bonded to the carbon atoms.

The specific interaction energies between a benzene molecule and a sodium ion acting as an active site of the zeolite have been evaluated using a CNDO technique [97]. The adsorption model with the sodium ion located in the plane of the aromatic ring affords a smaller interaction energy than the configurations where the ion is situated (i) on the six-fold axis of symmetry, and (ii) below one π-bond, respectively.

The alkali–naphthalene ion pair has been the subject of many investigations in order to calculate modifications of the hyperfine structure (hfs) due to ion-pair association. Iwaizumi et al. [98] performed McClelland-type [99] calculations of the proton hfs and found that the sodium counterion is centered approximately 3.5 Å above the centre of the naphthalene. However, two other groups of workers [100,101], using more advanced theoretical models and calculating the alkali hfs, concluded that in dimethoxyethane and 2-methyltetrahydrofuran solutions the sodium ion is centred 3 Å above one six-membered ring. Borczyskowski and Möbius [102] have studied sodium phenylnaphthalene ion pairs and used McLachlan-type calculations [103] to rationalise the observed barrier to internal rotation. It appears that the lateral positioning of the counterion is sensitive to its distance above the ring. At a height of 3 Å above the plane of the C-atoms an equilibrium position of the counterion above the pair of benzene rings is most probable. On the other hand, at 4 Å, the most probable position of the sodium ion is above the 5–10 bond. However, in the latter position there is a lower association energy. For the related ion pair sodium–indenyl the proton chemical shifts were calculated and it was shown that sodium is located at 3 Å above the five-membered ring [104].

(iii) Organopotassium, organorubidium and organocaesium compounds

A small number of calculations on organometallic compounds of potassium, rubidium and caesium have been reported. These investigations were initiated either to interpret the ESR spectra of a system or to evaluate the binding of the alkali metal to a bio-organic substrate.

The ion-pair systems formed by potassium, rubidium and caesium with naphthalene, anthracene, biphenylene [100] and benzene [105] have been examined by a simple molecular-orbital treatment. This provides an estimate of the unpaired electron density on the alkali-metal ion as a function of the position of the ion relative to the molecular plane. Hence the alkali–metal hyperfine splittings have been interpreted in terms of the most likely positions for the alkali-metal ion. The electronic structures of the potassium-2,2′-bipyridine complexes [106] and the potassium σ-dimesitoylbenzene system [91] have also been reported.

Pullman and co-workers have investigated the affinity of K^+ for a variety of biomolecules including those containing peptide and ester carbonyl groups [93], those containing the fundamental components of depsipeptides [107] and the dimethylphosphate anion [108]. The latter system has also been reported by Marynick and Schaeffer [109].

The electron distributions in methylpotassium and methylrubidium have been reported by Ohkubo et al. [110]. In both molecules all the valence electron density has been withdrawn from the alkali-metal atom and redistributed solely to the carbon atom. The hydrogen atoms bear a small positive charge of +0.098 and +0.111 for methylpotassium and methylrubidium, respectively. The M–C bond populations of MeK and MeRb are −0.190 and −0.054, respectively.

C. PERIODIC GROUP II

(i) Organoberyllium compounds

The simplest organometallic compound of beryllium, CH_2Be, has been studied by two groups of investigators [1,5,111]. They found that a triplet state ($^3B_1$) is more stable than the singlet state ($^1A_1$) and that both these states are more stable than the probable dissociation products [$CH_2(^3B_1)$ + Be]. Pople and co-workers also included electron correlation in their evaluation of the dissociation energy [111]; this amounts to 62.3 kcal mole^{-1} and 33.1 kcal mole^{-1} for the triplet and singlet states, respectively. The optimised Be–C distances are 1.652 Å and 1.472 Å for the triplet and singlet states [5,111]. The Mulliken population analysis for the singlet state indicates that there is a drift of electrons away from the beryllium, resulting in a

charge of +0.156. The π orbital population is almost equally shared between the Be (0.93) and C (1.07) atoms [111]. The calculated heat of hydrogenation of singlet $BeCH_2$ is -135.7 kcal mole^{-1} and for the triplet state it is -80.9 kcal mole^{-1} [5].

Both semi-empirical [8,110] and ab initio calculations [3,5,6] have been performed on dimethylberyllium. The latter yields a charge on the metal of +0.297 and with the carbon possessing an excess of electrons (0.306), the bonding is clearly partially ionic. Dewar and Rzepa [112] have reported the electronic structure of the beryllium alkyls $BeMe_2$, $BeEt_2$ and Be_2Me_4, using the MNDO method. The calculated Be–C bond lengths indicate that the dimer bonds, Be–C_t (1.698 Å) and Be–C_B (1.878 Å) are, not surprisingly, longer than the Be–C distance (1.660 Å) in the monomer. The dimerisation energy of $BeMe_2$ is calculated to be 25.1 kcal mole^{-1}, although this is thought to be high.

The beryllium π-orbital occupancy in $Be(CH_3)_2$ is 0.136 with an accompanying small Be–C π overlap bond population. Calculations in which the angle of rotation was varied show that essentially free rotation occurs: the rotational force constant is extremely small (1.3×10^{-4} mdyne Å^{-1}) [3].

The charge distribution in $HBeCH_3$ [2] can be interpreted in terms of two-centre, two-electron bonds with ionic character of ca. 15% for the H–Be bond polarised in the sense ($H^- - Be^+$) and 13% for the Be–C bond ($Be^+ - C^-$). This yields a +0.296 charge on Be. A later calculation postulated a transfer of 0.15 electrons from BeH to the CH_3 group [5]. The geometry optimised bond lengths of $HBeCH_3$ are Be–C (1.698 Å), Be–H (1.335 Å) and C–H (1.089 Å), while the Be–C–H angle is found to be 111.8° [5]. The heat of hydrogenation of $HBeCH_3$ is computed to be -11.3 kcal mole^{-1} [5]. The value calculated for the hyperconjugation energy for $HBeCH_3$ is 7.1 kcal mole^{-1} [3].

$(HBeCH_3)_2$ was used as an archetype for the polymeric dialkyl beryllium systems, the methyl groups forming the bridge between the beryllium atoms [2]. The energy difference between the dimer and the sum of two isolated monomers was calculated to be -3.8 kcal mole^{-1}. This is somewhat unsatisfactory, as it predicts the former to be the least stable. It was argued that changes in correlation energy must dominate the dimerisation energy for beryllium alkyl compounds. The total overlap population increases upon dimerisation and this is principally due to the creation of a Be–Be bond with an overlap population of 0.322. The charge distribution in the dimer shows only minor changes from the monomer, with the beryllium having a slightly less positive charge and the bridging carbon atoms gaining more electron density.

The energies of several geometrical configurations of $BeCH_6$ have been calculated: these include $H_2Be{=}H_2{=}CH_2$, $H_2Be{\equiv}H_3{\equiv}CH$, $HBe{\equiv}H_3$

$\equiv CH_2$ and $H_2-Be-H-CH_3$ (i.e. double-bridged, triple-bridged and beryllium-bridged) [112]. They are all unstable with respect to CH_4 and BeH_2. This contrasts with the related $LiH-CH_4$ species, which is more stable than the separated components [5].

A double-zeta basis of Gaussian orbitals has been employed to obtain the geometrical structure of CH_3BeF [113]. The predicted C–Be and Be–F distances are 1.70 Å and 1.40 Å, respectively, in a linear molecule. The charge distribution reflects the electronegative nature of F: i.e. H (+0.21), C (−1.06), Be (+1.04) and F (−0.62). The highest filled orbital lies at −0.45 a.u. and the electron population is C 2*s* (0.04), C 2*p* (1.34) and Be 2*s* (0.27), Be 2*p* (0.19).

Pople and co-workers have computed the electronic energies for a series of molecules of structure $HBe-CH_2Y$ where Y = Li, BeH, BH_2, CH_3, NH_2, OH and F [22]. Interaction between the HBe group and Y is gauged by the relevant bond-separation energy (BSE), which is defined as the energy change over the formal reaction

$$HBeCH_2Y + CH_4 \rightarrow CH_3BeH + CH_3Y$$

The values (in kcal mole^{-1}) are, for Y = Li (9.8), HBe (7.8), H_2B (8.4), H_3C (−4.2), H_2N (−4.4), HO (−3.1) and F (−5.9). The positive values of the

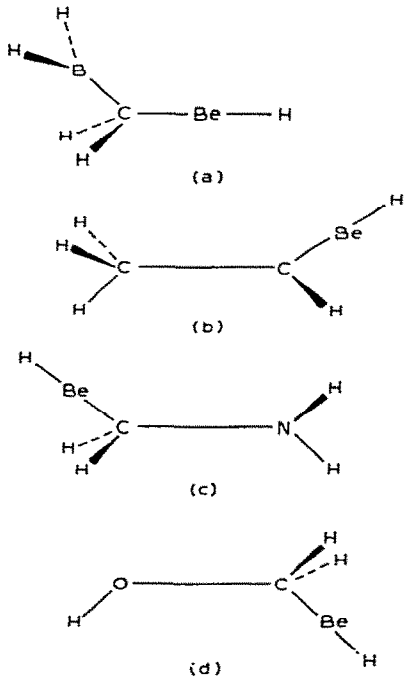

Fig. 10. The stable conformations of the molecules $HBeCH_2X$, where X = (a) BH_2, (b) CH_3, (c) NH_2, (d) OH.

BSE correspond to stabilising interactions of a σ–π nature involving a π acceptor and a σ-donor. The negative values are due to destabilising σ–π interactions and so, in the lowest energy conformations, such interactions are at a minimum.

The perpendicular conformation of $HBeCH_2BH_2$ is more stable by 9.26 kcal mole^{-1} than the coplanar geometry. A much lower barrier to rotation is present in $HBeCH_2CH_3$, where the staggered configuration is favoured by 3.12 kcal mole^{-1}. The synclinal conformation in $HBeCH_2NH_2$ is the most stable of four possible structures, while the antiperiplanar configuration of $HBeCH_2NH_2$ possesses the lowest energy (Fig. 10).

The optimised geometry has been obtained for both a tetrahedral and a planar arrangement about carbon for the series, $CH_x(BeH)_{4-x}$, $x = 0$, 1, 2 and 3 [14]. As the substitution of HBe groups increases, so the planar – tetrahedral energy difference decreases from 240 to 32 kcal mole^{-1} and the calculated C–Be distances in the tetrahedral geometry decrease from 1.666 Å to 1.630 Å.

Ab initio SCF Hartree–Fock calculations [114] have been carried out on the reaction of triplet-state beryllium atoms with methane. The only reaction channel available is hydrogen-atom transfer to give the ground states of BeH_2 and CH_3. The calculated enthalpy change of the reaction

$$Be(2P^3) + CH_4 \rightarrow BeH(^2\tilde{X}) + CH_3(^2\tilde{X})$$

is -2.6 kcal mole^{-1}, which compares favourably with the experimental value of -13.4 kcal mole^{-1}.

Swope and Schaefer [115] have studied the interaction between neutral Be and its positive ion, with the unsaturated hydrocarbons acetylene and ethylene. The bonding of Be^+ with both molecules is attractive, yielding Be–midpoint separations of 2.03 Å and 2.09 Å with the binding energies of 30 and 33 kcal mole^{-1} for C_2H_4 and C_2H_2 complexes, respectively. These ion–molecule interactions appear to be essentially electrostatic in nature. By contrast, the interaction of $Be(^1S)$ with the unsaturated hydrocarbons is a repulsive interaction. The threefold-degenerate excited state $Be(^3P)$ splits into $^3A_1$, $^3B_1$ and $^3B_2$ components as it approaches the unsaturated molecules. The $^3B_2$ state is strongly bound, by 19 kcal mole^{-1} and the Be–C_2H_2 distance is 1.771 Å, whilst the corresponding values for Be–C_2H_4 are 1.782 Å and 24.5 kcal mole^{-1}. The $^3A_1$ state is strongly repulsive, whilst the $^3B_1$ state assumes an intermediate role. In the $Be(^3B_2)$-C_2H_4 and $Be(^3B_2)$-C_2H_2 systems there is a net electron transfer to the hydrocarbons, i.e. 0.09 to (C_2H_2) and 0.16 to (C_2H_4). In both systems this can be thought of as electron donation to the highest bonding orbital of the hydrocarbon ($3b_2$), plus back donation of electrons to the Be in the $5a_1$ orbital.

Apeloig et al. have analysed the electronic energies and structures of the

β-substituted cations $HBeCH_2CH_2^+$ and $HBeHCCH^+$ [36]. The BeH group stabilises the ethyl cation and vinyl cation by 27.1 and 26.4 kcal mole^{-1}, respectively. For $HBeCH_2CH_2^+$, a large barrier to rotation about the C–C$^+$ bond was predicted (22.8 kcal mole^{-1}). This arises from the hyperconjugative effect present in the perpendicular and most stable conformation between the C–Be bond and the empty cationic $2p$ orbital. The resulting number of electrons in the formally vacant $2p$ orbital is 0.270 with an accompanying C–C π overlap population totalling 0.131.

The α-substituted cations $HBeCH_2^+$, $HBeCHCH_3^+$ and $HBeCCH_2^+$ were studied [35] and the effect of the group HBe on the stability of the α-cations determined. The methyl, ethyl and vinyl cations are stabilised by 20.4, 17.1 and 31.7 kcal mole^{-1} by the HBe group. This large stabilisation is due primarily to σ charge transfer (e.g. in $HBeCH_2^+$ there are 0.470 electrons transferred to the CH_2 group).

The structure of $(HBe)_2$ C=C: and HBeCH=C: have been examined [49] by an RHF/STO-3G method. The HBe substituent stabilises the carbene with two substituents having a substantially larger stabilising effect than a single substituent $\times 2$. The importance of hyperconjugation in this stabilisation can be adjudged from the population of the formally empty $2p$ carbenic orbital, which is 0.166 and 0.263 electrons for HBeCH=C: and HBeC=C:, respectively.

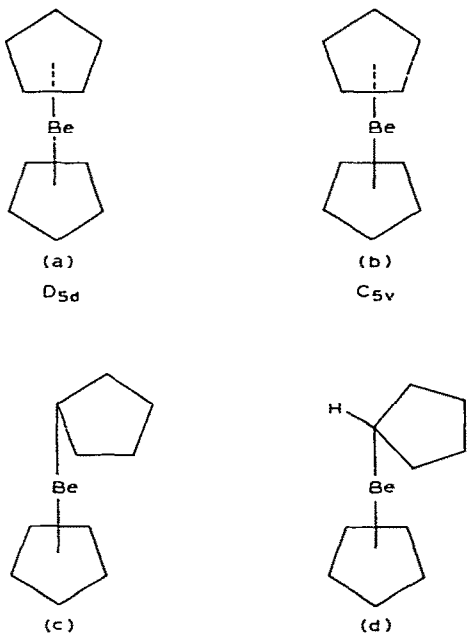

Fig. 11. The structures of cyclopentadienylberyllium.

The gas-phase geometrical structure of dicyclopentadienylberyllium differs from similar complexes in that the position of Be between the rings is not symmetrical and is displaced towards one of the rings by 0.5 Å [116] (Fig. 11). Dyatkina and co-workers [117] calculated that this C_{5v} structure is ca. 7.2 eV more stable than the alternative D_{5d} structure. They explained the lowering in energy in terms of the strengthening of the covalent bonds corresponding to a loss of ionicity. The less symmetrical structure affords a lower positive charge on the beryllium atom (+0.50 against +0.79). The beryllium valence orbital occupancy ($s^{0.34}p^{1.16}$) reflects the dominance of the p orbitals in the covalency of the compound.

Glidewell [118] has invoked the second-order Jahn–Teller effect to rationalise the structure of $(C_5H_5)_2Be$. The only possible distorting vibration is Σ_u^+, which corresponds to the observed distortion.

The low-temperature structure of $(C_5H_5)_2Be$ has a 'slipped' sandwich structure, with the Be 'π-bonded' to one Cp ring and 'σ-bonded' to the other ring (Fig. 11) [119]. Liu [120] has suggested that Be is too small to form effective π bonding to both rings. Therefore, the shifting of the rings allows interplanar repulsion to decline and the rings to come closer. The two cyclopentadienyl rings are parallel and this is rationalised in terms of the σ-bonded carbon using a pure p orbital to bond with Be rather than an sp^3-type hybrid.

Marynick used the PRDDO method to investigate the electronic structure of beryllocene [121]. He considered 6 structures, including the C_{5v} and D_{5d} and the 'slipped' models. The C_{5v} conformation was found to be 26 kcal mole^{-1} less stable than the structure of D_{5d} symmetry. The most stable structure was one where the Be atom lies on the axis which cuts the midpoint of one of the cyclopentadienyl rings and coincides with a carbon atom of the second ring. The angle between these rings is 117° with the Be–C_σ ring = 1.72 Å and the Be–C_π ring = 1.87 Å. The localised molecular-orbital analysis describes the bonding in the most stable conformation as (a) one ring bound to the beryllium by a localised Be–C two-centre σ-bond and (b) a second ring bound by two C–C–Be central three-centre bonds and a delocalised Be–C two-centre bond. The bonding of this ring to the central atom is primarily through carbon p_z and beryllium p_x and p_y orbitals. The resulting charge on the Be is +0.05, there are negative charges on all carbon atoms and positive charges on the hydrogen atoms. The Be–C overlap population is 0.68 while the three Be–Cπ overlap populations are 0.17.

Collins and Schleyer [122] have used orbital interaction diagrams to rationalise the gas-phase conformation of beryllocene. They argue that the D_{5h} and D_{5d} models of $Be(C_6H_5)_2$ have twelve 'interstitial' electrons and this means that they have four electrons in an antibonding e_1'' orbital. Asymmetric distortion of the D_{5h} giving the C_{5v} model reduces the destabilisation of

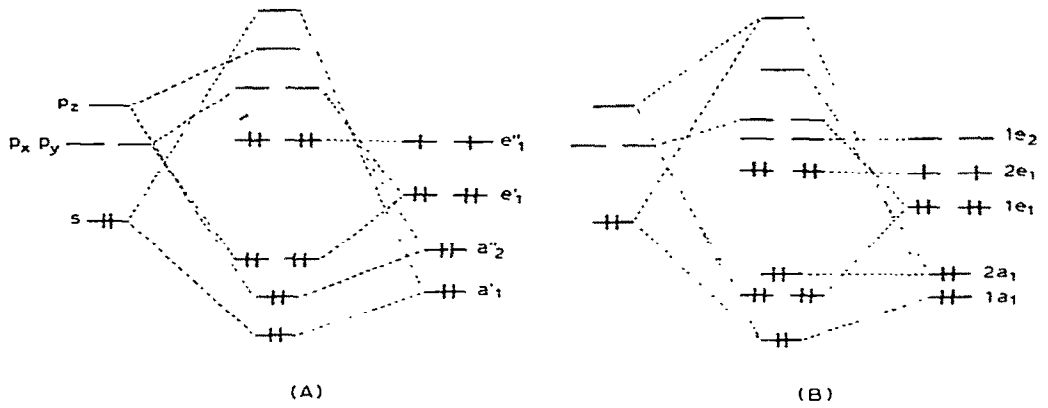

Fig. 12. The orbital correlation diagrams of beryllocene for the (A) D_{5d} and (B) C_{5v} structures.

the antibonding orbital and, relative to the symmetric distortion, gives a weaker destabilisation of the lower-lying bonding orbitals (Fig. 12).

Collins and Schleyer [122] argue that stable, symmetrical, sandwich molecules of beryllium could be found with ligands which provided fewer interstitial electrons, ideally eight in total. They investigated the following three- and four-membered rings: C_3H_3, BC_3H_4 and BC_2H_3, as possible ligands. The $\eta^1\eta^1$ configuration is more stable than the sandwich arrangement for the first two ligands. The hypothetical $Be(C_2BH_3)_2$ is shown computationally to have a stable, symmetrical, sandwich conformation; this awaits experimental confirmation.

In 1978–1979 there was a plethora of reports dealing with the enigmatic structure of beryllocene. All of these investigations found that the D_{5d} model is more stable than the C_{5v} conformation. The various energy differences are 14–18 kcal mole^{-1} [125], 10.5 kcal mole^{-1} [124], 2.8 kcal mole^{-1} [123]. The barrier to rotation of the Cp rings for the D_{5d} model is 0.2 kcal mole^{-1} [112] and 0.4 kcal mole^{-1} [125]. The slipped ring structure obtained by moving one of the rings so that one of the carbon atoms is directly over the Be atom is calculated to be less stable than the D_{5d} model by 24.3 kcal mole^{-1} [123], and 21.1 kcal mole^{-1} [125]. However, when the geometry about the carbon atom of the η^1 ring is optimised, the most stable state is obtained. A tetrahedral arrangement about the carbon atom, with the resulting non-parallel alignment of the Cp rings, is obtained. This geometry is predicted to be more stable than the D_{5d} configuration by varying amounts of energy ranging from 0.7 kcal mole^{-1} [125], 7.4 kcal mole^{-1} [123], and 15.6 kcal mole^{-1} [112]. A $\eta^1\eta^1$ isomer is higher in energy than the optimised $\eta^1\eta^5$ configuration with an energy slightly lower than the D_{5d} model [123]. The atomic charges of the D_{5d} model have been detailed and they show that there

is an electron transfer of 0.19 electrons to each Cp ring where the carbon atoms possess a negative charge (−0.129) and the hydrogen atoms are positively charged (+0.090).

Perhaps the most comprehensive study of beryllocene has been performed by Haaland and co-workers [126,127]. They have re-investigated the structure by gas-phase electron diffraction [126], performed ab initio calculations on various models [127] and interpreted the photoelectron spectra of beryllocene [127]. They find that models of D_{5d} symmetry or models containing one π bonded and one σ bonded Cp model are not compatible with the electron diffraction data. The possibility that gaseous Cp_2Be consists of a mixture of D_{5d} and π-Cp, σ-Cp conformers is considered and rejected. A model of C_{5v} symmetry can be brought into satisfactory agreement with the data. A slip sandwich model obtained from the C_{5v} model by moving sideways the ring which is at the greater distance from Be, while keeping the two rings essentially parallel, is compatible with the electron diffraction data. The best fit between experimental and calculated intensity curves is obtained with a model with a sideways slip of 0.8 Å. They suggest that the potential energy of the molecule does not change much as the magnitude of the slip changes and that the molecule thus undergoes large amplitude vibration.

The total energies obtained by ab initio molecular-orbital calculations [127] on the various models of Cp_2Be disagree with the experimental results. The lowest energies are obtained with the two models (D_{5d} and π-Cp, σ-Cp) which are incompatible with the gas-phase electron diffraction data. The highest energy is obtained for the C_{5v} model but the energy decreases somewhat on sideways displacement of the Cp′ ring. A sideways displacement of 0.79 Å leads to an energy decrease of 3.3 kcal mole^{-1} and, when the displacement is increased to 1.21 Å, the energy is decreased by another 0.6 kcal mole^{-1}. This indicates that this potential energy minimum is very broad.

The ionisation potentials of the first bands of Cp_2Be were compared with the orbital energies obtained from the various models studied by ab initio molecular-orbital techniques [127]. A satisfactory fit between experiment and calculations was obtained for a slip sandwich model of C_s symmetry. A model of C_{5v} symmetry is only compatible with the photoelectron spectrum if the Jahn–Teller splitting of the lowest $^2E_1$ state of the molecular ion is exceptionally large.

The Raman spectrum [128] of solid and liquid Cp_2Be suggests that there are two different Cp rings in the molecule of solid and liquid Cp_2Be. One of these rings possesses C_{5v} local symmetry, while the second ring deviates from the local C_{5v} symmetry and is probably polyhapto-bonded to the metal. There is no significant difference between the spectrum of Cp_2Be in the solid at −160°C and 25°C and that of the liquid at 65°C. Charkin has also

investigated the structure of beryllocene by ab initio calculations [129,130].

The monocyclopentadienyl derivatives of beryllium have been scrutinised by two groups of investigators [112,123]. Both found that the η^5 isomer is more stable than the η^1 isomer, in agreement with microwave spectroscopy. The MNDO method gives the relative stability as 9.1 kcal mole^{-1} [112], while an STO-3G calculation yields a 58.6 kcal mole^{-1} difference [123]. The calculated structural parameters are in reasonable agreement with experiment. Of particular interest is the bending of the C–H bonds towards the beryllium by 0.8° [123]. This contrasts with CpLi [54], where the C–H bonds are bent away from the lithium atom. The π orbitals of the Cp ring bond more effectively with the Be *p* orbitals if the C–H bonds are bent towards the Be. In CpLi the *p* orbitals of Li are more diffuse and better overlap with the Cp π orbitals is obtained by a bending away from the Li.

The two investigations disagree with respect to the charge distribution. The MNDO calculation [112] reveals that there is a small electron transfer (0.05 e) to the cyclopentadienyl ring from the Be–H moiety where Be has a +0.25 charge and H possesses 0.20 excess electrons. The ab initio calculation [123] gives a somewhat surprising result with a negative charge (−0.016) on the Be as well as the bonded hydrogen atom (−0.053). The charge migration occurs via the π orbitals of the cyclopentadienyl moiety to the *p* orbitals of the beryllium.

The stable isomer of CpBeCCH is calculated to be the η^5 conformation; the η^1 isomer has a higher energy (7.6 kcal mole^{-1}) [112]. Two possible structural arrangements were employed for the molecule $CpBeBH_4$ [112]. The more stable structure has a double bridge, i.e. $CpBeH_2BH_2$ and is a mere 0.5 kcal mole^{-1} more stable than the triple-bridged isomer $CpBeH_3BH$.

Dewar and Rezpa have reported MNDO calculations [131] for beryllium hydride or chloride half-sandwich complexes with the indenyl and fluorenyl complexes. Three stable isomers were located for the indenyl complexes, the calculated energies increasing with the coordination $\eta^1 > \eta^5 > \eta^6$. For the fluorenyl complex no minimum energy could be obtained for the η^5 isomer, as all geometry optimisations resulted in the location of the 9-η^1 isomer. This 9-η^1 is more stable than the η^6 isomer. The authors state, however, that the calculated energies of the η^6 and η^5 isomers of both complexes are too high with respect to the η^1 isomer.

Bicerano and Lipscomb have investigated [132] by the PRDDO method some *nido* structures of $B_5H_{10}BeX$ where $X = BH_4$, B_5H_{10}, CH_3 and C_5H_5. The charge on Be for the three ligands BH_4, B_5H_{10} or CH_3 is highly positive (+0.69, +0.42 and +0.40, respectively) but is slightly negative for C_5H_5 (−0.01). The overall charges on the ligands are −0.16 to −0.21 for B_5H_{10}, −0.48 for BH_4, −0.22 for CH_3, and +0.17 for C_5H_5. Thus, C_5H_5 is in a different category as a ligand compared to BH_4, B_5H_{10} and CH_3. The H_B

(BeB) are more negative than the H_B (BB). The bonding in the $B_5H_{10}Be$ unit is nearly constant among the four compounds. The σ bond between B and C in $B_5H_{10}BeCH_3$ is a strong single bond, and the C–C bonds in the C_5H_5 unit of $B_5H_{10}BeC_5H_5$ have an average degree of bonding which is characteristic of substantial aromatic character.

Localised molecular-orbital (LMO) studies show that Be is bonded to B_5H_{10} only through fractional bonds. The concept of approximate average hybridisation (sp^h) for each LMO allows the following observations to be made: (a) the hybrids ($sp^{6.7}$) for C in $C_5H_5 \cdots Be$ bonds are essentially of π type while the C–C bonds with the C_5H_5 group are $sp^{2.0}$; (b) the Be hybrids ($sp^{4.3}$) towards C_5H_5 have more p character than bonds to the boron framework ($sp^{1.4}$) or the Be–C bond ($sp^{1.3}$) in $B_5H_{10}BeCH_3$; and (c) the largest deviation from tetrahedral hybridisation at C in $B_5H_{10}BeCH_3$ occurs in the Be–C bond, ($sp^{2.2}$).

Streitweiser and Williams have examined the electronic structure of beryllium cyclooctatetraenide [133]. The small size of Be^{2+} suggests that it could fit inside the planar cyclooctatetraenide dianion ring. However, the geometry optimisation exercise indicated that the Be is situated on the C_8 axis at a

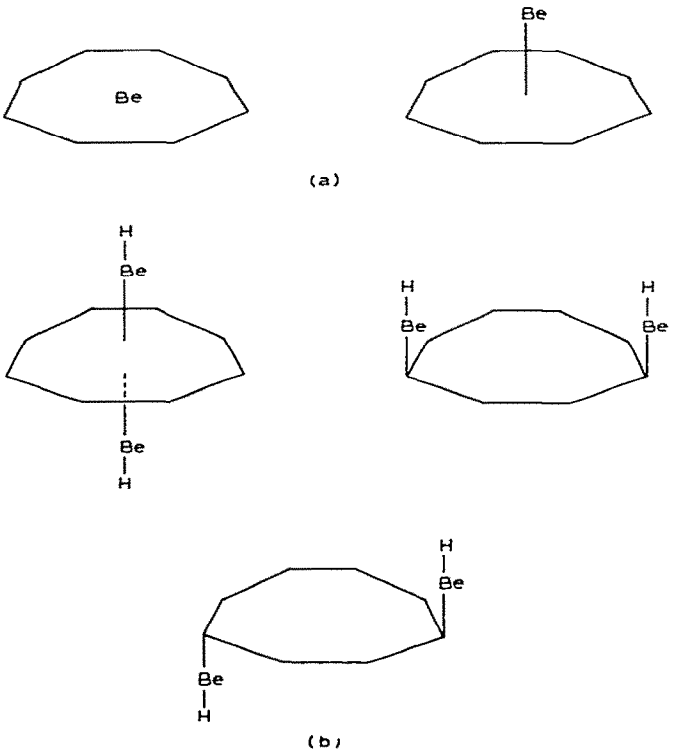

Fig. 13. Structures of (a) cyclooctatetraeneberyllium and (b) $HBe \cdot C_8H_8 \cdot BeH$.

height of 1.0 Å above the plane. Moving the Be out of the plane reduces the positive charge on Be to +0.772 and increases the C–C overlap population to 0.450. The calculated energy change for the isodesmic reaction

$$C_8H_8Be + BeH_2 \rightarrow HBe \cdot C_8H_8 \cdot BeH$$

indicates that the product is energetically favoured over the reactants by 60 kcal mole^{-1} (Fig. 13).

The molecular complexes of dimethylberyllium with aliphatic amines have been studied using a CNDO/2 technique [134]. The energy of complexation increases with methyl substitution from 71.9 kcal mole^{-1} for NH_3 to 99.0 kcal mole^{-1} for $N(CH_3)_3$. The calculated Be–N distances in these complexes measure between 1.85 and 1.95 Å. The charge transfer to the $Be(CH_3)_2$ moiety increases from 0.25 electrons for NH_3 to 0.31 electrons for $(CH_3)_3N$. As expected, this extra charge resides on the Be atom.

Ab initio calculations on $Cl_2Be(NCCH_3)_2$ [135] show that there is a transfer of 0.05 electrons from each methyl cyanide moiety to the $BeCl_2$: σ-donation of 0.25 electrons is dominant and is coupled with π back-donation totalling 0.20 electrons. The Be–N coordinate bond population is a mere 0.07. The charges on the Be, N and Cl atoms are +1.28, −0.33 and −0.69, respectively, indicating the ionic nature of the complex. The interaction between Be^{2+} and formamide has also been reported [85,86].

Dewar and Rezpa have calculated the electronic structure of 9,10-berylloxaronaphthalene [112]. They predict that the 9,10 central bond is long (1.833 Å). The five π MOs are similar to those in naphthalene, especially the two with no density on atoms 9 and 10. The highest occupied MO, however, is bonding in the Be–O region, in contrast to the situation in the unsubstituted naphthalene. There is no σ orbital which is appreciably bonding along the Be–O bond, and this suggests that the molecule may be homoaromatic.

Pople and co-workers have examined the electronic structures of $HBeC_6H_4^+$ [56]. For both singlet and triplet states, the order of stability is *ortho* > *meta* > *para*, with the triplet state having the lower energy. There is an expected σ-electron transfer from the HBe group to the C_6H_4 unit, coupled with a small π electron movement to the HBe. The stabilisation energies calculated from the reaction

$$HBeC_6H_4^+ + C_6H_6 \rightarrow C_6H_5^+ + HBeC_6H_5$$

are 11.6 kcal mole^{-1} (*ortho* singlet) and 6.5 kcal mole^{-1} (*ortho* triplet). The corresponding *para* and *meta* values are smaller.

(ii) Organomagnesium compounds

Organomagnesium compounds in the form of the versatile Grignard reagents are perhaps the most widely known of all organometallic compounds. Hence, it is not surprising that their electronic structure has been thoroughly examined [113,136–142].

Ab initio studies have been concerned with the electronic energies and atomic charges of the monomers $Mg(CH_3)_2$, $MgCH_3F$, and $MgCH_3Cl$. In all cases, linear geometry is the most stable. Reorganisation of CH_3MgF into angular geometry (C–Mg–F = 109°) as a preliminary to tetracoordination by solvent molecules requires 20.6 kcal mole^{-1}. The charge distribution indicates that the bonding is largely ionic. Electron density maps [136] also confirm this view.

The energy of bond-breaking in these compounds has been calculated [136], e.g. CH_3MgF

$$CH_3MgF \longrightarrow \begin{cases} \cdot MgF + CH_3^{\cdot} & \Delta H = 39 \text{ kcal mole}^{-1} \\ \cdot MgCH_3 + F\cdot & \Delta H = 84 \text{ kcal mole}^{-1} \\ MgF^- + CH_3^+ & \Delta H = 244 \text{ kcal mole}^{-1} \\ MgCH_3^+ + F^- & \Delta H = 254 \text{ kcal mole}^{-1} \end{cases}$$

For all three magnesium compounds, scission to radicals is more favoured than the ionic mechanisms. The results for $MgCH_3Cl$ and $Mg(CH_3)_2$ show that breaking of the Mg–C bond to give radicals requires the same energy (39 kcal mole^{-1}), independently of the nature of the second bond. The energies required for breaking the second bond, giving radicals, are in the order ΔH(Mg–F) > ΔH(Mg–Cl) > ΔH(Mg–C). By contrast, an ionic mechanism is favoured for the solvated magnesium compound [137].

RMgX species, in solvents such as diethyl ether, are said [138] to associate according to

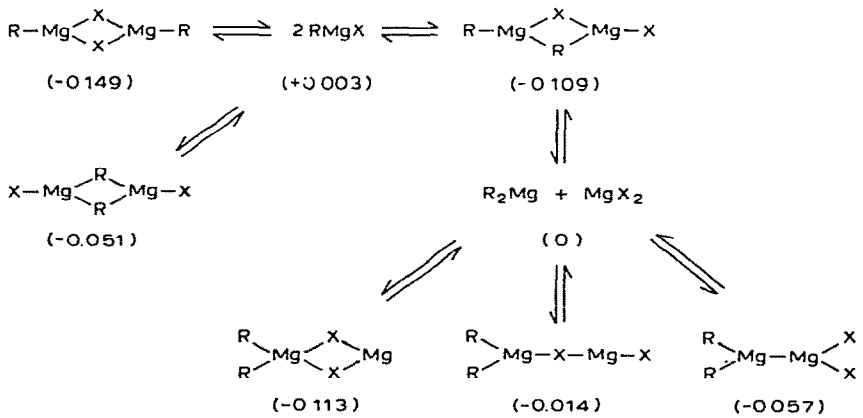

The figures in parentheses are the energy differences (in a.u.) from the sum of the energies of linear MgR_2 and MgX_2. The dimers are found to be more stable than their constituent monomers. This disagrees with earlier calculations [139]. The halogen-bridged structures are more stable than those which involve an alkyl group and those possessing a direct Mg–Mg bond. The latter two types are, surprisingly, of comparable stability. The presence of bridging groups reduces the high polarity associated with the monomer. All in all, the stability of the dimeric species appears mainly to depend on the electron-deficient character of the magnesium atoms as well as the electron-rich nature of the bridgehead atoms. The exchange of alkyl groups associated with Grignard reagents can be explained by the existence of the intermediate mixed alkyl–halogen bridge structure.

Ohkubo and Watanabe [139] calculated the energies of solvation of C_2H_5MgBr by $(CH_3)_2O$, C_4H_8O and $(CH_3)_3N$ as 1.13 eV, 1.06 eV and 1.18 eV, respectively. Unfortunately, this fails to explain the observation that dimerisation of RMgX occurs in only one of these solvents, i.e. $(CH_3)_2O$.

Pseudo-potential calculations have been reported for $(CH_3)_2Mg$ and CH_3MgCl [140]. A simple picture shows most of the bonding interactions to be of σ type, although there is some minor additional contribution from metal–ligand π bonds. A four-electron, two-orbital picture is presented of the bonding. The lower orbital is formally bonding in a two-centre and in a three-centre sense with contributions from the *s* and *d* metal orbitals. The higher orbital has a node at the metal and contains only *p* contributions from the metal. The charges on the atoms are, for dimethylmagnesium, +0.60 (Mg), −0.71 (C) and +0.14 (H), whilst for methylmagnesium chloride they are +0.64 (Mg), −0.69 (C), +0.15 (H) and −0.38 (Cl).

The electron distribution for $Mg(CH_3)_2$, $MgFCH_3$ and $MgClCH_3$ has also been reported by Charkin [141] and by Ohkubo et al. [142]. Their results agree with the main features of the bonding described above.

The π allyl complex of magnesium surrounded by oxygen atoms in an octahedral arrangement has been studied [143] by an SCCC method. This complex is thought to be an initial intermediate in the selective oxidation of propylene by $MgMoO_4$. The allyl ligand is found to be almost electronically neutral, hence indicating weak bonding of the allyl ligand. This contrasts with the cases of Fe, Co and Ni, where 1–1.6 π electrons are shifted to the metal and the allyl ligand is stabilised. It is not surprising, therefore, that the transition-metal molybdates are highly active catalysts whilst $MgMoO_4$ is virtually inactive.

Experimentally [144,145], dicyclopentadienylmagnesium, Cp_2Mg, appears to have the eclipsed rather than the staggered ring configuration. CNDO/2 calculations [144] indicate a very small barrier to rotation (0.03 kcal $mole^{-1}$), the staggered conformation possessing the lower energy. However, since this

barrier is much lower than the thermal energy available at room temperature, effective free movement of the rings is expected.

The electron distribution indicates that Cp_2Mg is best regarded as a covalent molecule, the bonding between metal and ring being effected mainly by a combination of $3p_x$ and $3p_y$ orbitals on the Mg with the e_{1u} π orbitals of the rings. The strength of the Mg–Cp bond is comparable with that of the Ni–Cp bond in Cp_2Ni. The orbital energies obtained from the calculation were in qualitative agreement with the photoelectron spectra [146].

Magnesium plays a vital role in several biological systems. The binding of Mg^{2+} to dimethylphosphate anion [108,109,147,148] has been studied.

Electronic energy computations [149] on the Mg^{2+}/uracil system indicate that Mg^{2+} binds preferentially to the oxygen atoms and, in particular, to the O_4 atom rather than the C–C π bonds, as previously believed [150]. Calculations on the magnesium complexes of phthalocyanine [151], tetrazaporphin [151] and porphyrin [152] have been reported and the nature of the absorption bands interpreted with respect to the filled and empty MOs. The electronic structure of magnesium porphine ($MgN_4C_{20}H_{12}$) and ethyl chlorophyllide a ($MgN_4C_{29}O_3H_{25}$) have been obtained by Christoffersen and co-workers [153] using their molecular fragment ab initio calculational technique.

(iii) Organocalcium, organostrontium and organobarium compounds

An Extended Hückel calculation [110] on dimethylcalcium yielded the following charge distribution Ca(+1.82), C(−1.26) and H(+0.16). Hence $(CH_3)_2Ca$ has considerable ionic character. The Ca–C covalent bond has an overlap population of 0.104 and is composed of a σ-component (0.106) and a π-component (−0.002).

The binding of the Ca^{2+} ion to a dimethylphosphate anion has been reported [108,109].

There have been no significant calculations on organostrontium or organobarium compounds.

D. PERIODIC GROUP III

(i) Organoboron compounds

The simple boron–carbon compounds, BCH, $HBCH_2$ and H_2BCH_3 have been studied by Dill et al. [154]. The first is of interest as it is isoelectronic with the ethynyl cation; likewise, it is predicted to exist as a triplet ground state $^3\Pi$. The linear BCH molecule shows the following optimised parame-

ters: B–C = 1.309 Å and C–H = 1.072 Å. The singlet states $^1\Delta$ and $^1\Sigma^+$ are considerably higher in energy (ca. 70 kcal mole^{-1}) and have shorter bond lengths.

The B–C bond length in $HBCH_2$ is short (1.339 Å) and, with a π-overlap population of 0.490, it may be defined as a double bond. The atomic charges of B and C are +0.252 and −0.339, with charge transfer from the BH group to the CH_2 moiety amounting to 0.204 electrons. The estimated heat of formation is 76 kcal mole^{-1}, with component B=C bond energy amounting to 97 kcal mole^{-1}.

H_2BCH_3 has a very small (0.07 kcal mole^{-1}) six-fold rotational barrier [154,155]. The most stable conformation involves a perpendicular HBCH fragment with a B–C bond length of 1.70 Å. The π-overlap population of the B–C bond amounts to 0.036 electrons and indicates the presence of hyperconjugation. The charges on th boron (+0.259) and carbon (−0.303) are similar to those in $HBCH_2$. The charge transferred, however, is 0.116 and is half that donated in $HBCH_2$. The heat of formation is estimated to be 15 kcal mole^{-1} and the B–C bond energy 74 kcal mole^{-1}.

Methylborane has also been studied, using a floating spherical Gaussian model [156,157]. In the calculated geometry the C_{3v} methyl group symmetry is broken by a distortion towards a B–H–C bridge structure and the electronic repulsion in this system passes through a minimum at the equilibrium geometry. The tilt and the asymmetry of the methyl group in CH_3BH_2 was the subject of a special study by Flood et al. [158]. The magnitude of this tilt is 2.6° away from the BH_2 group for the eclipsed configuration and 2.9° towards the BH_2 group for the staggered molecule. The rotational barrier for dimethylborane has been computed [155]. The staggered-eclipsed conformation, II, is found to be more stable than the

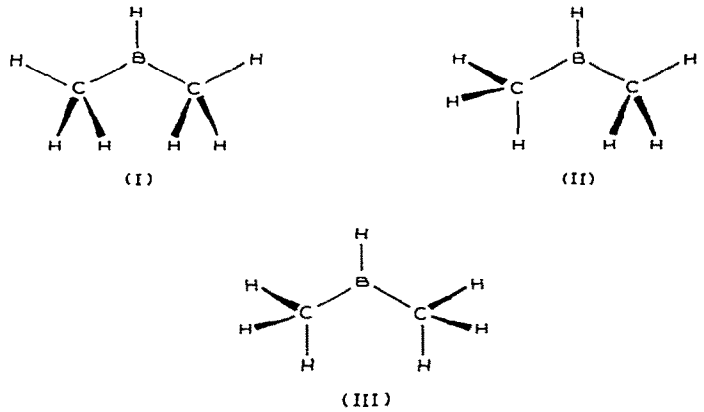

Fig. 14. The conformations of dimethylborane.

double staggered conformation I by 0.47 kcal mole^{-1} and the double eclipsed conformation, III, by 0.14 kcal mole^{-1} (see Fig. 14).

The bonding in trimethylboron has attracted much attention. Here the interest stems from a desire to explain the monomeric nature of the compound, in contrast with the dimeric bridged character of $(CH_3)_3Al$. Carbon–boron π bonding in trimethylborane was first proposed by Mulliken in 1947 to account for the above observation [159] and there have been many calculations dealing with the electronic structure of $(CH_3)_3B$. One of the first investigations was by Cowley and White, who employed a SCCC approach [8]. From this the atomic charges for $B(CH_3)_3$ are B (+0.179), C (−0.099) and H (+0.016), indicating, as expected, a flow of charge away from the boron atom. They obtained a B–C π overlap population of 0.062 compared with a B–C σ overlap population of 0.786. Since the percentage of π bonding in the total bonding is the same as in $(CH_3)_3Al$, it cannot account for the monomeric nature of $(CH_3)_3B$. However, the total overlap population about B is 2.5, whereas it amounts to 2.2 about Al in these compounds. Cowley and White argue that polymerisation will occur if a value of the single M–C overlap population is less than 0.8 and that this will result in an increase in the total overlap population about M. The total overlap population about Al does, indeed, increase due to dimerisation and totals 2.50 for $Al(CH_3)_3$ dimer. In contrast, Ohkubo et al. [110] report that the B–C π bond population in $B(CH_3)_3$ is 10% while that of Al–C in $Al(CH_3)_3$ is 15%. This, they opine, would explain the instability of the latter on the basis of comparative bond strengths.

More recently, Guest et al. investigated BMe_3 using a double-zeta basis set [6]. They obtained a very polar electron distribution with a charge of +1.06 on the boron, while the carbon atoms host 0.70 excess electrons. The boron $2p_\pi$ population amounts to a mere 0.08 electrons, with a $B_{2p\pi}-C_{2p\pi}$ bond population of 0.03. Hence, there is a non-negligible hyperconjugation element in the B–C bond. Localisation calculations show that each carbon–boron bond is described by a single bond-orbital polarised towards the carbon atom. Each carbon atom is approximately 'sp^3 hybridised' in the localised C–H and B–C bonds, while the trigonal boron atom is, not unexpectedly, approximately 'sp^2 hybridised'.

Cross-ring B–B bonding is possible in an organoboron dimer although for such cases, the atomic $3s$, $3p$ and $3d$ levels are energetically too remote to contribute effectively. Hence, for there to be strong cross-ring bonds it would be necessary for the boron atoms to approach each other quite closely. Overlap of the contracted $2s$ and $2p$ orbitals would only then be effective. If both methyl and hydrogen bridging were possible in such a compound, it would reasonably be expected that the latter would be favoured because the nuclear repulsion of two methyl groups in bridge positions

would force the two boron atoms apart. This type of bridging seems, therefore, less likely to exist in boron than in the analogous aluminium compounds, e.g. B_2Me_6 is likely to be less stable than Al_2Me_6. Indeed, this is the conclusion reached by all the detailed calculations [160].

Since the boron and aluminium systems appear to differ so markedly in their quantitative features, the intermediate compound containing both boron and aluminium is of obvious interest. The compound $AlBMe_6$ has been synthesised from BMe_3 and Al_2Me_6 [161] and calculations [160] have shown that the $AlBMe_2H_4$ model has lower total energy than the former pair of compounds $B_2Me_2H_4$ and $Al_2Me_2H_4$. This result is consistent with the chemical evidence that the formation of the isolated known compound, $AlBMe_6$, is thermodynamically favoured over a mixture of BMe_3 and Al_2Me_6.

Geometry-optimised ab initio calculations have been reported for CH_3BF_2, $(CH_3)_2BF$ and $(CH_3)_3B$ [162]. The B–C bond lengths are 1.590 Å, 1.592 Å and 1.587 Å, respectively, while the B–F bond length decreases from 1.307 Å for CH_3BF_2 to 1.300 Å for $(CH_3)_2BF$. For all three molecules there is a positive charge on the boron, with negative charges residing on the carbon and fluorine atoms. The π electron population of boron in $B(CH_3)_3$ is 0.108 and is of a similar magnitude to that obtained by Guest et al. [6]. The ionisation potentials of CH_3BF_2, $(CH_3)_2BF$ and $(CH_3)_3B$ are predicted as 10.83, 9.83 and 10.45 eV, respectively and the electron originates from a σ-orbital in all three cases. The He(1) photoelectron spectra of trimethylboron and the mixed halogenomethyl compounds of boron have been analysed in terms of the bonding [163,164].

Nöth and co-workers [164] have produced a detailed description of the bonding in methylhalogenoboron with the aid of photoelectron spectra of six methylhalogenoboranes $Me_{3-n}BX_n$ (where X = F, Cl, Br, and $n = 1, 2$) and ab initio calculations using STO-3G, STO-4G basis sets. In the photoelectron spectra better separated bands are obtained over the series F → Cl → Br. Thus, the typical halogen orbital ionisation of Cl and Br are more revealed and therefore more easily identifiable than for F. The halogen bands are clearly differentiated from the methyl bands.

For the methylfluoroboranes, substitution of the fluorine atoms by the methyl groups leads to an expected raising of the orbital energies and a lowering of the ionisation potential. In $MeBF_2$ the first ionisation electron originates from an orbital localised about the B–C bond. The higher ionisation energies stem from Me orbitals, followed by B–F bonds and localised fluorine orbitals. There is only one band observed in the low-energy σ-region of Me_2BF and it originates from B–C bonds. The broad band at 13.4 eV stems from at least three methyl orbitals of the σ and π type. The orbital energy sequence in BMe_3 is $\sigma_{BC} > \sigma_{CH_3} > \pi_{CH_3} > \sigma_{BC}$.

The first band of $MeBCl_2$ stems from chlorine non-bonding orbitals. This

is followed by σ orbital with B–C and B–Cl character, π_{Cl} and π_{BCl} orbitals. The HOMO of Me_2BCl is a σ orbital incorporating B–C and B–Cl bonds. The order of lower-energy orbitals is $\sigma > \pi_{BCl} > \sigma > \sigma > \pi_{CH_3}$.

An approximate index for the size of the π interaction in trigonal boron compounds is the splitting Δ_3 between the non-bonding and the BX bonding orbitals of the BX_3 systems. The splitting order is $X = F > Cl > OCH_3 > SCH_3 > N(CH_3)_2 > Br > CH_3$. The π electron population on boron for these BX_3 compounds is 0.52 (F), 0.38 (Cl), 0.51 (OCH_3), 0.47 (SCH_3), 0.48 [$N(CH_3)_2$] and 0.11 (CH_3). The overlap population of the B–X bonds of BX_3 is 0.27 (B–F), 0.30 (B–Cl), 0.33 (B–OCH_3), 0.34 (B–SCH_3), 0.42 [B–$N(CH_3)_2$] and 0.39 (B–CH_3).

The acceptor properties of BMe_3 have been probed by Gropen and Haaland [165]. Using a CNDO technique, they examined both the electronic structures of $Me_3B \cdot NMe_3$ and the separate donor and acceptor components. The boron atom in uncomplexed trimethylboron carries a small positive charge (+0.12). Complexation with NMe_3 results in the transfer of 0.42 electrons to the acceptor moiety There is then no resultant charge on the boron atom and the methyl groups each carry a charge of −0.14. The methyl groups of the acceptor moiety, by contrast, carry a positive charge of +0.13 whilst the nitrogen atom possesses a +0.02 charge. The barrier to rotation about the donor–acceptor bond is 1.7 kcal $mole^{-1}$, with the staggered conformation of methyl groups corresponding to the more stable geometry. The calculated binding energy predicts stability (by −95 kcal $mole^{-1}$) of $Me_3B \cdot NMe_3$ with respect to the separated components. A MNDO investigation [166] of $(CH_3)_3N \cdot B(CH_3)_3$ and $H_3N \cdot B(CH_3)_3$ has also been reported. The calculated dipole moments are 5.3 D and 5.46 D, respectively, while the first ionisation potentials are 10.49 eV and 10.58 eV, respectively.

Gropen and Haaland [165] have also investigated the anion $[Me_4B]^-$. The anionic electron is smeared over all the molecule, resulting in charges on B and Me of −0.11 and −0.22, respectively.

Pople and co-workers [14] have studied the planar and tetrahedral forms of CH_3BH_2 and $C(BH_2)_4$. The tetrahedral − planar energy differences, ΔE_{TP}, are lower for CH_4. This arises from the σ-donor and π-acceptor properties of the BH_2 group. Increased substitution of H atoms in CH_4 by BH_2 groups produces much smaller ΔE_{TP} differences than expected, due to increased repulsion between the BH_2 groups.

$CH_3B(OH)_2$ and $(CH_3)_2B(OH)$ have been examined by the MNDO technique [166]. The heats of formation, ionisation potentials, dipole moments and geometries of these molecules are reported.

The series of molecules H_2BCH_2Y, where Y = Li, BeH, BH_2, CH_3, NH_2, OH and F has been studied [22]. The rotational barriers about the H_2B–CH_2Y bond were analysed by decomposition into the potential constants V_1,

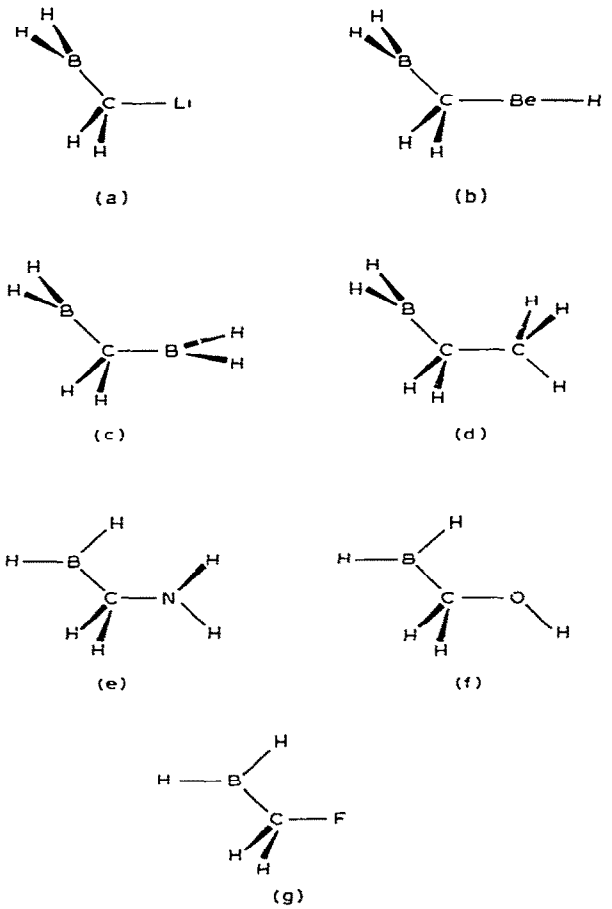

Fig. 15. The stable conformations of H_2BCH_2Y, where Y = (a) Li, (b) BeH, (c) BH_2, (d) CH_3, (e) NH_2, (f) OH and (g) F.

V_2 and V_3. The rotation is dominated by the high π-acceptor ability of the BH_2 group, while the nature of the barrier is dominated by the electronegativity of Y. For Y = Li the perpendicular conformation is the more stable by 20.4 kcal mole^{-1}, whereas for Y = F the planar configuration is lower in energy by 7.1 kcal mole^{-1}. When Y = BeH, BH_2 and OH, coupled rotation between the double rotors is exhibited. For $BH_2CH_2BH_2$, the most stable configuration involves the double perpendicular form of the BH_2 groups with respect to the methylene group. This is as expected from the σ-donor and π-acceptor properties of the BH_2 groups. The most stable geometry for $Y = NH_2$ places the rotors coplanar in a synclinal configuration, while for Y = OH the coplanar rotors are in an antiperiplanar configuration (see Fig. 15).

The stable conformation of ethyl borane incorporates a perpendicular arrangement of the CH_3 and BH_2 groups with a staggered conformation about the C–C bonds. This geometry has been rationalised in terms of hyperconjugation between the vacant BH_2 orbital with the C–C bond rather than the two C–H bonds. The geometry, ionisation potential and heat of formation of triethylboron have been evaluated [166].

The energy changes in the process

$$BH_2CH_2Y + CH_4 \rightarrow BH_2CH_3 + CH_3Y$$

for Y = Li, BeH, BH_2, CH_3, NH_2, OH and F are calculated to be 18.4, 8.4, 4.1, −1.5, −0.3, +1.5 and +1.2 kcal mole^{-1}, respectively [22]. The levelling-off of the energies for the electronegative elements arises from the adoption of coplanar conformation which thereby eliminates the unfavourable σ–π interactions.

Calculations have been performed on the reaction of BH_3 with C_2H_4 [167]. It is found that the reaction proceeds exothermally via an intermediate π-complex but without an overall activation barrier. The dominant interaction in the early stages of the reaction between the ethylene π HOMO and the vacant boron $2p\pi$ LUMO leads to the formation of the π complex. This then proceeds smoothly to the ethylborane, with the HOMO of the π complex converting to a C–B bonding orbital. The interaction of one of the BH_3 HOMOs with the ethylene LUMO becomes more important as the reaction proceeds, as it eventually leads to C–H bonding. The calculated enthalpy of hydroboration of ethylene by BH_3 is −63 kcal mole^{-1} (from STO-3G) and −33 kcal mole^{-1} (from 4–31G). Dewar and McKee [168] have studied the reactions of borane with ethylene, propene, isobutene, vinyl chloride, vinyl fluoride, acetylene and methylacetylene and of methylborane and dimethylborane with propene. The calculated minimum energy reaction path of the first three reactions showed that a loose adduct of π-complex-like type was formed as a marginally stable intermediate, this being the rate-determining step for the overall reaction with an activation energy of 7.6 kcal mole^{-1} (ethylene), 9.9 kcal mole^{-1} (propene, anti-Markownikoff), 9.7 kcal mole^{-1} (propene, Markownikoff), 11.8 kcal mole^{-1} (isobutene, anti-Markownikoff), and 11.0 kcal mole^{-1} (isobutene, Markownikoff). The increase in the activation energy with the number of methyl groups indicates that steric repulsions outweigh the electronic effects which would be expected to lower the activation energy.

The addition of the monomethylborane and dimethylborane to propene yields models for the second and third steps in the hydroboration reaction. In the addition of CH_3BH_2, the *trans* orientation of the methyl groups is more favourable in the π-complex-like intermediate than the *cis* arrangement. This difference is reasonably attributed to the steric repulsions be-

tween the methyl groups. The activation energy is predicted to be 9.1 kcal mole^{-1} and 8.9 kcal mole^{-1} for the Markownikoff and anti-Markownikoff addition, respectively. In the addition of $(CH_3)_2BH$ to propene, *cis* orientations of the methyl groups in the intermediate complex cannot be avoided and so no stable intermediates are formed. The activation energies, 16.5 kcal mole^{-1} for the anti-Markownikoff addition and 21.8 kcal mole^{-1} for the Markownikoff addition, are much higher than those from the other reactions.

All the addition reactions of borane to vinyl chloride and vinyl fluoride take place via marginally stable intermediates of the π-complex type except the anti-Markownikoff addition to vinyl fluoride. Vinyl fluoride is predicted to add in anti-Markownikoff fashion with a corresponding activation energy of 9.3 kcal mole^{-1}, while vinyl chloride adds in a Markownikoff orientation and with an activation energy of 11.6 kcal mole^{-1}. This difference can be rationalised in terms of a differing $-E$ (electromeric) activity of the halogen atoms.

The addition reactions of BH_3 to acetylene and methylacetylene are predicted to occur via intermediate π complexes which are much more stable than those in the olefin addition reactions. The calculated activation energies predict that methylacetylene (7.4 kcal mole^{-1}) should react faster than acetylene (9.3 kcal mole^{-1}). In this case the electronic effect of the methyl group outweighs the steric effects.

In a related study, Dewar and McKee [169] have made a MNDO examination of the reduction of formaldehyde and methyl formate by the borohydride ion. They predict that both reactions are strongly exothermic. Reaction profile calculations indicate that the reactions in the gas phase are 'forbidden' processes.

The reactions of borane with acetone and ketene have also been investigated [169]. The minimum-energy reaction path for the addition of BH_3 with acetone gives the intermediate complex $(CH_3)_2C{=}O{-}BH_3$, which rearranges to the product $(CH_3)_2CHOBH_2$. The first step is predicted to be almost thermoneutral with a low activation energy (12.3 kcal mole^{-1}) while the second stage is strongly exothermic with a much higher activation energy (21 kcal mole^{-1}). A similar reaction path was obtained for the addition of BH_3 to the carbonyl portion of ketene. The corresponding activation barriers are predicted to be much higher than those for the acetone reaction.

Ketene can also undergo hydroboration to give H_2BCH_2CHO. The first step of the reaction is the formation of a zwitterionic intermediate $H_3B^- - CH_2 - C{\equiv}O^+$ with a low activation energy (5.8 kcal mole^{-1}), while the conversion of the intermediate requires 7.8 kcal mole^{-1}. The ease of hydroboration has been explained in terms of a cyclic conjugated system previously recognised in the phosphonitrilic chlorides [170].

Datta and co-workers [171] have investigated, by the CNDO method, the transition state of the hydroboration reaction between ethylene and borane. They find that the three-centre transition state is more stable by 50 kcal $mole^{-1}$ than the four-membered transition state and may be regarded as part of the preferred pathway. The localised molecular orbital picture shows the existence of a two-electron three-centre bond between the two carbon atoms and the boron atom. The ethylene donates 0.344 electrons to the borane portion, resulting in negatively charged boron (−0.18) and positively charged carbon atoms (+0.10).

The fifth examination of the hydroboration reaction has been performed by Lipscomb and co-workers [172]: PRDDO, ab initio minimal and extended basis sets, and configuration-interaction calculations are used in this investigation. The PRDDO and the extended basis set calculations yield a reaction energy of −71 kcal $mole^{-1}$ and −33 kcal $mole^{-1}$, respectively, and an activation energy of +19 kcal $mole^{-1}$ and +15 kcal $mole^{-1}$, respectively. Both methods yield a short-range maximum defining the transition state in their reaction paths. This transition state is a highly polarised structure and the dynamics of its formation from BH_3 and C_2H_4 and its distortion into ethylborane suggest that the hydroboration process can legitimately be called a donation-back-donation mechanism. As the transition state is formed, a donation is made to the boron atom, and as the reaction is completed, these electrons are donated back to the rest of the molecule.

The CI calculations yield a reaction energy of −45 kcal $mole^{-1}$, and the reaction energy of the transition state from BH_3 and C_2H_4 is −10 kcal $mole^{-1}$, and so the reaction has no activation energy at the zero-order configuration-interaction level.

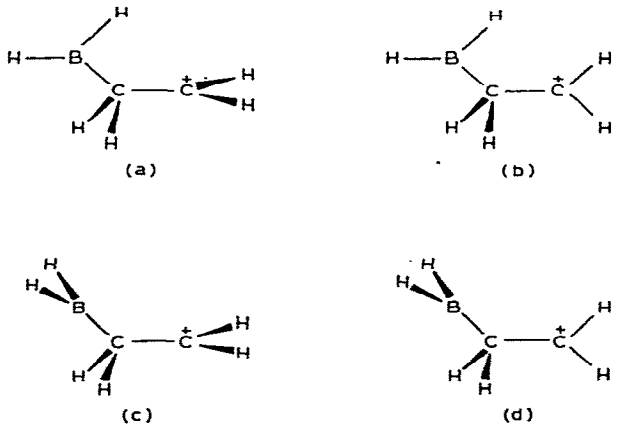

Fig. 16. The conformations of $BH_2CH_2CH_2^+$.

Geometry-optimised ab initio calculations have been reported [173] for $R_2C_3O \cdot BY_3$ (where Y = F or H and R = CH_3 or H), i.e. the cyclopropenone and its dimethyl derivative adducts with BH_3 and BF_3. The results show that in the above series, BH_3 is a stronger Lewis acid than BF_3 while dimethylation increases the basicity of the cyclopropenone system.

INDO calculations have been performed on the $Me_3B \cdot O_2$ adduct, which is considered to be present in the initial stages of the oxidation of Me_3B by O_2 [174]. The irreversible formation of $Me_3B \cdot O_2$ is considered to be a charge-transfer process in which a spontaneous transition from the triplet state of molecular oxygen is possible.

The electronic structure of the cations $BH_2CH_2CH_2^+$ and $BH_2CH{=}CH^+$ have been analysed in an attempt to assess the effect of BH_2 as a β-substituent on the ethyl and vinyl cations [36,175]. It is found that BH_2 stabilises the ethyl cation by 12.3 kcal $mole^{-1}$ and the vinyl cation by 7 kcal $mole^{-1}$.

Four possible conformations of $BH_2CH_2CH_2^+$ are shown in Fig. 16. Preference for the perpendicular conformation, i.e. (a) and (c), arises from hyperconjugation of the vacant $2p$ orbital on the boron, with the methylene π-type orbital of the CH_2 group. Rotation to the eclipsed conformation, (b) and (d), precludes this interaction and allows interaction only with the $C{-}C^+$ bond. The most stable conformation is (a), in which the empty orbitals on B and C^+ can hyperconjugate with the best available adjacent occupied orbital of the appropriate symmetry.

The effect of BH_2 on the stabilities of α-substituted methyl, ethyl and vinyl cations has been investigated [35]. It is found that BH_2 is roughly as effective as CH_3 in stabilising those cations. This is because hyperconjugation is chiefly responsible for the stabilisation induced by both groups. In $BH_2CH_2^+$ the perpendicular form is more stable than the planar configuration, due to a double hyperconjugation between the pseudo π BH_2 orbital and the C^+ $2p$ orbital and between the pseudo π CH_2 orbital and the B $2p$ orbital.

The equilibrium structures of the isoelectronic molecules HBC^{2-}, HCB^{2-} and $HBCH^-$ have been studied [176]. The following optimised bond lengths were obtained for HBC^{2-}, B–C (1.364 Å) and B–H (1.231 Å), for HCB^{2-} B–C (1.383 Å) and C–H (1.098 Å), whilst for $HBCH^-$ B–C (1.303 Å), B–H (1.183 Å) and C–H (1.063 Å). Total energy considerations predict that HCB^{2-} is more stable than the isomeric HBC^{2-}.

There have been many researches into the electronic structure of the intriguing molecule BH_3CO [177–196]. The first investigation was by Armstrong and Perkins [177], who employed ab initio methods to determine the electronic structure of the molecule. From the energies of the components and the complex, a heat of formation in reasonable agreement with experiment was determined. Moreover, the calculated C–O bond population

in the complex turned out to be higher than that in free CO, thus affording a natural explanation of the experimental spectroscopic observation that the C–O stretching frequency is increased by complexing with borane.

Basch computed the wavefunction for BH_3CO [178] in order to test the quality of an approximate MO method against the exact non-empirical SCF result. He also compared different definitions of the group orbital populations [179–183] and found that charge separation is smallest for Löwdin's definition [179–181] and largest for Christoffersen and Baker's [182], with Mulliken's definition [183] being somewhere in between but much closer to Löwdin's.

Runtz and Bader [184] used the virial partitioning method [185] to examine the electron distribution and energy of formation of BH_3CO. The technique involves a spatial partitioning of a molecule into atomic-like fragments and partitioning its properties into a sum of the fragments' contributions. The virial theorem is obeyed separately within the domain of each fragment. The (B) fragment in BH_3 has a net charge of $+2.14$ and the (C) fragment in CO has a net charge of $+1.36$. Thus, the formation of BH_3CO involves a joining of two positively charged fragments. In order to stabilise the complex, electrons are transferred from both the (H) and (O) fragments to the (B) and (C) fragments. It is interesting to note that the overall transfer in the complex is 0.123 e from BH_3 to CO! The energy of formation of the complex from BH_3 and CO is calculated to be -6.3 kcal $mole^{-1}$.

Using a double-zeta basis set, the dipole moment of BH_3CO is calculated to be 1.6223 D [186], compared with the experimental value 1.80 ± 0.04 D [187]. BH_3CO was one of the few molecules out of the 34 studied which produced a calculated value smaller than the experimental dipole moment.

Kern and co-workers [188,189] employed a large basis set and so an estimate of the Hartree–Fock limit could be made (-139.210 ± 0.004 a.u.). This allows the evaluation of the molecular extra correlation energy as 0.21 a.u. The energy of the reaction

$$BH_3CO \rightarrow BH_3 + CO$$

has been evaluated and electron correlation energy is found to be the main energy term. The population analysis of the largest basis set yields the following atomic charges: H (-0.020), B (-0.116), C (0.485) and O (-0.308). Thus, there is a donation of electrons (0.178) from the CO to the BH_3 group. The B–C overlap population is 0.184 (σ contribution) and 0.133 (π contribution), emphasising the σ–π nature of the bond. The C–O and B–H bond overlap populations increase on complexing and this may rationalise the stability of the complex over its components. Plots of the localised molecular orbitals indicate that the CO portion is almost identical to that obtained for

the uncomplexed molecule. The carbon–oxygen 'banana bonds' show a slight tendency to delocalise onto the hydrogen atoms. The B–C bond LMO density has the appearance of a distorted carbon lone pair. The density of the B–H bond is somewhat delocalised towards the B–C region and, hence, has a three-centre bond appearance. This description of BH_3CO is, therefore, of two identifiable fragments which interact weakly through a dative B–C bond.

An alternative description [190] uses the resonance-structure concept and the molecular wavefunction can be written

$$\psi = a\psi_0(H_3BCO) + b\psi_1\left(H_3B^- - \overset{+}{C}O\right) + c\psi_2(H_3B^+ - CO^-)$$

ψ_0 represents the no-bond structure
ψ_1 represents the n-donor action of CO
ψ_2 represents the π-acceptor action of CO

where $a = 0.548$, $b = 0.298$ and $c = 0.147$. The chemical bond between the carbon and boron atoms stems from the charge-transfer actions in both directions. The σ-transfer is greater than the π-component.

Umeyama and Morokuma [191] have analysed the energy terms involved in the formation of BH_3CO. They opine that the stability of BH_3CO is due to three attractive components; these are the electrostatic, polarisation and charge-transfer energy terms. The third contribution is important and is significant even at large internuclear separations. Lack of any one of these three terms would render BH_3CO unstable. They conclude that BH_3 prefers the pyramidal structure in the complex in order to reduce the exchange repulsion energy term.

The oxygen-bonded species $CO \rightarrow BH_3$ was also investigated [191] and it was found to be both unstable with respect to $OC \rightarrow BH_3$ and with respect to the separate components. The relative instability of $COBH_3$ is due to a decrease in the charge-transfer energy term coupled with smaller electrostatic and polarisation stabilisation. The smaller charge-transfer stabilisation may be attributed to two factors: (i) the highest occupied σ-orbital of CO is more localised on carbon than on oxygen; and (ii) the atomic orbitals of oxygen are smaller than those on carbon so that, at a given separation, the B–O overlap is less than the B–C overlap.

Ha probed the electronic structure of BH_3CO, using CI calculations [192]. The SCF ground state composed from a double-zeta basis set was augmented by singly and doubly excited configurations formed from the eight highest-occupied and eight lowest-lying orbitals. Inclusion of the CI wavefunctions improved the agreement between the calculated heat of formation from -10.98 to -14.56 kcal mole^{-1} and the experimentally deduced value of -16.6 kcal mole^{-1} [177].

The binding energy of BH_3CO was obtained from the many-body perturbation theory [193]. Results are given for basis sets of double-zeta quality with polarisation functions added on all atoms. The binding energy is calculated to be 21 kcal $mole^{-1}$, with correlation effects accounting for 62% of the binding. When the theoretical values are corrected for vibrational zero-point energies and the experimental data are adjusted for temperature effects ($\Delta H_f^{calc}(0\ K) = -18.5$ kcal $mole^{-1}$; $\Delta H_f^{exp}(0\ K) = -19.4$ kcal $mole^{-1}$), the results agree within 5%.

There have been significant semi-empirical investigations [194–196] on BH_3CO. Purcell and Martin [194] concentrated on the hyperconjugative properties of BH_3CO using the INDO method. They calculated NMR spin–spin couplings, electric field gradients, ionisation potentials, geometries and infrared intensities, both with and without the hyperconjugation interactions. Results of the finite difference calculations for $^1J_{HB}$, $^1J_{BC}$, $^2J_{HH}$ and $^2J_{HC}$ indicate that the latter three terms are affected by hyperconjugation, whilst the first term is not influenced by this interaction. Hence, comparison of the $^1J_{BD}$ term for $H_3B{\cdot}D$ and $R_3B{\cdot}D$ adducts could afford information about σ–π synergism. Likewise, $^2J_{HH}$ is a promising probe. The asymmetry $f_z = (q_\sigma - \frac{1}{2} q_\pi)$ in the boron p orbitals is markedly influenced by hyperconjugation. It has the value -0.262 for a non-hyperconjugated situation and -0.099 for full hyperconjugation. These f_z values are related to the boron-field gradient and, thus, the ^{11}B nuclear quadrupole moment may be another useful probe to study hyperconjugation.

The orbital energies are not greatly affected by hyperconjugation. The BH_3 molecular orbitals of e symmetry are stabilised by 0.25 eV, while the a_1 molecular orbital is destabilised by about 0.25 eV. Thus, photoelectron spectroscopy is unlikely to yield any useful information about hyperconjugation. Hyperconjugation also produces a marked shortening of the B–C bond length amounting to 0.18 Å; however, the B–H bond distance and the HBC angle are not altered by removing the hyperconjugative interactions.

The electronic structure of $B_2H_4(CO)_2$ and B_3H_7CO have been examined [197,198] by ab initio techniques. The energies of formation of the borane carbonyl from the parent borane and carbon monoxide are in the order ΔE_f $(BH_3CO) > \Delta E_f$ $(B_2H_4(CO)_2) > \Delta E_f$ (B_3H_7CO), with BH_3 showing the greatest gain in stability, while B_3H_7 is the borane least stabilised by CO. The electron donation from the carbonyl moiety amounts to 0.133 electrons for the mono- and diborane carbonyls, while it is 0.219 electrons for the triborane carbonyl. An interesting feature of the three borane carbonyl molecules is the increase in the CO bond population upon complexing. This is, perhaps, the important factor in the complexing nature of the CO ligand.

Dorschner and Kaufmann [199] have calculated by ab initio techniques the geometric and electronic structures of BH_3CN^- and BH_3NC^-. The

cyanoborohydride ion is predicted to be the more stable isomer by 7.9 kcal $mole^{-1}$. The structural parameters for BH_3CN^- are B–C = 1.62 Å, B–H = 1.23 Å and the angle C–B–H = 108.5°. The geometry of BH_3NC^- is similar, with B–N = 1.58 Å, N–C = 1.17 Å, B–H = 1.23 Å and the angle N–B–H = 108.5°.

The charge of the BH_3CN^- ion is essentially localised on the boron and nitrogen atoms, while the carbon and the hydrogen atoms can be considered as neutral species. By contrast, the charge of the BH_3NC^- is delocalised over the whole molecule. The B–N overlap population of BH_3NC^- (0.354) is smaller than the B–C overlap of BH_3CN^- (0.486). The different reducing properties of BH_3CN^- and BH_4^- are explained in terms of the charge on the hydrogen atoms, as in the latter compound there is a high localisation of charge (0.27) on each hydrogen.

When the empty boron orbitals are of very similar energy to those of the valence orbitals, we would expect appreciable interaction to occur with peripheral organic groups. Thus, in some early work Good and Ritter [200] found that the UV spectrum of trivinylboron shows an intense peak at 234 nm whereas ethylene itself absorbs in the vacuum UV near 162 nm [201].

Other vinylboranes exhibit similar spectral shifts [202] but when triarylboranes are examined, it is found that the first band of the aryl group is not very different from that of benzene. It is perhaps wise to point out here that the experimental work on compounds such as these has proved to be difficult because of their extreme sensitivity to oxygen, moisture and solvents with any degree of electron-donor power.

A fairly complete early theoretical treatment of the electronic spectra of representative organoboron compounds of the type $R_{3-x}BX_x$, where R = vinyl or aryl and X = F, Cl, Br, Me, OH and NH_2, was put forward by Armstrong and Perkins [203–207]. This was based on a self-consistent field molecular-orbital treatment of the Pariser–Parr–Pople type involving the π electrons of the organic group and the substituent X, together with the empty p_π orbital situated on the boron atom. By this method it has been possible to rationalise the electronic spectra and to interpret almost all the

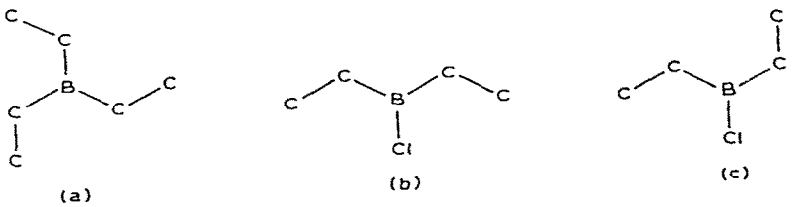

Fig. 17. The geometry of (a) trivinylborane and (b) the C_{2v} and (c) the C_s structure of divinylborane chloride.

features of them which arise. Some of the points brought out are of general application for main-group organometallic compounds.

In order to show how progress has been made and what may result from it, we examine trivinylborane and divinylboron chloride. The symmetries of these compounds are shown in Fig. 17. The swastika form of Vi_3B has C_{3h} symmetry, whilst Vi_2BCl could have either C_{2v} or C_s symmetry. It is of interest to see whether the UV spectrum can decide between the two latter possibilities.

The electronic states of the C_{2v} model generated by excitations of the $\pi \rightarrow \pi^*$ type are all either of A_1 or B_1 symmetry whilst for the C_s model they are all of the same type, i.e. A'. In both cases all transitions to singlet states are space-allowed and are polarised in the molecular plane coincident with or at right angles to the B–Cl bond. By contrast, the states of trivinylboron are of A' or E' type and transitions are only allowed to the latter state: these are polarised in the xy plane. For both compounds the states resulting from π excitations can be calculated very satisfactorily.

The main band of Vi_3B can be satisfactorily assigned to the $^1A' \rightarrow {}^1E'$ transition which is strongly allowed. The next band (at 5.77 eV) is a weak one in the experimental spectrum and can be assigned to the $^1A' \rightarrow {}^1A'$ transition. Although a transition to the pure electronic state is formally forbidden, it will be allowed if the upper state is coupled with an in-plane degenerate vibration of the B–C skeleton.

In divinylboron chloride an intense band turns up at 5.57 eV and this corresponds well with the $^1A_1 \rightarrow {}^1B_1$ transition (under C_{2v} symmetry). The next band lies at 5.98 eV and corresponds to the $^1A_1 \rightarrow {}^1A_1$ transition polarised at right angles to the first. It is clear from these and other results of the calculations that there is a considerable degree of π delocalisation from the π molecular orbitals of the vinyl group to the empty p_π orbital of the boron atom. The pronounced red-shifting and intensification of the first ethylene band is brought about by the interposition of a boron orbital in the energy sequence for the vinyl group. What is important is that π electron delocalisation is revealed by a study of the UV spectrum of these molecules and in these cases, the first transition band is a sensitive index of the phenomenon.

It was suggested earlier that the UV spectrum of the Vi_2BCl molecule might help in deciding its configuration, i.e. whether its symmetry is C_{2v} or C_s. The excited-state energies calculated for the two models are very similar and they cannot be distinguished on this basis. The relative intensities of the transitions to the $^1B_1$ and $^1A_1$ states are, however, much more revealing. For a C_{2v} model the calculated relative intensities of the transitions to the $^1B_1$ and $^1A_1$ states are 83 : 1 whilst for the swastika model the same intensities are in the ratio 3 : 2. By comparison, the experimental bands fall in the intensity

ratio 4:3 and so it seems reasonable to suppose that the compound is mainly composed of the swastika isomer at room temperature. The reason for the existence of this geometry is unclear but it may reflect the stereochemistry of the transition state in the reaction by which it is produced.

Kuehnlenz and Jaffé have also calculated the electronic transitions of the methylvinylboranes [208]. The weak low-energy transitions in the experimental spectrum which occur in addition to the 'π bands' are due to σ–π^* transitions where the σ bond is localised about the B–C orbital and this conclusion is identical to that arrived at earlier by Armstrong and Perkins [209]. The molecular skeleton is probably somewhat twisted, as the bands would otherwise be forbidden. For the related methylvinylboron chlorides, the longest wavelength transition is calculated to be a weak σ–π^* transition emanating from the molecular orbital localised on the chlorine atom and terminating on an orbital largely composed of the boron $2p\pi$ orbital.

Allinger and Siefert [210] have performed conformational studies on vinylboranes. The CNDO and INDO methods indicate that both vinylborane and dimethylvinylborane are twisted by 90°. By contrast, ab initio studies indicate that the planar form of vinylborane is favoured. The energy of rotation is 16.2 kcal mole^{-1}. Williams and Streitweiser [211] and Seip and Jensen [212] also found that the planar form was the preferred geometry, although the rotational barrier was considerably reduced to 8.8 kcal mole^{-1} [211], and 7.35 kcal mole^{-1} [212]. Allinger and Siefert [210] maintain that dimethylvinylborane, methylvinylborane and trivinylborane are probably not planar, with the vinyl groups in each case being twisted from the plane by perhaps 30° or so.

Ab initio calculations [162] have been performed on vinylboron difluoride, divinylboron fluoride and trivinylborane. The optimised B–C bond lengths are 1.564, 1.569 and 1.571 Å, respectively. These bond lengths are about 0.02 Å shorter than for the corresponding methylboron fluoride compounds. The population analysis reveals that there is the expected positive charge on the boron atoms and this decreases with increasing number of vinyl groups. This charge is lower than in the corresponding methyl compound due to a greater π-electron population which stems from delocalisation from the vinyl group. The boron π population for trivinylborane totals 0.028 electrons while the electron distribution within the vinyl group is 0.976 (C_α) and 0.948 (C_β). The calculated first ionisation energies of the vinylboron fluorides are lower than those of the corresponding methyl compounds and are 9.14 eV ($C_2H_3BF_2$), 8.63 eV ($(C_2H_3)_2BF$), and 8.40 eV ($(C_2H_3)_3B$). In each case, the electron is removed from a π orbital centred on the vinyl groups.

The attack of Cl^- on $CH_2{=}CH{-}BH_2$ has been investigated by an ab initio method [213]. During the approach of the radical, the bond lengths of the substrate and all bond angles were allowed to relax from their initial to their

final values. The attack on the substituted carbon becomes competitive with the unsubstituted position and seems even to be slightly favoured; hence the preferred attack is at the carbon, which gives the thermodynamically less stable product CH_2CHBH_2Cl. By contrast, the preferred attack of $H^\bullet$ on $CH_2{=}CH{-}BH_2$ is at the unsubstituted end, giving the thermodynamically more stable product CH_3CHBH_2.

Van 't Hoff proposed stereochemical rules regarding the basic shapes of cumulenes, $H_2C(=C)_nH_2$ [214]. When n is odd, planarity is preferred but when n is even, a perpendicular conformation is obtained. Schleyer and co-workers [215] have theoretically examined the first four members ($n = 0$–4) of the cumulenes with the two geminal hydrogens replaced by a three-membered ring comprised of two BH groups. They find that the more stable conformations (by 15–20 kcal mole^{-1}) are the anti-Van 't Hoff geometries, i.e. $(HB)_2CH_2$, planar; $(HB)_2C{=}CH_2$, perpendicular; $(HB)_2C{=}C{=}CH_2$, planar; and $(HB)_2C{=}C{=}C{=}CH_2$, perpendicular. The Van 't Hoff forms exhibit classical Lewis two-centre two-electron bonding, with six σ electrons for the three diboracyclopropane ring bonds. In the anti-Van 't Hoff configuration, the same rings have only four σ electrons, the two remaining electrons occupying an aromatic cyclopropenium–ion-like π orbital. The geometrical consequences are shortening of the BB bonds and widening of the HBB angles in the anti-Van 't Hoff geometries over the Van 't Hoff configurations.

Singlet states of $H_2BCH{=}C{:}$ and $(H_2B)_2C{=}C{:}$ were examined by the RHF/STO-3G method [49]. The BH_2 group and the BCC atoms lay in the same plane. There is a small stabilisation of the parent carbene by the BH_2 group. This arises from the hyperconjugation effects and π acceptor ability of the BH_2 group.

The electronic structures of $CH_2{=}CH{-}BH{-}NH_2$ and $NH_2{-}BH{-}BH{-}NH_2$ have been calculated [216] in order to help rationalise the photochemistry of 1,2-bis(dimethylamine)-1,2-diphenyl(diborane(4)) [217]. This is best explained in terms of photolytic boron–boron homolysis. This contrasts with the photochemical electrocyclic ring closure of the isoelectronic 2,3-diphenyl-1,3-butadiene. The calculations predict an inversion in the ordering of the two highest filled molecular orbitals, one σ and one π type, accompanying the stepwise replacement of C=C units by B–N linkages. Thus, the highest filled MO of $H_2NBHBHNH_2$ is essentially a boron–boron σ-bond.

Kuehnlenz and Jaffé have calculated the excited states of various borazine derivatives [208]. The main transitions of *B*-trimethyl borazine are π–π^* in nature and lie at 6.4 eV ($^1A_2'$), 7.0 eV ($^1A_1'$) and 7.1 eV ($^1E'$). These are lower in energy as compared with the unsubstituted borazine. This energy reduction is considerably higher than for the corresponding *N*-trimethylborazine. Independent earlier work [218] agrees with the above that the lowest-energy

transitions in borazines are of π–π^* type. However, from the latter, a clear result is that the shift in absorption energies consequent on substitution is greater for substitution at nitrogen than it is for boron substitution.

The bonding in *B*-trimethylborazine as well as other substituted borazines is discussed through ab initio SCF-MO calculations [219]. The calculated molecular energies predict *B*-trimethylborazine to be 2.8 eV more stable than the *N*-trimethyl substituted derivative. The population analysis of $(BCH_3NH)_3$ suggests that the methyl group gains 0.25 e by a σ mechanism while back-donating 0.02 electrons into the borazine π ring system. The atomic charges are B (+0.70), N (−0.79), C (−0.81), methyl H (+0.20), H (+0.31). The calculated ionisation potentials indicate that the sequence for the three highest occupied orbitals is the same as in borazine, i.e. $\pi > \sigma > \pi$. The low-energy photoelectron spectrum [220,221] has been satisfactorily interpreted. CNDO calculations [220,221] have also been used to aid the assignment of the spectra.

The π molecular complex, benzene/borazine, has been studied by the CNDO method [222]. A modification of this method, in which pairs of atoms associated with the same molecule and with different molecules are differentiated, leads to reduced intermolecular bonding and provides reasonable stabilisation energies and intermolecular separations. The molecules in the complex are symmetrically disposed in parallel planes. The stabilisation energies are calculated to be in the range 2–5 kcal $mole^{-1}$ with interplanar separations near 3 Å.

All-valence IEHT and CNDO calculations have been carried out [223] for the 1,1,4,4-tetramethyl-1,4-diazonia-2,5-diborazacyclohexane. The calculations show that the B–C bond is relatively stronger than the B–N bond. Partial electron transfer from N to B has occurred in the formation of the B–H bond. The stretching force constants for the B–N and B–C bonds are 2.19 and 3.33 mdyn $Å^{-1}$, respectively.

The electronic spectra of the phenylboranes have been analysed [205–207] and the excited states can be calculated just as in the case of the aforementioned vinyl compounds. However, because the orbital degeneracy of benzene becomes lifted on lowering the symmetry to C_{2v} (as in the $PhBX_2$ and Ph_2BX cases), the number of individual electronic states becomes considerably larger. Furthermore, since the calculated states are spread over a small energy range, configuration interaction is extensive and strong and the final states are mixtures of one-electron states [205–207].

It is not really possible, therefore, to correlate each state with a band in the experimental spectrum of a given molecule and the most informative procedure is to trace the shifts in energy and intensity of the bands which, in free benzene, correspond to the three lowest excited states. Under D_{6h} symmetry these belong to representations $^1B_{2u}$, $^1B_{1u}$ and $^1E_{1u}$ and occur at

4.71, 5.96 and 6.76 eV, respectively [224]. The first two give rise to weak bands but the last is very intense.

With halides of the $PhBX_2$ type one finds calculationally [205], that the first band (corresponding to the $^1B_{2u}$ benzene state) occurs at almost the same energy as in benzene. This contrasts sharply with the analogous vinyl series where the first band of ethylene was strongly shifted. The reason for the difference lies in the fact that, in $PhBX_2$, the first state does not arise from a transition to the first antibonding orbital which is strongly 'boron' in character. The next two benzene bands are, however, bathochromically shifted quite strongly and the $^1E_{1u}$ state is split into its two components.

A similar situation exists in the diphenyl series [206] and there is a similarity between the spectra and electronic states of these compounds and of diphenyl. Here the lowest electronic states arise from symmetric and anti-symmetric combinations of the locally excited $^1B_{2u}$, $^1B_{1u}$, $^1E_{1u}$, and $^1E'_{1u}$ states of the two rings. As with simpler phenylboranes, the first transition bands are virtually unshifted with respect to the parent benzene bands and it is the higher-energy states which exhibit evidence for π-electron delocalisation from the rings. These states correspond roughly to combinations of the $^1E_{1u}$ components but the benzene character of these is rather lost in this energy region and the exciton states are in admixture with ring–ring charge-transfer states. Similar analysis has been followed through for borafluorenes [225], organoboronic acids [226] and cyclic boroxanes [227].

Ramsey and O'Neill [228] discuss the UV, ^1H NMR and photoelectron spectra of boron-substituted monophenylboranes with the aid of CNDO/2 calculations on $C_6H_5BX_2$ where X = F, OH and CH_3. It is found that only for X = Cl is there a net electron withdrawal from the phenyl ring although, for all the BX_2 groups, there is a calculated electron donation to the sigma framework of the benzene ring. Perturbation of the electronic spectrum of benzene by the BX_2 group is determined both by the competition between X and the hydrocarbon π system for the vacant boron $2p\pi$ orbital as well as electronegativity differences which produce a reorganisation of σ-electron density.

Ramsey and O'Neill [228] define four categories to which substituent X can belong: (i) strongly electronegative with strong π bonding; (ii) moderately to weakly electronegative with strong π bonding; (iii) weakly electronegative with weak π bonding; (iv) strongly electronegative with weak π bonding. Substituents in categories (i) and (ii) will probably not give rise to low-energy charge-transfer transitions, although the normal $\pi \rightarrow \pi^*$ transitions of the substituted hydrocarbons will be shifted to low energy. On the other hand, substituents in categories (iii) and (iv) may be expected to give rise to low-energy charge-transfer transitions in benzene.

Electron-releasing σ-inductive effects should be important for substituents

in categories (ii) and (iii), producing decreases in ionisation energy. Substituents in category (iv) should produce the largest effects on chemical and spectroscopic properties associated with net inductive electron withdrawal and boron $2p\pi$ bonding to the unsaturated hydrocarbon system. Combination of inductive, field and resonance effects of BX_2 substituents in categories (i) and (iv) should lead to increase in ionisation energies, particularly in those involving π orbitals and, except for BF_2, should give large downfield hydrogen NMR chemical shifts.

Mislow and coworkers [229] have discussed the conformational dynamics of triarylboranes. The isoelectronic triarylcarbonium ions, Ar_3C^+, have substantially higher barriers than the triarylboranes, due to the greater length of the C–B bond compared with the corresponding C–C bond (1.58 Å cf. 1.45 Å). Furthermore, the π conjugation between boron and the phenyl rings is said to be negligible (3 ± 2 kcal mole^{-1}) whereas, for arylcarbonium ions, a much higher resonance energy is indicated by calculation. Ab initio calculations of the barrier to rotation for $C_6H_5C^+H_2$ yield 36.6 kcal mole^{-1} whilst for $C_6H_5BH_2$ a value of 6.3 kcal mole^{-1} has been obtained. The Mulliken population analysis for the two bonds illustrates the weaker nature of the B–C π bond. In the planar benzyl cation the π overlap population of the C–C bond is 0.185, while upon rotation this reduces to 0.060. For phenylborane the values are 0.072 and 0.022, respectively.

Finnocchiaro et al. [230] have examined the temperature-dependent NMR spectral behaviour of alkoxydiarylboranes and they discuss the conformation of these compounds. Boron–oxygen π bonding influences not only the magnitudes of the rotational barriers about the B–O bonds but also, indirectly, the height of the barriers to rotation about the B–C bonds of alkoxydiarylboranes. The barrier to flipping of a mesityl group is ca. 3 kcal mole^{-1} lower than that of the less bulky methoxy group. Ab initio calculations indicate that the rotational barrier for $HOBH_2$ is greater than that for $PhBH_2$. The Mulliken population of the B–X π bonding parallels that of the rotational barrier.

Calculations have been performed on boracyclopropene within the INDO approximation [231]. The calculated geometry reveals that the B–C bond spans 1.457 Å while the C–C bond is 1.382 Å long and the B–C–C angle is 61.7°. As the former distance is shorter than that found in BMe_3 and the latter distance is similar to that found in benzene, considerable delocalisation is indicated. The π electron density distribution shows that conjugation indeed occurs, with 0.53 electrons occupying the formally vacant boron π orbital. The C–C π bond order (0.74) is of the same order as the C–B π bond orders (0.62).

Collins and Schleyer [122] have calculated the energies of bis-(cyclopropenyl) boron cation isomers. They found that the η_1, η_1 conforma-

tion is predicted to be more stable than the sandwich-type η_3, η_3 molecule.

Pople and co-workers have investigated the effect of the BH_2 group on the stability of the phenyl cation [56]. The triplet states of $C_6H_4^+ BH_2$ are found to be more stable than the corresponding singlet states. The most stable triplet state corresponds to a geometry in which the BH_2 group is perpendicular to the phenyl group and substituted in a *para* position to the C^+ atom. The most stable conformation of the singlet state occurs when the BH_2 group is coplanar with the phenyl group and substituted in the *meta* position.

Ab initio calculations [232,233] have been used to demonstrate bond-stretching isomerism in the 1-aza-4-boratricyclo [2.2.2.$0^{1,4}$] octane–1-aza-4-borabicyclo [2.2.2] octane system

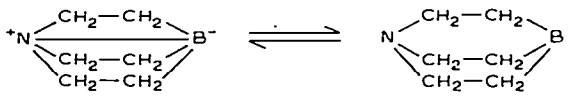

(I) ABTO (II) ABBO

Here (I) and (II) are isomers which are related by a simple bond stretching and this transformation was investigated through the variation in the calculated energy accompanying the bond-stretching of the inter-bridgehead distance. There are two potential minima although the one which corresponds to the ABTO structure is shallow. The minimum for the ABBO isomer is 8 kcal $mole^{-1}$ lower than for the ABTO isomer and occurs at B–N = 2.4 Å. The relative weakness of the ABTO form may be attributed to the weak long-distance interaction between boron and nitrogen, which is inadequate to compensate for additional ring strain. The stability of ABTO can be increased by stabilising the boron $2p$ orbital (for example, by electron-withdrawing groups attached to positions 3, 5 and 8) and/or by destabilizing the nitrogen $2p$ orbitals (by electron-releasing groups at positions 2, 6 and 7).

Linear relationships are observed between the calculated charge densities q_B^{total} or q_B^P at boron and $\delta^{11}B$ for a considerable number of organoboron compounds [234]. CNDO calculations yield the following: $q_B^{total} = 0.0026\ \delta^{11}B + 2.8346$, standard error = 0.0112, and the correlation coefficient = 0.98. Ab initio calculations give a similar linear relationship; $q_B^{total} = 0.0029\ \delta^{11}B + 4.8913$, standard error = 0.0636, and the correlation coefficient = 0.70. The term P^2_{B2S}–H from the density matrix, correlates linearly with $^1J(^{11}B\ ^1H)$ for both the CNDO and ab initio calculations.

Jallali-Heravi and Webb have calculated [235] the boron chemical shifts for 20 boron compounds with the use of MINDO/3 computational program. The comparison with the experimental values reveals that the calculated chemical shifts are overestimated.

The carboranes are an extremely important, though rather different class from those considered till now and there have been many calculations of their electronic structure [240–280]. A separate review would be necessary to do justice to the extensive work carried through, and here we present a somewhat abbreviated text.

Localised molecular-orbital (LMO) techniques provide a picture of molecular bonding which can be more readily interpreted chemically. The use of LMOs has yielded a description of bonding consistent with the classical three-centre bonding theory developed to describe electron-deficient molecules. Hence, LMO studies of the carboranes have been quite extensive. There are two procedures for obtaining the localised orbitals from the canonical molecular orbitals. The Edmiston–Ruedenberg method [236] maximises the self-repulsion energy

$$J = \sum_i (\phi_i\phi_i/\phi_i\phi_i) = \sum_i \int \phi_i(1)\phi_i(1)\frac{1}{r_{12}}\phi_i(2)\phi_i(2)\mathrm{d}v_1\mathrm{d}v_2$$

This method has two serious drawbacks from a computational standpoint. Firstly, the method requires all two-electron integrals over the n occupied canonical molecular orbitals. Hence, a transformation must be made from the atomic orbitals and the computational effort for this transformation is proportional to the fifth power of the number of basis orbitals. Secondly, the method is an iterative process involving a series of unitary transformations of the n occupied MOs. This updating of the two-electron integrals is computationally an η^5 process. As a consequence, the Edmiston–Ruedenberg procedure is impractical for very large molecules.

The second localisation method is due to Boys [237–239]. Here the localised orbitals are those which maximise the sum of the squares of the distance between the orbital centroids I where

$$I = \sum_{i>j=1}^{n} \left[\langle\phi_i|r|\phi_i\rangle - \langle\phi_j|r|\phi_j\rangle\right]^2$$

This, therefore, involves repeated transformations of the $3m^2$ dipole moment integrals where m is the number of basis functions and so is more readily applicable to the larger molecular systems.

Ab initio [240–243] and semi-empirical [244,245] calculations on 1,5-$C_2B_3H_5$ indicate that there is weak B–B bonding and so the structure can be represented by a classical scheme where each carbon is bonded to one hydrogen and three boron atoms and each boron is bonded to a hydrogen and two carbon atoms. The charge distribution shows that all the hydrogen atoms bear a positive charge, those bonded to the carbons donating more electron density than those attached to boron. This released electron density ends up on the carbon atoms while the boron atoms possess only a small positive charge.

Fitzpatrick and Fanning [242] have reported geometry-optimised ab initio calculations, which complement the earlier CNDO calculations [244], on the unstable isomer 1,2-$C_2B_3H_5$. The boron–origin distances are greater for the 1,2-isomer than the 1,5-isomer, while the opposite is true for the carbon–origin distances. The carbon atoms are negatively charged, although the magnitude of the charges is less than those on the 1,5-isomer. The boron atoms are positively charged with the exception of the apical boron atom, which has a slight negative charge. The charge distribution of the B–H and C–H moieties are −0.130 and −0.069, respectively, for the apical positions, while the corresponding planar values are 0.008 and 0.096. For both isomers the apical groups are negatively charged while the planar diatomic moieties are positive. The overlap populations of 1,2-$C_2B_3H_5$ indicate that the bonding in the equatorial plane is small while the apical–planar bonding is important, although the populations are less than those of the 1,5-$C_2B_3H_5$. These weaker apical–planar bonds are said to be one of the reasons for the relative instability of the 1,2-isomer, which is calculated to be 63.5 kcal $mole^{-1}$ higher in energy than the 1,5-isomer.

The reduced carborane $C_2B_3H_5^{2-}$ has been investigated [246,247]. If D_{3h} symmetry is retained, then $C_2B_3H_5^{2-}$ has orbital degeneracy and should not be stable. Certain isomeric forms of $C_2B_3H_5^{2-}$ of different symmetry are deemed energetically inaccessible if the structure retains a nominally trigonal-bipyramid structure. However, if the descent in symmetry is realised by distortion to a square-pyramid skeleton, then all of the isomeric forms of $C_2B_3H_5^{2-}$ are energetically accessible. The symmetry-allowed low-energy mode of interconversion between isomeric square-pyramidal forms of $C_2B_3H_5^{2-}$ amounts to an arcing of one atom position (Fig. 18).

Comparison of the total energies of 1,2-$C_2B_4H_6$ and 1,6-$C_2B_4H_6$ reveals that the latter is the more stable isomer [248]. Electron density distributions from SCF calculations on 1,2-$C_2B_4H_6$ [240] show that $B_4(B_6)$ carry a −0.05 charge, while the $B_3(B_5)$ atoms are neutral. The schematic representation of the localised molecular orbital (LMO) bonding for 1,2-$C_2B_4H_6$ is shown in Fig. 19 [240]. This MO contains two three-centre boron–boron bonds which are polarised towards the $B_3(B_5)$ atoms. Each carbon atom is involved in two equivalent asymmetric three-centre B–C–B bonds. These orbitals are polarised towards the carbon atoms which have approximately half the total orbital population. The bonding between the adjacent carbon atoms can be

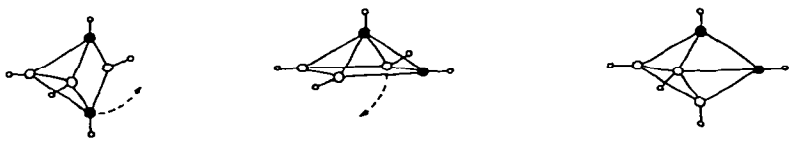

Fig. 18. The mode of interconversion between isomeric square pyramidal forms of $C_2B_3H_5^{2-}$.

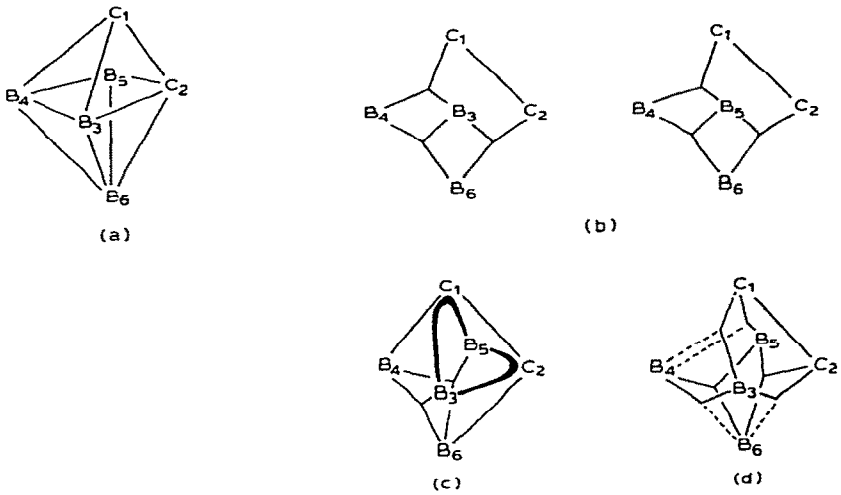

Fig. 19. Bonding in 1,2-$C_2B_4H_6$. (a) The geometrical structure; (b) the localised molecular orbitals calculated by Guest and Hillier (ref. 240); (c) the localised molecular orbitals calculated by Lipscomb (ref. 250) using the Edmiston–Ruedenberg procedure; and (d) the localised molecular orbitals calculated by Lipscomb (ref. 250) using the Boys method.

thought of as a two-centre bond orbital, although the electron density plot shows a delocalisation of the bond orbital onto the neighbouring boron orbitals. Atoms B_4 and B_6 participate in five bonds (2B–C–B, 2B–B–B and 1B–H) and therefore Lipscomb and co-workers represent this by fractional bonding at these atoms [243,249,250]. Lipscomb and co-workers [250] find that the Boys and the Edmiston–Ruedenburg procedures yield different structures for 1,2-$C_2B_4H_6$ (Fig. 19). The bonding features from the latter method are two open three-centre bonds ($B_3-C_1-B_5$ and $B_3-C_2-B_5$), two central three-centre bonds ($B_3-B_1-B_6$ and $B_4-B_5-B_6$), and three two-centre bonds (C_1-C_2, C_1-B_4 and C_2-B_6). Of particular interest is the absence of fractional bonding and the presence of the open three-centre bonds.

The charge distribution for 1,6-$C_2B_4H_6$ [240,241] exhibits small negative charges on the boron atoms and large negative charges on the carbon atoms.

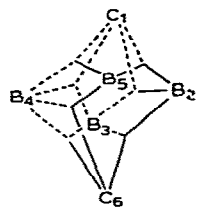

Fig. 20. The localised molecular orbitals for 1,6-$C_2B_4H_6$.

This excess electron density is released mainly from the hydrogens, especially those bonded to the carbon atoms.

For $1,6\text{-}C_2B_4H_6$, the localisation of the ab initio wave-functions [240,243,250,251] predicts that all the LMOs contain finite, non-local contributions. The bonding scheme given in Fig. 20 shows that one carbon atom appears in four framework orbitals, with the second carbon atom in three orbitals. In a similar manner, two of the boron atoms have four LMO contributions and two boron atoms participate in three LMOs. Hence, the former atoms, C_1, B_4 and B_3, are involved in fractional bonding.

MS-X_α calculations [252] on $1,6\text{-}C_2B_4H_6$ afford good agreement between the transition-state orbital energies and the measured photoelectron spectroscopic ionisation potentials.

PRDDO [253] and CNDO [244] studies on the rearrangement of $1,2\text{-}C_2B_4H_6$ to $1,6\text{-}C_2B_4H_6$ have been directed towards finding an energetically accessible pathway. The latter failed to find an energetically accessible pathway, while the former study reveals that the rearrangement passes through a distorted trigonal pyramid DTP (Fig. 21). The barrier to the rearrangements are 35 kcal $mole^{-1}$ for $1,2\text{-}B_2C_4H_6 \rightarrow$ DTP, and 14 kcal $mole^{-1}$ for DTP $\rightarrow 1,6\text{-}B_2C_4H_6$. The intermediate DTP structure lies about 8 kcal $mole^{-1}$ and 20 kcal $mole^{-1}$ above 1,2- and $1,6\text{-}C_2B_4H_6$, respectively.

The rearrangements of the reduced carboranes 1,2- and $1,6\text{-}C_2B_4H_6^{2-}$ are predicted [247] to involve pentagonal pyramidal isomers. This result, coupled with the findings of the aforementioned rearrangement of $C_2B_3H_5^{2-}$, sug-

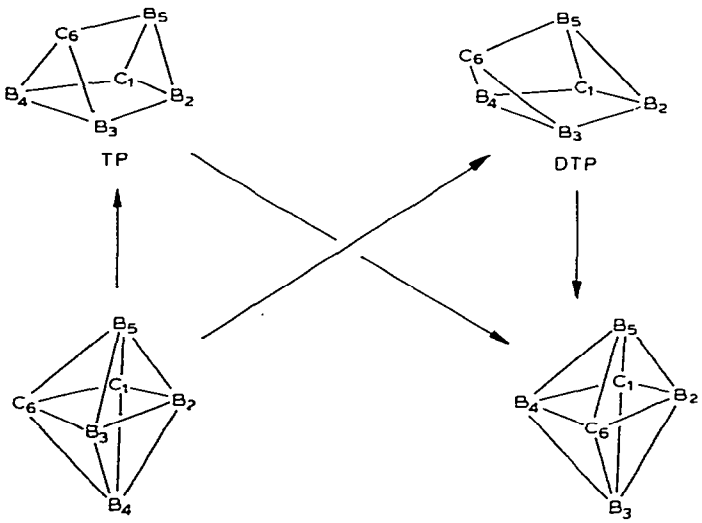

Fig. 21. The rearrangement schemes of $1,2\text{-}C_2B_4H_6$ to $1,6\text{-}C_2B_4H_6$.

gests that the two-electron reduction of *closo*-carboranes in general opens the deltahedron to the corresponding *nido* counterpart.

4,5-$C_2B_4H_8$ has been studied by both SCF techniques and by LMO approaches [249,251,254]. The most electropositive atom is B_2, whilst B_3 and

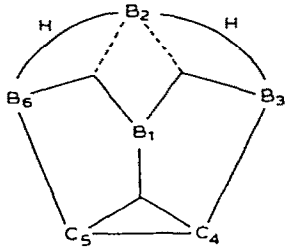

Fig. 22. The localised molecular orbitals for 4,5-$C_2B_4H_8$.

B_6 atoms also possess a comparable charge. The negative charge resides on the hydrogen atoms, with H_1, H_3 and H_4 collecting the most electron density. Comparison of the overlap populations of the framework bonds indicates that of the B_1-B_2 bond to be the largest (0.58) followed by the B_1-B_3 bond (0.36) and the B_2-B_3 bond (0.35). The equatorial B_3-C_4 interaction is 0.86 and is considerably stronger than the apical B_1-C_4 bond (0.24). The localised molecular orbitals for $C_2B_4H_8$ are sketched in Fig. 22. Here there is one atom B_2 which is participating in five bonding LMOs including two fractional three-centre BBB bonds. The hybrids of the carbon atoms involved in the CCB orbitals are essentially *p* orbitals and very close to π orbital in character.

The geometry optimised structure of 2,3,4,5-tetracarba-*nido* hexaborane (6) has been calculated [255] by an ab initio method using an STO-3G basis. The structure has a pentagonal pyramidal geometry with an apical B atom. The bonding between neighbouring atoms in the basal plane is strong, while the interactions between the apical boron and the basal plane are weak. There is π electron donation from the basal ring but σ-electron donor interaction to the ring is symmetry-forbidden. The similarity between the BH moiety in this molecule and the grouping $Mn(CO)_3$ in the molecule $C_5H_5Mn(CO)_3$ is discussed.

Lipscomb and co-workers have examined [256] the relative stabilities of several classical structures possessing formal orbital vacancies associated with three well-known non-classical molecules $C_2B_3H_5$, $C_2B_4H_6$ and $C_4B_2H_6$. In each case, classical structures may be postulated that are comparable in energy with their non-classical counterparts and are plausible as intermediates in rearrangements. This is especially true for $C_2B_4H_6$ where the

classical structure is a mere 2 kcal $mole^{-1}$ higher in energy than the non-classical geometry.

The existence of formally vacant orbitals in the classical structure suggests that placing electron-rich substituents on boron should stabilise these structures. Calculations on the B-fluoro derivatives of the above classical and non-classical structures reveal that the classical $C_2H_2B_3F_3$ is now only 2 kcal $mole^{-1}$ less stable than the non-classical structure. The classical isomers of $C_4H_4B_2F_2$ and $C_2H_2B_4F_4$ are found to have lower energy than their non-classical counterparts.

The He(I) photoelectron spectra of 1- and 2-$CH_3B_5H_8$ have been reported [257]. The effect of substitution on the highest filled molecular orbital of the borane fragment (4*e*) is examined and analysed using a linear combination of bond orbitals (LCBO) method. In the methylpentaborane, the methyl group acts both inductively, by affecting the effective core charge of the substituted atom and conjugatively, by interaction of the 4*e* framework orbital with the C–H group orbitals of CH_3 having π symmetry.

The position of the bridge hydrogen of CB_5H_7 has interested two research groups [258,259]. The molecule is best described as a distorted octahedron (see Fig. 23) and the bridge hydrogen tautomerises rapidly, equating borons 2, 3, 4 and 5 on the NMR time scale [260]. CNDO calculations [258] support the suggestion of a four-centre bond linking the hydrogen to borons 2, 3 and 6. PRDDO calculations [259], however, indicate that the hydrogen is present as a slightly delocalised equatorial–equatorial bridge hydrogen which interacts only weakly with boron 6 and undergoes tautomerism at room temperature by passing through an equatorial–apical BHB bridge.

2,4-$C_2B_5H_7$ has been studied both by Guest and Hillier [240] and by Lipscomb and coworkers [243,250,261]. The least positively charged boron is B_5 and, in fact, electrophilic chlorination and bromination yield exclusively the 5-halo derivative. Overlap-population analysis indicates that bonds from the apex atom are weaker than the equatorial bonds. The localised valence structures are shown in Fig. 24. The apex boron atoms participate in three three-centre bonds. A similar bonding arrangement occurs for B_5 and B_6 while the third equatorial boron atom possesses fractional bonds, as it is a

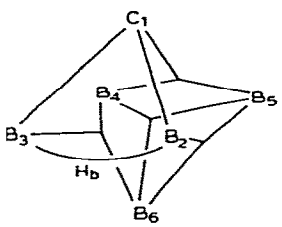

Fig. 23. The localised molecular orbitals for CB_5H_7.

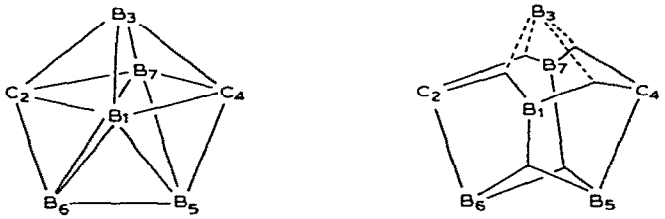

Fig. 24. The localised molecular orbitals for 2,4-$C_2B_5H_7$.

participant in four three-centre bonds as well as a terminal B–H bond.

The electronic structure of 1,7-$C_2B_6H_8$ has been reported [243]. The carbon atoms possess 0.11 extra electrons while the charges on the borons 2, 3 and 5 are +0.07, +0.11 and +0.04, respectively. The LMOs exhibit C_2 symmetry and are similar to those of $B_8H_8^{2-}$ [243] (Fig. 25). There are four three-centre bonds in each cap and one B–B bond in the equatorial regions.

The charge distribution of 1,6-$C_2B_7H_9$ [243] is similar to that of the other carboranes,with a negative charge (−0.12) on the carbon atoms and positive charges on borons 2, 4 and 8 totalling +0.12, +0.07 and +0.01, respectively. The LMOs for $C_2B_7H_9$ show a significant degree of delocalisation (Fig. 26). The four equivalent BCB bonds show low populations on the two borons adjacent to the two carbons. This deficiency is made up by delocalisation of the B–B single bonds. Boron atoms 2 and 3 participate in five framework bonds and are fractional centres. The boron atom 8 is also a fractional centre participating in two normal BBB bonds and in delocalisation from the two B–B single bonds.

The atomic charges of 8,9-$C_2B_7H_{13}$ [240,262] show that atoms B_4 and B_5

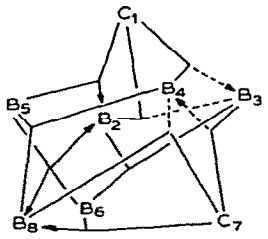

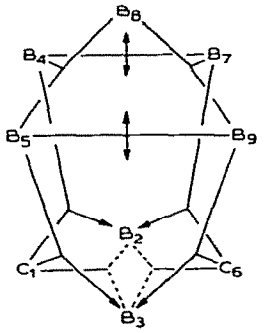

Fig. 25. The localised molecular orbitals for 1,7-$C_2B_6H_8$.

Fig. 26. The localised molecular orbitals for 1,6-$C_2B_7H_9$.

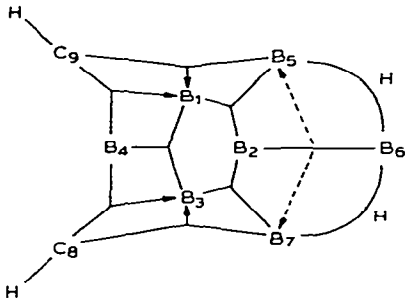

Fig. 27. The localised molecular orbitals for 8,9-$C_2B_7H_{13}$.

(B_7) possess the highest positive charge, while the carbon atoms, as expected, end up with the highest negative charge. The localised molecular orbitals of 8,9-$C_2B_7H_{13}$ (see Fig. 27) result in fractional bonds at atoms B_1 and B_3 as they are involved in two CBB bonds and two BBB bonds. The B_2-B_6 bond is predicted to be a single delocalised bond while the hydrogen bridges are unsymmetrical, resulting in 0.61 electrons on B_6 and 0.41 electrons on B_7 (B_7).

The charge distribution in 1,6-$C_2B_8H_{10}$ [240,243] results in electropositive boron atoms with B_2 and B_3 atoms possessing the highest charge (+0.17, +0.14, respectively). The bonding at the five-coordinate carbon C_1 consists of a symmetric three-centre bond ($B_5-C_1-B_2$) and two equivalent orbitals ($B_4-C_1-B_5$) which have largely two-centre character with little bonding participation of the third boron, i.e. B_5 and B_2, respectively. The six-coordinate carbon atom, C_6, participates in three three-centre BCB bond orbitals (see Fig. 28).

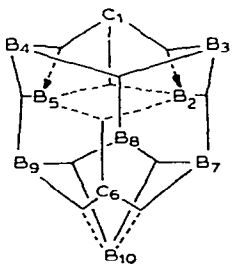

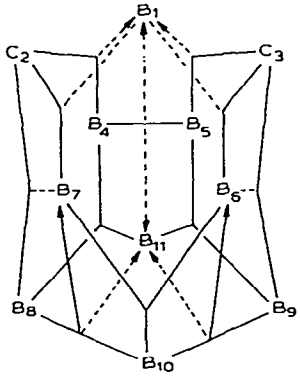

Fig. 28. The localised molecular orbitals for 1,6-$C_2B_8H_{10}$.

Fig. 29. The localised molecular orbitals for 2,3-$C_2B_9H_{11}$.

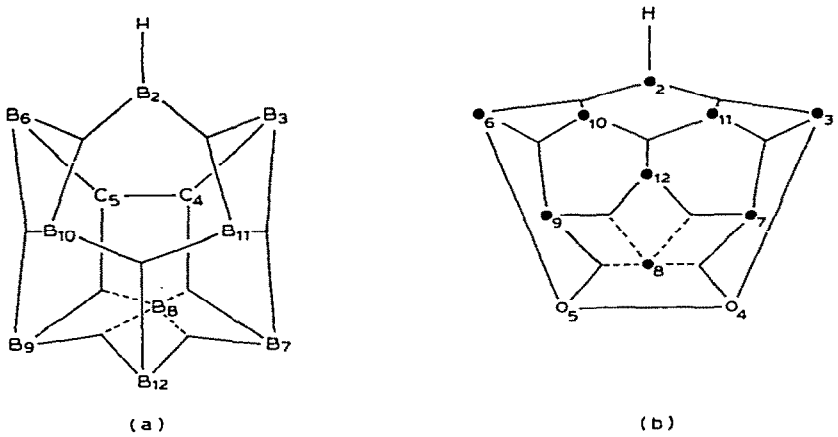

Fig. 30. The localised molecular orbitals for 4,5-$C_2B_9H_{12}^-$: (a) a three-dimensional scheme and (b) a planar projection.

The electronic structure of 2,3-$C_2B_9H_{11}$, calculated by Lipscomb and co-workers [243] results in a negative charge (−0.02) at boron atom 10. Boron atoms 1, 4 and 8 have charges +0.14, +0.08 and +0.08, respectively, while the carbon atoms possess a −0.08 charge. The LMOs presented in Fig. 29 show that B_1 is a fractional centre with four framework bonds, while B_{11} has five framework bonds.

The LMOs for $C_2B_9H_{12}^-$ (Fig. 30) are found to be similar to those calculated for the $B_{11}H_{13}^{2-}$ ion [262]. There are seven B–B–B bonds, one C–C bond, and two B–C–B bonds. Boron atom B_8 participates in two of the B–B–B bonds as well as in two B–C–B bonds and so it is designated as a fractional bonding centre.

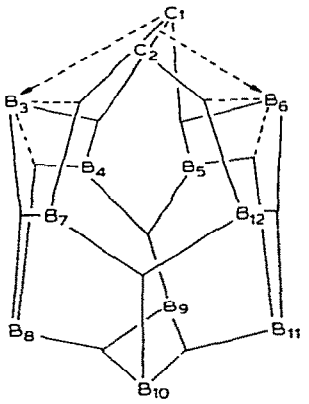

Fig. 31. The localised molecular orbitals for 1,2-$C_2B_{10}H_{12}$.

The scheme for the localised orbitals of 1,2-$C_2B_{10}H_{12}$ is presented in Fig. 31 [240,243]. There is a total of eight boron framework orbitals which are three-centre in character, a two-centre carbon–carbon bond and four B–C–B bonds. Mulliken population analysis of the SCF wavefunction [240] predicts that the B_3 (B_6) atoms have the largest positive charge.

The localisation scheme [240,243] for the 1,7-$C_2B_{10}H_{12}$ isomer yields six three-centre boron framework bonds and one two-centre boron–boron bond and this totals one less than the 1,2-$C_2B_{10}H_{12}$ isomer. The carbon atoms are involved in three B–C–B bonds, although two of these bonds are largely two-centre in character leaving B_5 and B_{12}, respectively, participating only fractionally in the bonding (see Fig. 32).

1,12-$C_2B_{10}H_{12}$ is calculated to be the most stable isomer [240,243]. The LMO structure in Fig. 33 is essentially the same as the other $C_2B_{10}H_{12}$ LMO structures. The carbons are involved in five BCB bonds and a delocalised B–C bond. There are five three-centre boron framework bonds and two B–B delocalised bonds.

2,13-$C_2B_{10}H_{13}^-$ is a carborane ion based on an icosahedron minus one vertex. Carbon 2 is placed in the uncapped ring of five heavy atoms, whilst C_{13} exists in a CH_2 group bridging boron atoms 4 and 5. The LMOs presented in Fig. 34 [262] are very close to those of $B_{11}H_{13}^{2-}$. There are eight B–B–B bonds, four B–C bonds and one B–C–B bond. The resulting structure contains no fractional bonding.

An ab initio calculation [263] of the electronic structure of $B_3C_2H_7Fe(CO)_3$ shows that the carborane portion attracts 2.03 electrons from the iron tricarbonyl species. The excess electron density on $B_3C_2H_7$ is smeared over

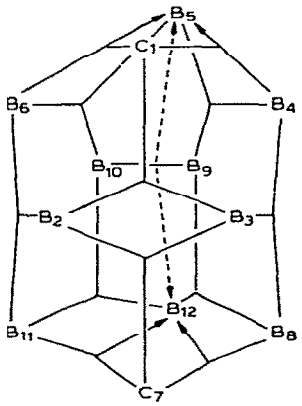

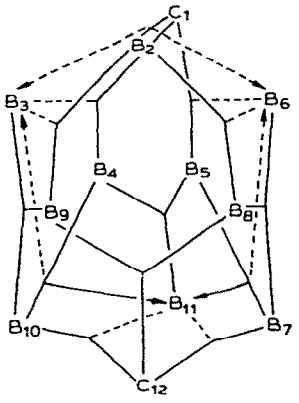

Fig. 32. The localised molecular orbitals for 1,7-$C_2B_{10}H_{12}$.

Fig. 33. The localised molecular orbitals for 1,12-$C_2B_{10}H_{12}$.

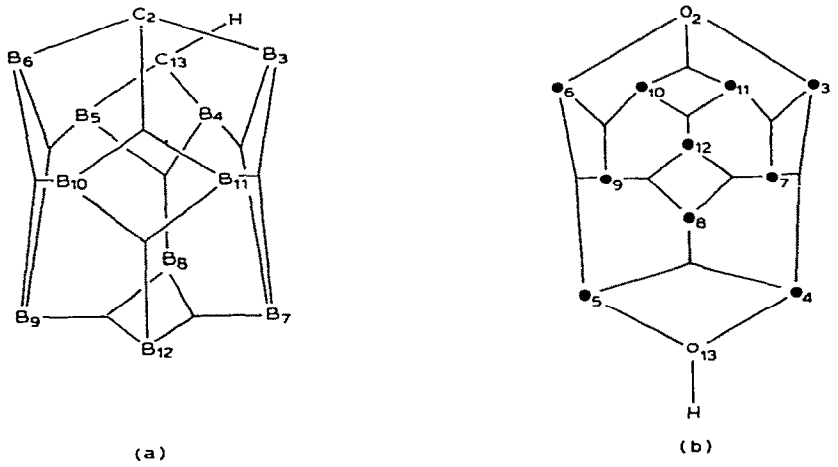

Fig. 34. The localised molecular orbitals for 2,13-$C_2B_{10}H_{13}^-$: (a) a three-dimensional structure and (b) a planar projection.

both the carbon and boron atoms and occupies both pseudo π orbitals and boron–boron σ framework bonds of the carborane. Covalent bonding between the two components is unimportant and the mode of combination is mainly ionic in character. A large energy of formation of the metalloborane with respect to the separated carborane and iron carbonyl fragments is calculated.

Bis complexes of 1,2- and 1,7-dicarbollide ligands ($C_2B_9H_{11}^{2-}$) have structural characteristics depending on the electronic configuration of the metal. For metals with a d^0–d^7 configuration, both ligands form complexes with the metal bound symmetrically to each of the two five-membered faces. However, for metals with d^8–d^{10} s^2 configurations, the dicarbollide ligands form complexes with the metal bound asymmetrically and a slipped or a *nido* structure results. Wegner [264] suggests, for metals having electronic configurations greater than d^6, that the electrons go into orbitals which are antibonding not only with respect to metal–ligand interactions but also with respect to maintaining icosahedral geometry. Hence, loss of icosahedral geometry leads ultimately to a cage-opened *nido* structure.

Glidewell has interpreted the slipped-cage structure of $Ni(C_2B_9H_{11})^{2-}$ and other structures on the basis of a second-order Jahn–Teller effect [118,265].

A later crystallographic investigation [266] suggested that the observed distortions may result from a folding of the ligand face coordinated to the metal. Further crystallographic results [267] demonstrate that the magnitude and direction of the slipped distortion depends on the substituents on the

open pentagonal face of the ligand. Extended Hückel calculations [267] rationalise the observed slipped and folded distortions. For the parent $B_{11}H_{11}^{2-}$ ligand, the overlap between the metal HOMO and the ligand LUMO is largest when the metal atom lies above the pentagonal face. This is not the case for the less symmetrical carboranes,where the ligand frontier orbitals are localised about the boron atoms. This accounts for the significant distortions. This localisation of electron density at the boron atoms also results in the strengthening of the metal–boron bonds and so distortion results.

Related molecular-orbital calculations [268,269] are reported for the icosahedral platinaboranes and carboranes, $[B_{11}H_{11}Pt(PH_3)_2]^{2-}$, $[B_{10}CH_{11}Pt(PH)_3)_2]^-$ and $B_9C_2H_{11}Pt(PH_3)_2$. The failure of the polyhedral skeletal electron-counting rules when applied to carbaplatinaboranes is attributed to the unequal bonding capabilities of the platinum $5d_{xz}$ and $5d_{yz}$ orbitals in the $Pt(PH_3)_2$ fragment. The conformations of icosahedral carbaplatinaboranes are rationalised on the basis of the symmetry characteristics of the lowest-unoccupied orbital of the carbaborane and the highest-occupied orbital of the metal–phosphine moiety.

Extended Hückel molecular-orbital calculations [270] on $[Cu(B_{11}H_{11})_2]^-$ and related carbaborane complexes have indicated that the electronic configuration of the metal and the substituents in the borane cage influence the extent of the slip distortion. The calculated atomic charges for the unslipped and slipped $Cu(B_{11}H_{11})_2^{3-}$ complex indicate a build-up of electron density at those boron atoms which lie farthest from the metal atom, i.e. (1, 2) and loss of electron density at the other positions (i.e. 3, 4 and 5). Electronegative substituents at 1, 2 position will encourage, and substituents at 3, 4 and 5 positions will discourage, the 'slip' distortion.

Structural studies on metallocarboranes derived from $7,8\text{-}C_2B_9H_{11}^{2-}$ allowed Wallbridge and coworkers [271] to demonstrate progressive opening of the carbaborane cage with increasing electron density on the metal. They invoke Wade's suggestion [272] that, in addition to the skeletal electron pairs of a polyhedral framework ($n + 1$ pairs for a *closo* system), up to 3 electron pairs may be accommodated in the 'non-bonding' d orbitals of the transition metal. This implies that $(n + 2)$, $(n + 3)$ and $(n + 4)$ skeletal electron pairs can be associated with the presence of d^8, d^{10} and $d^{10}s^2$ ions leading to a progressive opening of the metallocarborane cage.

The SCCC MO method has been used [273] to examine the electronic structure of $(C_5H_5FeC_2B_9H_{11})^-$ and its carbon analogue ferrocene. The predominant interactions between the iron atom and the dicarbollide dianion involve σ orbitals on the dicarbollide species, whereas the predominant interactions between the iron atom and the cyclopentadienide anion involve π orbitals of the latter. On complexing of the dicarbollide dianion, there is a

net loss of 1.037 electrons involving a reduction of electron density on all three sites, the ring open base, the closed face and the apex, with the greatest proportional change occurring on the open face. In contrast, the cyclopentadienide anion loses only 0.164 electrons, which comprise a σ electron gain and a greater π electron loss. The calculations support the qualitative view [274] that a transition metal could bond to the open rear pentagonal face of a carborane in a similar way to the bonding of the metal to a cyclopentadienyl ring, inasmuch as the σ orbitals of the dicarbollide are of the same symmetry type as the π orbitals of the Cp^- ring.

The aforementioned polyhedral skeletal electron-pair theory has recently rationalised the geometries of the carboranes and the metallocarboranes [271,275]. The skeletal structures of the carboranes are related to the number of skeletal bonding electron-pairs they contain. Species with n skeletal atoms adopt *closo*-structures if they are held together by $n+2$ pairs and *arachno* structures if held together by $n+3$ pairs of skeletal bonding electrons. Each B–H and C–H unit in a carborane is said to provide 2 and 3 skeletal electrons, respectively, while further electrons are obtained from the extra hydrogens and the anionic charge.

The axially symmetric metal carbonyl fragments $M(CO)_n$ (where $n = 1, 3, 4$) have three outpointing hybrid orbitals which are suitable for forming cluster skeletal molecular orbitals [275–278]. These fragments possess $(6-n)$ nonbonding molecular orbitals and so the frontier orbitals of the $M(CO)_n$ fragment are occupied by $(x-2-(6-n))$ skeletal electrons, where x is the number of valence electrons of M. Hence, the moieties B–H and $Fe(CO)_3$ both possess two skeletal electrons and are structurally interchangeable.

King and Rouvray [279] have analysed the bonding topology in the carboranes in an analogous fashion to that in a delocalised two-dimensional polygonal system by algebraic graph-theoretical methods. The close relationship between delocalisation in the three-dimensional polyhedral systems with n vertices and $2n+2$ skeletal electrons and the delocalisation in two-dimensional polygonal systems with $4k+2$ π electrons is outlined.

Nishimura [280] proposes that *closo*-metallaheteroboranes which appear to have fewer than $(n+1)$ skeletal electron pairs to hold their n skeletal atoms together may have incompletely filled metal *d*-orbitals or hyperpolyhedral metal–metal bonding. He describes the first example of hyperpolyhedral metal–metal bonding in metalloborane chemistry, $[(\eta\text{-}C_5H_5)_2Fe_2B_6H_8]$.

(ii) Organoaluminium compounds

The ability of trimethylaluminium to dimerise led originally to suggestions of three-centre bonding across the Al–C–Al bridge which has been shown to exist in this material [281]. This would involve an already formally 4-valent

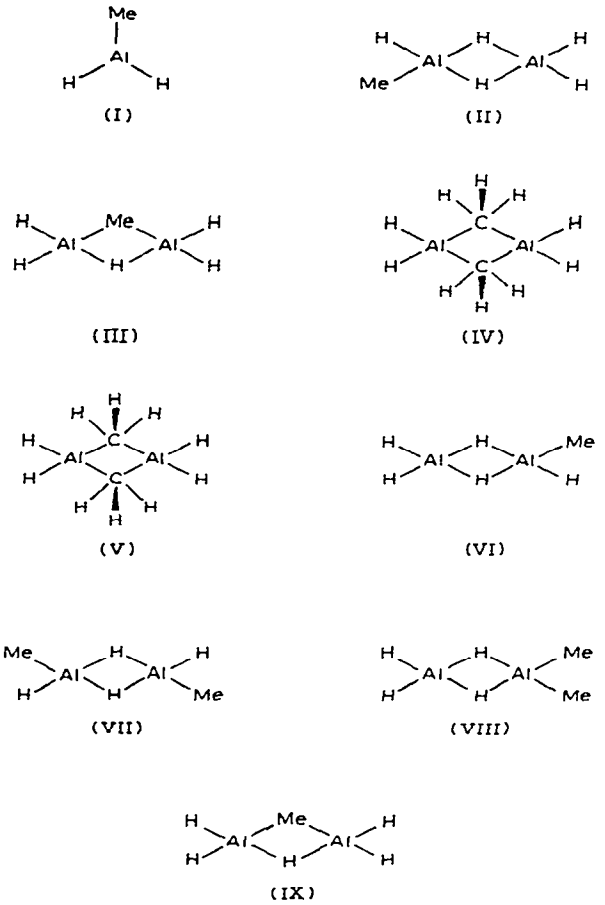

Fig. 35. Organoaluminium hydride isomers.

carbon atom. This is plausible but leaves unexplained the fact that this type of bonding does not occur in the corresponding boron compound. This is all the more puzzling when one remembers that boron forms numerous hydrides which bond by an analogous type of mechanism. This problem, together with an analysis of the type of bridging likely, in general, in methylaluminium and methylboron hydrides, was first systematically tackled theoretically by Levison and Perkins in 1970 [160], using a CNDO-based method. Since one of the differences between boron and aluminium is that the latter possesses empty 3*d* orbitals which are likely to exert an important effect on the bonding, the participation of these was examined in some detail. Because of the relatively low computing power available at that time, it was necessary to restrict the size of the orbital basis set as far as possible in the calculations; thus only one methyl group per aluminium atom could be considered. The remainder of the substituents were hydrogen atoms. Thus,

the series of systems included various isomers of $Al_2Me_2H_4$ and Al_2MeH_5 (Fig. 35).

Perhaps the first important point about such dimeric compounds is whether the bridging moieties are more likely to be methyl groups or hydrogen atoms. Two associated features are (i) what positions the methyl groups would occupy if terminal, (ii) whether the methyl hydrogen atoms are staggered or eclipsed with respect to each other when the methyl group acts as a bridge.

Calculations including the 3*d* orbitals showed that if methyl groups occupy terminal positions, the favoured conformation of the molecules is that in which they lie mutually *trans*. Curiously enough, the *gem*-dimethyl compound (VI) is more stable electronically than VII (i.e. the sum of its bonding and electronic repulsion energies is greater) but here the nuclear repulsion factor dominates and, hence, the total energy of the latter isomer is greater. If all the hydrogen atoms were replaced by chlorine (which has a large core charge), then the *gem*-dimethyl compound might well be the more stable of the two and, indeed, evidence for the formulation of $Al_2Me_2Cl_4$ as $Me_2Al^+AlCl_4^-$ has been adduced [281].

In models IV and V, when the methyl group is acting as a bridge (as it must in Al_2Me_6), the electronic and nuclear energies are mutually compensating so that similar total energies result for the staggered and eclipsed isomers. Thus, the bridge geometry is not unequivocally established and the equilibrium between the two forms may well be labile.

Finally, the relative efficacies of the methyl group and the hydrogen atom as bridging units may be compared. Calculations on Models IV, V and VII lead to the conclusion that a hydrogen-bridged dimer should be more stable. It is interesting that the methyl-bridged isomer is electronically more stable but the juxtaposition of a methyl group to two aluminium atoms and a second methyl across a small ring increases the nuclear energy drastically and precludes this type of bridging if there is an alternative. This result may be extrapolated to the known trimer $Al_3Me_3H_6$ which appears to have a ring structure and in which, it is believed, hydrogen bridging exists [282]. Again, the nuclear energy must be a greater destabilising force which cannot be adequately compensated when the methyl group is inserted between two aluminium atoms.

In the series $Al_2Me_{6-n}Cl_n$, the members in which n is odd are unknown. This has been explained [281] on the basis of disproportionation to the compound with n even and which contains the stable Me_2Al^+ unit. In the case of Al_2MeH_5, the products of disproportionation would be $Al_2Me_2H_4$ and Al_2H_6

$$2\,Al_2MeH_5 \rightarrow Al_2Me_2H_4 + Al_2H_6$$

In this case also, the total energies support Glick and Zwickel's [281] disproportionation argument.

It is important to assess to what extent the $3d$ orbitals actually contribute to the molecular energy and this can be accomplished by comparing the energies of the isomers, calculated with or without inclusion of the d-functions. It turns out that, firstly, participation of d orbitals in the dimer (VII) lowers the total energy of the system by 4–6 times the comparable stabilisation energy of the monomer (I). It seems that the cross-ring Al–Al bonding, not possible in the monomer, is an important stabilising factor. This is not surprising in view of the short Al–Al distance (0.04 Å greater than the covalent diameter of aluminium). Such Al–Al bonding was first suggested by Lewis and Rundle [283].

Another point of interest here is that the effective electronic environment of the aluminium atom has a marked effect on the lowering of energy by the d orbitals. This means that d-orbital participation should be particularly strong when the aluminium atom is surrounded by electronegative ligands and so will affect the bonding much more in such cases.

When methyl groups form the bridge (as must be the case in Al_2Me_6) there is a strong drift of electrons to the aluminium atoms. Al–Al cross-ring bonding exists and its most important contributors are the p orbitals. The d orbitals do participate and it appears that $3d_\delta 3d_\delta$ bonding is a factor which helps to account for the stability of this type of organoaluminium compound. The role which the d orbitals play in the bridge ring is mainly confined to the metal–metal bond and is barely concerned with the bridging itself. This is consistent with chemical experience, because B_2H_6 is stable yet the $3d$ orbitals would be expected to be of negligible importance here.

The original suggestion [282] that methyl bridge bonding can be described by overlap between an 'sp^3' hybrid of carbon and another hybrid of aluminium is inappropriate because only the $2s$ and two $2p$ orbitals on carbon (in the ring plane) take part in the bridge bonding: the other $2p$ orbital bonds only to the terminal hydrogen atoms (on carbon).

It is found for Al_2Me_6 [284] that the dimeric species is stabilised by the d orbitals more than twice as much as is the monomer $AlMe_3$. This suggests that, despite the greater distance apart of the aluminium atoms, there is a degree of Al–Al bonding when methyl rather than hydrogen acts as the bridging group. However, participation of the aluminium $3d$ orbitals in the bridging bond, though not negligible, is much weaker than that of the aluminium $3s$ and $3p$ basis sets. Hence, it seems that the $3d$ orbitals of aluminium influence the dimerisation of some compounds of the element by their contribution to a metal–metal bond rather than by bringing about any unique modification of the electronic stucture of the bonds.

The electronic structure of $(CH_3)_3Al$ has also been studied by Ohkubo et

al. [110]. They propose that the weak π bond nature of the Al–C bond is responsible for the instability of the monomeric state and that this rationalises the dimerisation. Cowley and White [8] reject this as an explanation for the dimeric $(CH_3)_6Al_2$ on the grounds that $(CH_3)_3B$ also has a low π energy but does not dimerise. The latter authors also cite the Al–Al bonding interaction as a substantial contributor to the stability of the dimer. Such metal–metal interactions are found also in the coordination compound $[(CH_3)_2NAlH_2]_3$ and this is said to be responsible for stabilising the preferred conformation [285]. The photoelectron spectrum [286,287] of $(CH_3)_6Al_2$ shows a symmetric first band at 9.76 eV corresponding to an ionisation from a single orbital which has an appreciable contribution from the $3p$ levels of the aluminium. The spectrum of the substituted halogen derivatives has been recorded and interpreted. For $(CH_3)_4Al_2Cl_2$ and $(CH_3)_4Al_2Br_2$, the highest filled orbitals lie at 10.25 eV and 9.9 eV, respectively. The nature of the bonding in both molecules is the same as that in $(CH_3)_6Al_2$, the increase in stabilisation being due to the inductive effect of the halogen atom. The lone pair on the halogen is responsible for the first band in $(CH_3)_2AlI$ and for the monomethyl species CH_3AlCl_2, CH_3AlBr_2 and CH_3AlI_2.

Lappert et al. [288] have performed a series of ab initio calculations on Me_2AlCl and its dimer $(Me_2AlCl)_2$. They find that the energy of dimerisation is 19 kcal mole^{-1}. (The corresponding value for $AlCl_3$ is 8 kcal mole^{-1}.) The population analysis of Me_2AlCl gives the following charge pattern: Al (+1.59), Cl (−0.67), C (−0.94) and H (+0.16). The charge on the chlorine atom arises from the large σ-electron drift from the aluminium, coupled with a small π electron back-donation to the central atom. The methyl group carries an overall negative charge (−0.46) and this stems from a σ-electron donation from the aluminium. The hyperconjugation of the methyl group with the formally vacant aluminium $3p\pi$ orbital is small and amounts to 0.015 electrons per methyl group donated to the aluminium $3p\pi$ orbital. The charge distribution of the dimer $(Me_2AlCl)_2$ is Al (+1.70), Cl (−0.98) and H (+0.16). Dimerisation increases the electron drift away from the aluminium to both the chlorine atom and the methyl group. A weak antibonding Al–Al interaction is present in the dimer.

Analysis of the valence molecular orbitals of Me_2AlCl shows that the first ionisation potential corresponds to an ionisation from an Al–C σ-bonding orbital. While two of the orbitals contributing to the second band are predominantly chlorine $3p\sigma$, the third orbital is an Al–C bonding orbital. The next five orbitals contribute to the third and all contain significant C $2p$ and H $1s$ character describing the bonding in the methyl groups. The two lowest-energy orbitals of this group of five also contain a significant Al–Cl bonding contribution.

Structural models have been proposed for the mixed methylcyclopropylaluminium compounds [289] on the basis of their NMR spectra and the known structure of tricyclopropylaluminium dimer. Of special interest is the molecule $Al_2(CH_3)_4(cycloC_3H_5)_2$ where there is averaging of the non-equivalent terminal methyl groups. It is proposed that rotation of the bridging cyclopropyl groups will lead to the magnetic equivalence of the terminal methyl groups. CNDO calculations were used to determine the minimum energy conformation. The most stable conformer has the bridging cyclopropyl groups in an *anti* rather than a *syn* conformation. The activation energy for rotation of the cyclopropyl groups is about 11 kcal mole^{-1}.

An important characteristic feature of the chemistry of trimethylaluminium is its Lewis acidity. This has been examined in the CNDO study [290] of the complex $(CH_3)_3Al\cdot N(CH_3)_3$. The calculated binding energy of this complex is -125 kcal mole^{-1}. This agrees poorly with the observed enthalpy of formation of $(CH_3)_3Al\cdot N(CH_3)_3$ (-31 kcal mole^{-1}). The inclusion of 3*d* orbitals on aluminium has a powerful effect on the electron distribution and drastically reduces the positive charge on the aluminium. For example, the charge on aluminium in $AlCl_3$ is zero, while in $(CH_3)_6Al_2$ it is $+0.21$; if 3*d* orbitals are neglected, the corresponding charges are $+0.92$ and $+0.63$.

The following general observations can, nevertheless, be made regarding the electron distribution in such complexes. Firstly, the amount of charge transferred overall from donor to acceptor increases if methyl groups on the acceptor are substituted by more electronegative groups or atoms. Moreover, the acceptor atom remains positively charged or neutral in the complex and the net negative charge is carried by the substituents. The N atom in the donor is either neutral or carries a small negative charge in the complex, whilst the net positive charge on the donor is carried by the methyl groups. The calculated equilibrium Al–N bond lengths of the complex are in excellent agreement with experiment. The calculated barrier to rotation about the Al–N is 5.0 kcal mole^{-1} for $Me_3Al\cdot NMe_3$ and a staggered conformation is predicted.

The complexes of $(CH_3)_3Al$ with amines, NH_3, CH_3NH_2, $C_2H_5NH_2$, $(CH_3)_2NH$ and $(CH_3)_3N$ have been studied by Ratajczak and co-workers [20]. The amount of charge transferred to the $(CH_3)_3Al$ increases from 0.30 for NH_3 to 0.37 for $(CH_3)_3N$, while the calculated Al–N coordination bond length decreases upon methyl substitution. The energy of coordination increases with increasing methyl groups from NH_3 (93.5 kcal mole^{-1}) to Me_3N (125.5 kcal mole^{-1}). The reaction of trimethylaminoalane with benzene has been investigated by CNDO calculations [290,291].

A simple molecular-orbital treatment has been used to discuss the donor–acceptor complexes of $Mo(phen)(P(C_6H_5)_3)_2(CO)_2$ with Lewis acids such as

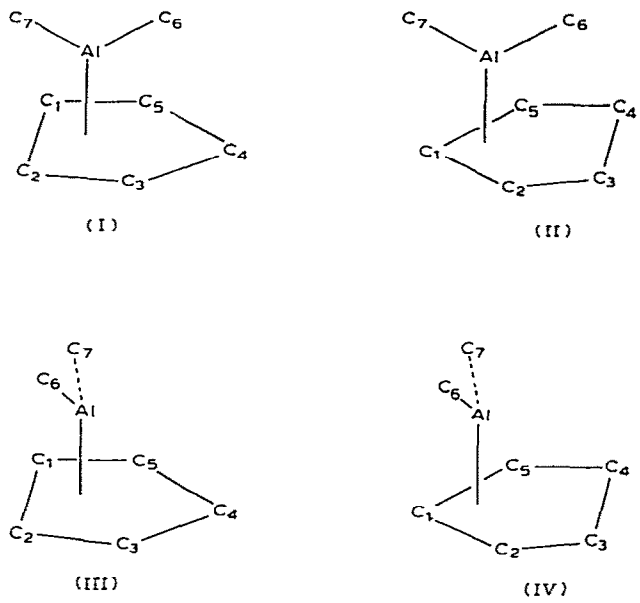

Fig. 36. The structures of dimethylcyclopentadienylaluminium.

$(C_2H_5)_3Al$, $(i\text{-}C_4H_9)_3Al$ and $(CH_3)_3Ga$ [293]. The Lewis acids add to the oxygen of a carbonyl group, lowering the energy of the π orbital of the $Mo(CO)_2$ moiety by increasing the Mo–carbonyl back-bonding.

The structure of dimethylcyclopentadienylaluminium, Me_2AlCp, has been determined by electron diffraction [293]. Models containing σ-bonding and symmetrically π-bonded rings are ruled out. Four models containing asymmetrically π-bonded rings have been considered (Fig. 36) and their energies obtained by a CNDO method [293]. The calculations indicate that model I is the most stable configuration. The barrier to internal rotation of the C_5H_5 ring is of the order of 5 kcal $mole^{-1}$ whilst the barrier to the exchange of the methyl groups is 10–20 kcal $mole^{-1}$. The asymmetric nature of $(CH_3)_2AlCp$ is supposed to arise because the Cp ring only needs to function as a three-electron ligand in order that the Al atom be associated with an octet of electrons.

Ab initio calculations [294] have been performed on the related H_2AlCp compound using Models I, II and III. Model I is found to be more stable than both Model II (by 2.36 kcal $mole^{-1}$) and Model III (by 11.83 kcal $mole^{-1}$). The total overlap population of Model I indicates substantial bonding between Al and $C_{1(2)}$, negligible bonding between Al and $C_{3(5)}$, and a net antibonding effect between Al and C_4. The overall bonding between Al and the ring seems to stem from the interaction of both the a_1 π orbital with

the 3*s* orbital of Al and the e_{1x} π orbital with the $3p_x$ orbital of the Al. The interaction between the e_{1y} π orbital and the atomic orbitals on the Al results in bonding between Al and $C_{1(2)}$, but antibonding between Al and the C_3, C_4 and C_5 atoms of Cp. It is thought reasonable to assume that this antibonding character originates from the non-availability of Al $3p_y$ (which is involved in the Al–H bonding). The resulting repulsion between Al and the $C_{3(5)}$ and C_4 atoms is responsible for the asymmetric structure of the π complex. Analysis of the electron distribution reveals that there is a transfer of 0.53 electrons from Al to the Cp ring in the *a'* molecular orbitals and a back donation of 0.194 electrons into the Al $3p_x$ orbital, together with a smaller transfer into the Al $3d_{xy}$ and $3d_{xz}$ orbitals. The charge on aluminium is +0.619, while both the hydrogens bonded to aluminium and the cyclopentadienyl ring carry a negative charge (the latter amounts to −0.377).

The bonding in organoaluminium compounds [295–297] has also been studied by ^{27}Al nuclear quadrupole spectroscopy and interpreted by the simple treatment of Townes and Dailey [298].

Kasai and McLeod [299] have investigated via the ESR technique the interaction of the aluminium atom with ethylene in a rare-gas matrix. The complex is formed through the dative bonds resulting from the interaction of the π orbitals of the olefin and the valence orbitals of the aluminium atom. The spin densities in the 3*s* and 3*p* Al orbitals in the complex are determined to be 0.015 and 0.70, respectively. The extremely small *s* character and the dominance of the *p* character of the semi-filled orbital are compatible with an '*sp* orbital hybridisation' on Al and the formation of two dative bonds, one resulting from migrations of electrons from the bonding π orbital of the olefin into the vacant *sp* orbital of Al and the other resulting from back donation into the vacant antibonding π orbital of ethylene from the semi-filled *p* orbitals of the aluminium atom. The corresponding aluminium–acetylene complex [300] is found, surprisingly, to have a vinyl structure. This is confirmed by INDO and EHT calculations, where the angle C_1-C_2-H is calculated to be 150° (C_2 is the nonsubstituted carbon atom).

Schaeffer and co-workers [301] have subjected the aluminium–acetylene system to their usual thorough analysis via a double-zeta SCF and CI calculational procedure. They find that there is no interaction with the π systems in either $Al-C_2H_2$ or $Al-C_2H_4$. The optimised geometries of three structures of the σ-bonded system were obtained, i.e. a vinylidene complex and *cis* and *trans* isomers of vinylaluminium. The vinylidene complex has a binding energy of 21.5 kcal mole^{-1}, whilst the corresponding values for the *cis* and *trans* isomers are 8.0 kcal mole^{-1} and 8.2 kcal mole^{-1}, respectively. Although these stabilities are in conflict with the ESR spectrum, the 1,2-hydrogen shift necessary to produce the vinylidene structure may not occur at room temperature, as the barrier height is estimated to be ca. 8 kcal

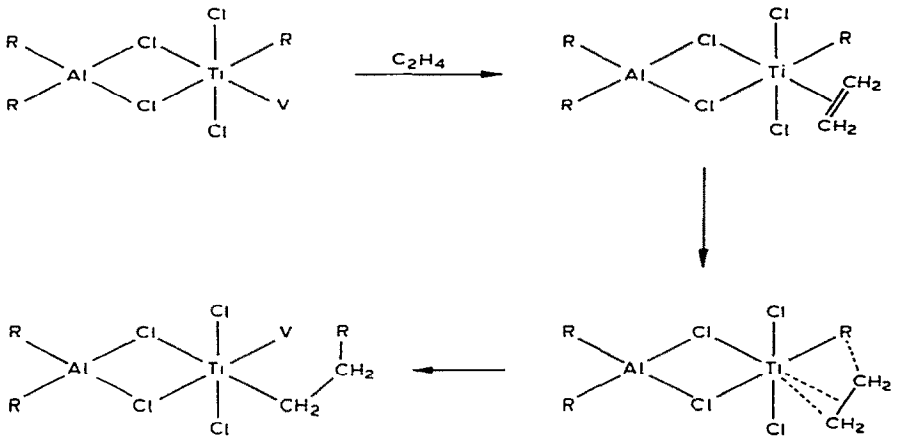

Fig. 37. The mechanism for Ziegler–Natta catalysis.

mole^{-1}. Schaeffer points out a fascinating feature which emerges from this study: while the isolated acetylene–vinylidene reaction is endothermic by 40 kcal mole^{-1}, the same process becomes exothermic in the presence of an aluminium atom. The relevance to catalysis is obvious.

The interactions of aromatic compounds with Al^{3+} have been studied by EHT calculations [302]. The degree of charge transfer is linearly related to the ionisation potential of the benzene compound.

The important discovery [303,304] of a catalyst system for the low-temperature polymerisation of olefins has led to a vast amount of experimental work. There have also been a small number of theoretical investigations [305–309] into the reaction mechanism of the catalytic process. The most favoured mechanism is due to Cossee [305], who envisaged that a titanium compound is first alkylated by an alkylaluminium derivative. With ethylene as the monomer, the sequence of steps for the homogeneous catalytic reaction is shown in Fig. 37.

The formation of a vacant site (V) in the octahedral coordination sphere of the titanium atom, the initial coordination of an ethylene molecule and the migration of the alkyl group R are the principal features of this mechanism. The electronic structure of a titanium–aluminium–ethylene complex has been studied as well as the sequence of steps in which the ethylene inserts into a titanium–methyl bond [306–309]. Armstrong et al. [306] discuss the role of the $\rightrightarrows AlR_2$ group in the complex and catalytic cycle. They find that the orbitals of the aluminium atom on the terminal group do not exercise any first-order effect on the important energy levels of the species involved in the process. However, it is of critical importance that the

symmetry of the titanium site be such that the titanium–alkyl bond can be localised in a labile molecular orbital which has considerable *d* character. Although a range of symmetries was not investigated, it seems that a trigonal bipyramidal or an octahedral site symmetry may best achieve this result. This suggests that the most important role fulfilled by the $\rightleftharpoons AlR_2$ group is to partake in bridge bonding with the titanium, thus compelling it to adopt a high coordination number.

Novaro and co-workers [308,309] have investigated the reaction pathway by an ab initio technique. Variation of the total energy along the reaction coordinate yields (1) an initial shallow minimum for the coordination of the ethylene, (2) an activation barrier of 15 kcal $mole^{-1}$ corresponding to the breaking of the π bond of ethylene and (3) an energy stabilisation for the production of the propyl chain. In this study the aluminium not only interacts with the methyl bonded to titanium but also interacts with the ethylene carbons at certain stages of the reaction.

A related study [310] has been performed on the complexes of alcohols with $EtAlCl_2$ which play an important role in the termination of growing chains formed in the cationic polymerisation of olefins. The nature of the active centres of the investigated system was elucidated by quantum chemical calculations on potentially active electrophilic catalytic centres.

A concerted four-centre thermal reaction classifiable as a (2 + 2) reaction is forbidden in the Woodward and Hoffmann sense [311]. When a metal atom partakes in this type of reaction, the orbital-symmetry rules are somewhat relaxed. The concept of triplet instability for Hartree–Fock molecular orbitals [312,313] has been applied to thermal (2 + 2) reactions of organometallic compounds in order to examine the extent of the feeble forbiddenness of the reactions [314]. The reactions considered are the insertion of an olefin into an aluminium–hydrogen bond and the epoxide cleavage catalysed by aluminium trihydride. The four-centre transition state shows the aluminium and one hydrogen of AlH_3 coordinated to the carbon atoms of the ethylene. For the olefin insertion reaction, there exist favourable reaction paths with no biradical character, although for certain values of the aluminium–carbon and hydrogen–carbon distances, there will be biradical character in the reaction intermediate. The insertion reaction is considered to consist of two elementary processes; the first is the formation of a π complex through the vacant p_π orbital of aluminium, whilst the second is the rearrangement of the π complex to a σ complex by the migration of the hydride anion to the β carbon. The bond indices and atomic charges bear out this description.

The cleavage of uncomplexed ethylene oxide is investigated theoretically by increasing the C–C–O angle. When this angle reaches 79°, triplet instability occurs as a result of the crossing between HOMO and LUMO:

hence, the ring-opened form should assume biradical character. The ethylene oxide–alane complex is assumed to have a four-centre transition state where the aluminium and the hydrogen of the AlH_3 are coordinated to the oxygen and the carbon atom, respectively, of the ethylene oxide. Variation of the geometry of the reacting system by altering both the coordination distances and the Al–C–O angle, failed to give triplet instability. Hence, in the catalysed cleavage of ethylene oxide there is an absence of biradical character.

(iii) Organogallium, organoindium and organothallium compounds

There have been no important calculations on organogallium or organoindium compounds and only one significant calculation on an organothallium compound.

Van Wazer and co-workers [315] have calculated the valence electronic structure of cyclopentadienylthallium (I). They used a pseudopotential approach to take into account the core orbitals of thallium and carbon. The fourteen filled valence molecular orbitals have orbital energies ranging from -1.12 to -0.14 au, with the orbital energy of the 14th orbital at an unusually high value. Thallium orbitals contribute significantly only to the four least-stable filled MO's of C_5H_5Tl, while the thirteen most stable orbitals are related to the corresponding orbitals of $C_5H_5^-$. The charge pattern of C_5H_5Tl is Tl (+0.101), C (−0.246) and H (+0.227). There is very little electron transfer between neutral thallium and the C_5H_5 ring, although the hydrogen-to-carbon polarisation is high. However, the overlap population between thallium and the cyclopentadienyl ring is quite high (0.474). This stems from the $3e_1$ orbital, which is based on thallium hydridisation of the form $\frac{1}{2}(p_x + 2d_{xz}) + \frac{1}{2}(p_y + 2d_{yz})$. This allows the thallium atom preferentially to direct its valence charge towards the C_5H_5 ring and form a stable π compound with only a single cyclopentadienyl moiety. Hence, it is not surprising that the electron distribution within the valence orbitals of thallium is $s^{1.75}p^{0.45}d^{0.71}$.

E. PERIODIC GROUP IV

(i) Organosilicon compounds

The electronic structure of CH_3SiH_3 has been calculated by ab initio techniques [316–326]. Veillard [316] concentrated on determining the barrier to rotation which he predicted to be 1.44 kcal mole^{-1}, in good agreement with the experimental value, 1.7 kcal mole^{-1} [317]. The dependence of the CH_3SiH_3 barrier to internal rotation of vibrational coordinates has been

examined [318]. It is estimated that the pure harmonic terms arising from just the A_1 vibrations contribute about 155 cal mole^{-1} and it is quite possible that the total correction could be three or four times larger.

Liskow and Schaeffer [319] list the orbital energies, calculated second moments, third moments, potentials, diamagnetic shielding force at the nuclei, and the electronic field gradient. They calculate a value of 0.58 D, in the direction $+\mathrm{CSi}-$, for the electric dipole moment. This is in good agreement with the experimental value of 0.73 D [320] and confirms the orientation assigned from molecular Zeeman-effect measurements [321]. Liskow and Schaeffer argue that the sign of the dipole is not consistent with the atomic charges obtained from the wavefunction, as this results in the carbon atom possessing a -0.607 charge while silicon bears a $+0.862$ charge. Bellama et al. [322], however, show that the orientation of the molecular dipole is actually determined by the M–H bond moments and, in particular, by the magnitude and orientation of the Si–H bond moment. The Si–H $+-$ bond moments will, therefore, oppose and dominate the Si–C $+-$ bond moment and so the overall direction is CH_3SiH_3 $+-$.

Blustin has performed an FSGO calculation [323] on CH_3SiH_3. The calculated geometry, dipole moment and rotational energy are in satisfactory agreement with experimental values. The calculated heats of reaction for

$$SiH_6 + CH_4 \rightarrow CH_3SiH_3 + SiH_4$$

and

$$C_2H_6 + SiH_4 \rightarrow CH_3SiH_3 + CH_4$$

are 18 kJ mole^{-1} and 30 kJ mole^{-1}, respectively. The calculated heat of formation is $+54$ kJ mole^{-1}, which shows some discrepancy with the recent experimental estimate of -17 kJ mole^{-1} [324].

CH_3SiH_3 and its Si $1s^*$, $2s^*$ and $2p^*$ core hole states and the double $2s^{**}$ core hole states have been calculated by a UHF calculation [325]. The results are used to discuss shifts in KL_1L_1 Auger energies in terms of hole state calculations, orbital energies and the equivalent core method. Shifts in the core electron binding energies have also been calculated and indicate that experimental shifts are overestimated.

The geometry and the binding energy of CH_3SiH_3 have been obtained from STO-3G and STO-3G* (addition of a d Gaussian orbital to the second-row atom) basis sets [326]. All the bond lengths, except for the Si–H bond length, and all angles are reproduced well for both basis sets. The binding energy is 657 kcal mole^{-1} for the STO-3G basis and 691 kcal mole^{-1} for the STO-3G* basis set.

There have been two pseudo-potential calculations [327,328] on CH_3SiH_3 and both concentrate on the rotational barrier. Ewig and Van Wazer [327]

obtain 1.22 kcal mole^{-1}, while the calculation of Nicolas et al. [328] yields 1.40 kcal mole^{-1}. The latter group assert that the HOMO is of *e* symmetry while Liskow and Schaeffer [319] report a_1 symmetry for the frontier orbital. A CNDO study of the rotational barrier and dipole moment of CH_3SiH_3 has also been published [329].

The molecular equilibrium geometry of $(CH_3)_3SiH$ [330] and $(CH_3)_2SiH_2$ [331] have been determined by a CNDO calculational procedure. The former has a calculated minimum energy in the LEM configuration, in which each methyl group is staggered with respect to the two opposite Si–C bonds. The barrier to rotation about the Si–C bond for a methyl group is calculated to be 2.8 kcal mole^{-1}. The most stable configuration of dimethyl silane occurs when one hydrogen of each methyl group lies in the Si–C–C plane but pointing outside the C–Si–C angle. A partitioning of the total energy of $(CH_3)_2SiH_2$ reveals that the variation in the total energy is governed by the term describing the spatial interactions between silicon and the six methyl hydrogens. This long-range Si---H interaction is also present in CH_3SiF_3 [332]. The most stable configuration is the staggered arrangement with a barrier to rotation calculated to be 2.2 kcal mole^{-1}, in reasonable agreement with the experimental value 0.93 kcal mole^{-1} [333].

The photoelectron spectra of methyl-substituted silanes have been reported and the bonding in these molecules has been described [334–338]. In particular, the vexed question of silicon *d*-orbital participation has been critically examined; the conclusion is that for this series of molecules, *d*-orbital bonding is not substantial. The photoelectron spectra of $S(Si(CH_3)_3)_2$ and $CH_3SSi(CH_3)_3$ have been assigned [339] on the basis of the 'semi-localised orbitals' approximation and from a consideration of symmetry and substituent effects.

Carbon–silicon nuclear spin-coupling constants of alkyl silanes have been calculated [340] using a finite perturbation procedure within the INDO scheme. Linear relationships are obtained between ^1J(Si–C) and the charge-density parameters reflecting (i) the electron deficiency of the C–Si moiety and (ii) the polarisation of the carbon–silicon bond in the sense (Si^+-C^-).

MINDO/3 calculations have been reported for the methylsilanes [341]. The calculated heat of formation is −11.28, −29.8, −44.5 and −55.5 kcal mole^{-1} for the mono-, di-, tri- and tetra-methylsilane, respectively. The first ionisation potential decreases upon methyl substitution from 11.28 eV for $MeSiH_3$ to 10.49 eV for Me_4Si. The optimised geometries of the methylsilanes are also reported.

A semi-empirical method for calculating the diamagnetic susceptibilities of organo-silicon compounds containing carbon–silicon bonds has been developed by Gupta [342]. Susceptibilities are considered to be contributed by the atoms, bonds and bond–bond interactions. Diamagnetic susceptibili-

ties have been calculated for alkylsilanes and agree to within 0.75% of the experimental values.

The electronic structure of some alkylsilanes is obtained [343,344] by application of the maximum overlap approximation. The calculated *s* character in the appropriate hybrid orbitals predicts the bond angles and J(C–Si) and J(Si–H) coupling constants with a good accuracy.

Two research groups [345,346] have invoked the parameter method of Del Re [347] to calculate the charge distribution and dipole moments of the alkylsilanes. The mass spectra of the methylsilanes were calculated using the quasi-equilibrium theory of mass spectra [348].

An investigation [349] of the *sp* and *pd* contributions to the dipole moments of some methylsilyl fluorides $MeSiH_{3-x}F_x$ (where $x = 0–3$) indicated the importance of the *pd* contribution to the increase in dipole moment as x increased. A related study [350] examined by CNDO the stable conformations of the methylsilyl fluorides $MeSiH_{3-x}F_x$ (where $x = 0–3$) as well as vinylsilane and phenylsilane. The calculated configurations gave good agreement with experiment and the equilibrium geometry of the latter two molecules is stabilised by p–$d\pi$ interactions.

The photoelectron spectra of Me_nSiCl_{4-n} ($n = 1,2,3$) [351] and Me_3SiX (X = Br,Cl) [352] have been published and assigned. The first group does not require silicon 3*d* orbital participation to explain the spectra in which the linear decrease in energy of the SiC and SiCl σ MOs across the series Me_nSiCl_{4-n} is predicted on the basis of inductive effects of Me and Cl groups. The second group suggests that the halogen lone pairs in Me_3SiX participate in the bonding via interaction with those orbitals of the $SiMe_3$ moiety which have the same symmetry. Participation of the lone pairs in bonding may occur via the 3*d* orbitals of silicon. This latter suggestion cannot be entirely excluded, since CNDO calculations with inclusion of 3*d* orbitals give a slightly better agreement with experiment.

Some of the features of the L_{II-III} X-ray absorption spectra of the methylchlorosilanes are explained by CNDO calculations [353]. The low-lying 3*d* levels must be taken into account in the calculation and in the interpretation of the spectra.

Paramagnetic screening constants in Me_nSiX_{4-n} (X = F,OMe, NMe_2Cl for $n = 0–4$) were evaluated [354,355] by the CNDO method with and without the ΔE approximation and the results compared with the experimental ^{29}Si values. The averaged excitation energies obtained from comparison of calculated values depend on the charge of the central atom and cannot be considered to be constant. A CNDO study [356] of ^{29}Si NMR chemical shifts for compounds Me_nSiX_{4-n} (X = H,F,Cl) has been reported. The general variation of the paramagnetic screening constants with n agrees fairly well with the variation of the observed chemical shift for X = H,F but

the correlation is not so good for X = Cl.

The geometries of $H_3SiCH_2CH_2X$ (where X = Cl,F) were optimised by CNDO/2 calculations [357] and the conformation with the *anti*-periplanar arrangement of Si–C and C–X bonds is the most stable one. The reaction enthalpies for

$$R-F + H^+ \rightarrow R-FH^+$$

and

$$R-Cl + H^+ \rightarrow R-ClH^+$$

were calculated for $R = H_3Si(CH_2)_n$ where $n = 1,2,3$. The calculated values of ΔH exhibit the same trends as the experimentally determined basicities and they are considerably affected by the conformation of the molecule.

$Me_3C(O)Me$ and $(Me_3Si)_2CO$ possess UV transitions near 370 nm and 500 nm, respectively [358], while the corresponding transition of Me_2CO is at 280 nm. Modified CNDO calculations [359] indicate the predominant character of the highest occupied orbital of the silanes is σ in character, composed of an antibonding combination of the oxygen lone pair and the Si–C localised orbital, while the oxygen lone pair is almost solely present in the HOMO of acetone. This strong mixing is suggested as the major origin of the wavelength shift.

The first calculation [360] of the electronic structure of vinylsilanes employed the FE method to rationalise the absorption spectrum of divinyltetramethyldisilane and divinyloctamethyltetrasilane in terms of $p \rightarrow d$ conjugation.

Nagy and Vandorffy [361,362] examined eight substituted silyl ethylene compounds by applying the method of Del Re [347] for the σ-electron system and a revised Pariser–Parr–Pople method for the π electrons. Good agreement with experiment was reported for energy transitions, oscillator strengths, dipole moments, bond lengths and ionisation energies.

The photoelectron spectra of vinylsilane and trimethylvinylsilane have been recorded and interpreted with the help of MINDO/1 and CNDO/2 calculations [363–365]. Inclusion of 3*d* orbitals on the silicon is considered essential and they afford a mechanism for delocalising and stabilising the ethylene π electrons.

Ensslin et al. [366] have measured the photoelectron spectra of *trans*-$Me_3SiXC{=}CXSiMe_3$ where X = H, Cl and Br. They find that the symmetry adapted group-orbital procedure [367] is most useful in assigning the bands to valence bond orbitals. *d*-Orbital participation is predicted to be negligible. The highest occupied orbital is a π orbital while the second orbital is localised about sigma Si–C bonds.

A perturbation scheme [368] is used to predict the dienophilic activity of $R_3SiCHCH_2$ and R_3SiCCH.

There have been two investigations of vinylsilane utilising an ab initio technique [369,370]. The photoelectron spectrum of vinylsilane indicates that the α-silyl group produces a negligible shift in the first band of ethylene. This behaviour is reproduced in calculations only when $3d$ orbitals are included in the basis set [369]. The $3d$ orbitals make their largest contribution to the virtual π^* orbitals of the molecule. The inclusion of $3d$ orbitals lowers the energy of the π orbital by 0.385 eV and that of the π^* orbital by 1.343 eV. Now, the lowering of the π–π^* transition of ethylene by the presence of a silyl group is approximately 0.8 eV and, hence, can be associated with the delocalisation of π^*-orbital population into the $3d$ orbitals of the silicon atom [369]. Zeeck [370] reports that the partial overlap population for the π orbitals of vinylsilane is 0.045 for the Si–C bond, indicative of a bonding interaction. The corresponding overlap population in propylene is -0.018, highlighting the absence of hyperconjugation between the methyl and the vinyl group.

There is considerable interest in the influence of the β-metallomethyl substituents on the properties of unsaturated hydrocarbons. Pitt [371] helped to stimulate the interest when he rationalised the trends of a number of experimental properties of silicon compounds in terms of the perturbational MO treatment of hyperconjugation in conjunction with CNDO/2 calculations. He lists the optimum requirements for hyperconjugation as:

(1) The energies of the σ and π orbitals involved should be similar. This is most likely for σ-MR_n groups when M and/or R are electropositive elements.

(2) The perturbation integral, which incorporates overlap, should be large. It is, therefore, better that the connecting atom of the σ group be in the first row of a given Periodic Group, although no more than a factor of two appears to be associated with this term if repulsion integrals are ignored.

(3) There should be high electron density in the p orbitals of the atoms connecting π and σ systems. This factor is generally inversely proportional to the size of the σ and π systems. The σ-electron density can be conformationally dependent and is favoured by polar bonds, i.e. $M^- - R^+$ which also have high p character. Interaction involving the σ^* orbitals of the MR_n group is favoured by the reverse polarity.

There have been several investigations by calculational and photoelectron techniques on the electronic structure of allylsilanes [363–365,372]. Weidner and Schweig [363,364] suggested that the properties of trimethylallylsilane are due to CH_2–$SiMe_3$ hyperconjugation, which is more effective than the corresponding CH_2CMe_3 conjugation because of the higher Si–C bond energy. Calculations on $CH_2{=}CH{-}CH_2{-}SiMe_3$ and $CH_2{=}CH{-}CH_2{-}CMe_3$ yield the energy of the highest bonding orbital to be -12.1 eV and -13.4 eV, respectively. This is in the same order as observed in photoelec-

tron spectra (9.0 eV and 9.6 eV, respectively). The inclusion of 3*d* orbitals only slightly modifies the results and hence they are not considered important in the structure of allylsilanes.

Schweig et al. [372] have quantitatively calculated the destabilisation of π orbital energies in allyl and benzyl compounds on the basis of a hyperconjugative M–C/π interaction model. They show unambiguously that the interaction between π systems and CH_2SiR_3 substituents is hyperconjugative.

Extended Hückel calculations were performed on the conformation of allylsilane and reveal a shallow energy minimum at $\alpha = 110°$ [373].

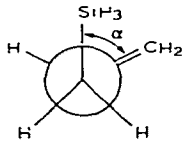

The σ–π conjugation effects should be maximised when the C–Si σ bond is parallel to the π orbitals of the double bond, i.e. when $\alpha = 90°$. So, in the $\alpha = 110°$ conformation, the σ–π conjugation will be significant.

The charge-transfer spectra of allylsilanes $X_3SiCH_2CH{=}CH_2$ (where X = Cl, C_2H_5O, H or CH_3) with tetracyanoethylene as an acceptor, were interpreted by CNDO calculations [374] on the basis of hyperconjugative interaction. It is further shown by perturbation theory that the acceptor properties of silicon are explained by the presence of low-lying σ^* (CH_2–Si) antibonding orbitals rather than 3*d* orbitals. As the electronegativity of X increases, the energy of σ and σ^* will decrease and, hence, (π–σ) with σ^* interaction becomes more important, leading to an increase in ionisation potential (see Fig. 38). The following sequence of the electron-accepting

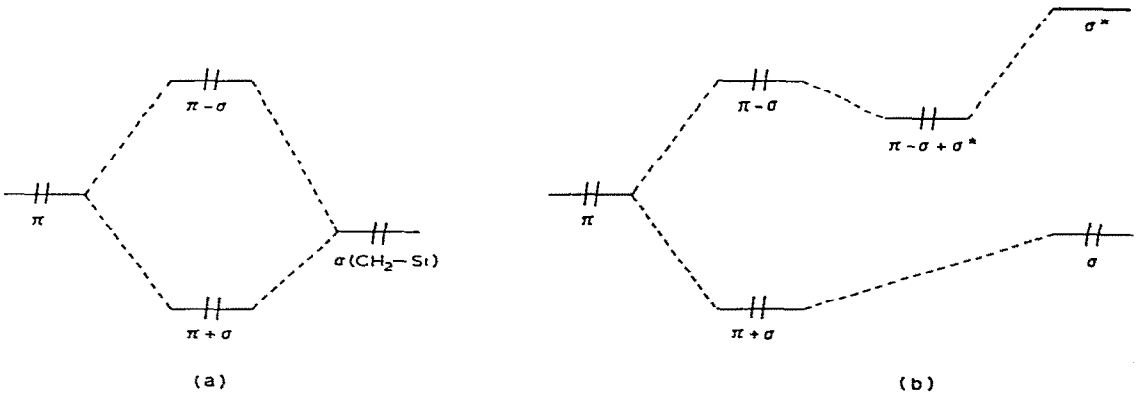

Fig. 38. Orbital diagrams of allylsilane: (a) in the absence of a σ^*(CH_2–Si) orbital and (b) in the presence of a low-lying σ^*(CH_2–Si) orbital.

strength of the β-silicon group was obtained: $SiCl_3 > SiH_3 > Si(OC_2H_5)_3 > Si(CH_3)_3$.

Horn and Murrell have investigated allylsilane by an ab initio technique [369]. It was found that there is a substantial energy difference between the two energy configurations, (i) parallel, where $\alpha = 0$, and (ii) perpendicular, where $\alpha = 90°$, with the latter more stable by 13 kJ mole^{-1}. The energy difference for the alkyl equivalent, 1-butene, is only 4 kJ mole^{-1}. This energy difference gives a measure of the relative importance of $(\sigma$–$\pi)$ hyperconjugation and inductive effects in allylsilane. The configuration of allylsilane is important in the interpretation of the photoelectron spectrum, with the perpendicular configuration giving better agreement.

The total π electrons of the β-silyl group are more effectively delocalised to the olefin than for the α-silyl group electrons in vinylsilane. The σ electrons of the α-silyl group are, however, much more influenced by changes in the π-electron density of the olefin than are the corresponding σ electrons of the β-silyl group. The atomic group charges of SiH_3 in allylsilane and vinylsilane are +0.101 and +0.084, respectively.

The photoelectron spectra of the simplest phosphorus ylide $(CH_3)_3P{=}CH_2$ and several C-silyl derivatives have been measured and CNDO calculations [375] performed on these compounds. The reason for 'silyl stabilisation' has proved not to be a stabilisation of the HOMO, i.e. the ylide π-level, but of a decrease of the MO coefficient at the ylidic, quasi-anionic carbon atom.

The influence of the silyl group on the cylindrical π system of acetylene has been the subject of some investigations [376–383]. The early rationalisation [376] of the different properties of trimethylsilyl- and tert-butylacetylenes was in terms of the differing inductive and conjugative effects of the silyl and alkyl groups. Pitt [377] showed by CNDO-type calculations on alkyl- and silyl-substituted acetylenes that experimentally observed trends in the charge distribution are reproduced despite the fact that 3*d* orbitals are omitted from the silicon basis set. He further proposed [371] a hyperconjugative model neglecting $p_\pi d_\pi$ back bonding to account for silicon substituent effects.

The photoelectron spectra of $(CH_3)_3SiCCX$ (where X = H, F, Cl, Br and I) [378] and mono- and di-substituted silylacetylenes [379] have been recorded. The bands have been assigned with the use of a parametrised model based on linear combinations of bond orbitals. Subsequently, calculations [379] were performed, using a modified CNDO/2 technique, to pinpoint the important interactions in these molecules. The inclusion of 3*d* orbitals yields poorer agreement with both experimental dipole moment and photoelectron spectra. In silylacetylenes the hyperconjugative destabilisation of the π orbital amounts to 0.32 eV while the inductive effect contributes 0.47 eV to the π orbital lowering from 12.68 eV in acetylene to 11.89 eV in silylacety-

lene. These are smaller than the corresponding values for the methyl group in methylacetylene.

The charge distribution in the *sp* basis calculation of silylacetylene indicates that there is a movement of 0.183 electrons from the silyl group to the acetylene and this excess is found on the carbon atoms. This compares with a similar movement of 0.096 electrons in methylacetylene, although for this molecule the source of the donated electrons is the methyl hydrogen atoms, whereas it is the silicon atom (+0.405) in silylacetylene which supplies the electrons.

The infrared absorption intensities of the CH and CC stretching vibrations of 13 silylacetylenes have been determined [380] and a linear relationship was obtained between the square root of the intensities and the Taft substituent parameters. Charge densities obtained from CNDO/2 calculations rationalise the results.

The barrier to internal rotation in SiH_3CCCH_3 has been evaluated [381], using an ab initio procedure and an STO-3G basis set. The molecule is predicted to have the hydrogen atoms eclipsed with a rotational barrier of 3.3 cal $mole^{-1}$. Dimethylacetylene adopts the same conformation with a rotational barrier of 5.0–7.3 cal $mole^{-1}$. The negative end of the dipole moment ($\mu = 0.09$ D) of SiH_3CCCH_3 points towards the silicon end of the molecule in a similar manner to that found in CH_3SiH_3 [319].

CNDO calculations have been performed on $SiH_3C \equiv CH$, $SiH_3C \equiv CN$, $(CH_3)_3SiC \equiv CH$ and $(CH_3)_3SiC \equiv CN$ in order to rationalise the variation of the Si–C bond lengths in these molecules [382]. Also reported are the 3*d*-orbital electron populations which are 0.72, 0.69, 1.36 and 1.38, respectively.

A second CNDO calculation [383] on silylcyanide examined its isomer, silylisocyanide. The former is more stable by 0.09 a.u. The silylcyanide dimer $(H_3SiCN)_2$ was also investigated. The calculated planar 6-membered ring consists of Si–C and Si–N bond lengths spanning 1.95 Å, C–N bonds of 1.21 Å, and CSiN angles of 103°. The energy of dimerisation is 0.13 a.u. and 0.33 a.u. for a silicon 3*d* exponent of 1.383 and 0.95, respectively.

One of the striking features of organosilicon chemistry is the absence of compounds with multiple bonds of the $p\pi$–$p\pi$ type that are stable under normal conditions. Consequently, there have been several theoretical examinations of the electronic structure of silaethylene in order to elucidate the factors responsible for the instability of the molecule. Initially there were three semi-empirical calculations [384–386] which concentrated mainly on the electron distribution, and they were followed by ab initio investigations [387–391] which were concerned with the structure and energy of CH_2SiH_2.

Extended Hückel and CNDO calculations were used to attain the electronic structure of CH_2SiH_2 [384, 385], CH_2SiF_2, CF_2SiH_2 and CF_2SiF_2

[386]. It is found that, firstly, carbon–silicon π bonds are exceedingly polar and secondly, the energy mismatching of the carbon and silicon p orbitals is responsible for the weakness of the π bond.

The barriers to rotation about the double bond increase in the order C=C > Si=Si > C=Si. In contrast to C_2H_4 and Si_2H_4, where the triplet state of the 90° twisted molecule has the lowest energy, the singlet state of twisted SiH_2–CH_2 is more stable and corresponds to $SiH_2^+ CH_2^-$.

Electrostatic calculations [385] indicate that $H_2Si{=}CH_2$ should react with itself in a simple head-to-tail fashion. $F_2Si{=}CH_2$ and $H_2Si{=}CF_2$ have reaction paths with a perpendicular head-to-tail route which will give a dimeric species, while $F_2Si{=}CF_2$ has no strongly attractive geometrical approaches for dimerisation to occur.

The electronic distribution is greatly affected by the presence of fluorine. A fluorine atom bonded to silicon increases the positive character of silicon from 0.4 (with hydrogen substituents) to 0.7. The effect on carbon is to bring about a similar change from −0.3 to 0.1. The total 3*d* orbital population of silicon in these four molecules is high, especially when the silicon bears fluorine substituents. Here the halogen atoms attached to the silicon withdraw σ-electron density and allow increased back donation from the fluorine π orbitals to the 3*d* orbitals.

The dipole moment of fluoro-silaethylene has been predicted by CNDO calculations [386]. Replacing the hydrogens on the carbon by fluorines decreases the dipole moment in the sense CSi +− and replacing the hydrogens on the silicon by fluorines increases the dipole moment. The orbital contributions to the dipole moment are described in terms of LMOs.

The first ab initio calculation on CH_2SiH_2 was performed by Schlegel et al. [387], who predicted the theoretical IR spectrum. Their optimised geometry stucture was planar, with Si–C = 1.639 Å and both H–C–H and H–Si–H angles spanning 114°. Force-constant calculations yielded in-plane vibration frequencies for CH_2SiH_2 and CD_2SiH_2.

An FSGO treatment of CH_2SiH_2 [323] yielded an optimised planar geometry with a C–Si bond length of 1.839 Å, a H–Si–H angle of 109° indicating a preference for the tetrahedral, and an angle of 122° for the methylene group. The heat of formation of CH_2SiH_2 is calculated to be more positive than that of SiH_2SiH_2 or that of CH_2CH_2.

Strausz et al. employed a minimum basis set [388] and an extended basis set [389] in their search for the most stable state. The minimum basis set calculation predicted that the triplet state was 1.4 kcal $mole^{-1}$ more stable than the singlet, while the extended basis set results indicated that the triplet state was 9.6 kcal $mole^{-1}$ less stable than the singlet state.

Ahlrichs and Heinzmann, who included electron correlation in their calculation procedure [390], confirmed that the planar singlet state is more

stable than the perpendicular triplet state (by ca. 28 kcal mole^{-1}). They found a strong Si–C $p\pi$–$p\pi$ bond in CH_2SiH_2 and this amounts to 70% of the value in C_2H_4. The rotational barrier is predicted to be ca. 46 kcal mole^{-1}. The energy barrier for the cycloaddition of CH_2SiH_2 to give $Si_2C_2H_8$ is less than 14 kcal mole^{-1} with a large reaction energy of 76 kcal mole^{-1}. The considerable polarity of the silicon–carbon bond relieves the symmetry restrictions and the reaction is no longer forbidden. The charge distribution is very polar, with carbon and silicon bearing a -0.4 and a $+0.5$ charge, respectively. The hydrogens bonded to carbon have a small $+0.05$ charge while those bonded to silicon have excess electrons (-0.1).

Hood and Schaeffer [391] used a double-zeta basis set to obtain the optimised geometry for the singlet and triplet states of silaethylene. The planar structure of singlet CH_2SiH_2 has a Si–C bond length of 1.715 Å, while the H–Si–H and H–C–H angles are 115°. The perpendicular geometry of the triplet state has the Si–C bond of length 1.880 Å, the H–C–H angle is 115°, the H–Si–H angle is 109°, and the SiH_2 rocking angle is 50°. Their calculations show that the singlet state is more stable than the triplet state by 13.7 kcal mole^{-1}. This energy separation is increased to 31.6 kcal mole^{-1} when a CI calculation is performed on the valence shell orbitals. Addition of polarisation functions to silicon and carbon enlarges the energy gap to 34.7 kcal mole^{-1}.

A possible source of the instability of the carbon–silicon double bond may be the rearrangement of CH_2SiH_2 to form either silylcarbene, SiH_3CH or methylsilylene, CH_3SiH. These isomers of silaethylene were therefore examined [392] and the geometry of the singlet and triplet states was obtained by using a minimum basis set augmented by 3*d* orbitals on silicon and with a small amount of CI. The most stable species is the singlet state of methylsilylene, while the most stable triplet state belongs to silylcarbene. The Si–C bond lengths of the singlet states of CH_3SiH, CH_2SiH_2 and $CHSiH_3$ are 1.89 Å, 1.64 Å and 1.99 Å. The silaethylene structure is not found to be most stable thermodynamically on either the singlet or triplet surface. Thus, a process which produces singlet methylsilylene or triplet silylcarbene in a low vibrational state is unlikely to result in the formation of the corresponding silaethylene.

The isomerisation of silylcarbene to silaethylene has been examined by Schlegel et al. [393]. The energy of isomerisation for the singlet state is -44 kcal mole^{-1} and for the triplet state is $+3$ kcal mole^{-1}. The formation of singlet ethylene from methylcarbene is 21 kcal mole^{-1} more exothermic and this is due partially to the lower strength of the Si–C π bond compared to the C–C π bond. The optimised geometries for the singlet and triplet states of both molecules from an STO-3G calculation are given.

The geometry and electronic properties of trimethylsilylcarbene, silylcar-

bene, carboxysilylcarbene and phenylsilylcarbene have been determined [394] by MINDO/3 calculations. The ground state of trimethylsilylcarbene is a triplet with 32.9 kcal mole^{-1} less energy than the singlet state. Both the singlet and triplet states are predicted to have a bent Si–C–H framework with the angle equalling 116° and 147° for the singlet and triplet state, respectively. The unsubstituted silylcarbene has a similar geometry. The most stable state of carboxysilylcarbene is a triplet lying 23.5 kcal mole^{-1} below the singlet state. The singlet state has a linear Si–C–C framework, while the triplet possesses a bent structure (Si–C–C = 170°). The ground state of phenylsilylcarbene is predicted to be triplet and has an angular geometry (Si–C–C = ca. 140°).

Introduction of silyl groups into the carbene centre results in a considerable decrease in the ionisation potential. This effect is also observed with phenyl and methyl substituents. Silyl moieties increase the $p\pi$ electron density of the carbene carbon but the degree of the effect is less than methyl or phenyl groups. So, in order to interpret the unique reactivity of silylcarbenes, the bulkiness of the SiH_3 group and the efficiency of the singlet–triplet interstate crossing should be taken into account.

Apeloig and Schreiber [49] have examined the electronic structure of $SiH_3CH{=}C$: and $(SiH_3)_2C{=}C$:. They find that SiH_3 groups stabilise the parent alkylidene carbene. The population of the formally vacant $2p$ carbenic orbital is 0.128 electrons, indicating an important hyperconjugative effect.

An FSGO treatment of CHSiH [324] yielded the following optimised geometrical parameters: C–H = 1.085 Å, Si–H = 1.444 Å and C–Si = 1.503 Å. The calculated heat of formation is +554 kJ mole^{-1} and, on comparison with SiHSiH (+353 kJ mole^{-1}) and CHCH (+227 kJ mole^{-1}), clearly indicates that carbon–silicon multiple bonding is less attractive than multiple bonding between the same element.

Murrell et al. [395] have calculated the geometries of the isomers CH_2Si and CHSiH using a double-zeta basis set. For CH_2Si the C–Si bond length is 1.72 Å and the H–C–H angle is 112.9°, showing a tetrahedral tendency about the carbon atom. The C–Si bond in CHSiH spans 1.587 Å. The CH_2Si structure is the more stable by 256 kJ mole^{-1}, illustrating that the divalent silicon compound is far more stable than the tetravalent silicon compound.

Pseudopotential calculations have been performed [396] on silylacetylene and four possible isomers, 2-silaallene, silacyclopropylidene, silacyclopropene and 2-silapropyne, to examine the relative stability of the isomers and their possible existence as short-lived intermediates. The relative energies of the C_2SiH_4 isomers compared to silylacetylene are 2-silaallene (+45.73 kcal mole^{-1}), silacyclopropylidene ($^1A_1$, +16.99 kcal mole^{-1}; $^3B_1$, +51.59 kcal mole^{-1}), silacyclopropene (+16.63 kcal mole^{-1}) and 2-silapropyne (60.74

kcal mole^{-1}). The reluctance of silicon to multiple-bond accounts for the relative instability of 2-silaallene and 2-silapropyne. Now, 2-silaallene has been suggested as a possible intermediate in a pyrolysis reaction [397]. From the calculations, silacyclopropylidene is predicted to be more stable than 2-silaallene and, as the interconversion involves no proton migration, it should be formed.

The electronic structure of the hypothetical dimethylsilafulvene has been examined by a CNDO technique [398]. The planar configuration is more stable by 19.8 kcal mole^{-1} than the perpendicular conformation of the CH_3SiCH_3 plane with respect to the ring. The silicon carries a +0.45 charge while the cyclopentadiene moiety carries an excess charge (−0.34).

CNDO calculations [399] have been performed on hexamethylsilacyclopropane and dimethyldispirosilacyclopropane in order to rationalise why the dispiro structure stabilises the silacyclopropane ring [400,401]. The calculations show that methyl substitution of the silacyclopropane ring decreases the C–Si overlap population and withdraws electron density from the ring carbon atoms. By contrast, the dispiro structure increases the C–Si overlap population due to the ability of the σ-orbitals of the cyclopropane rings to interact with the low-lying silicon 3*d* orbitals.

Extended Hückel calculations [402] reinforce the suggestion that *d*–σ hyperconjugation may be the reason for the stability of these silacyclopropanes. They also indicate that this interaction should be present in the yet unknown cyclopropylidenesilanes. Comparison of overlap populations for olefins and alkylidenesilanes reveals that the carbon–carbon bond population of ethylene and methylenecyclopropane is essentially the same (1.303). In contrast, the silicon–carbon overlap population in cyclopropylidenesilane (1.317) is greater than that in methylenesilane (1.180) due to the aforementioned *d*–σ hyperconjugation.

Jones and White have obtained optimised geometries [403] for silacyclopropene and four substituted silacyclopropenes by a CNDO approach. A small average C–Si–C bond angle of 43.6° is found to be insensitive to ring substituents. The average ring C–C bond length is 1.38 Å and approaches the value observed in aromatic rings. Equivalent π character found for both the C–Si and C–C bonds also suggests an aromatic type of π delocalisation. The main orbital contributing to this π delocalisation on silicon is a *d* orbital of the appropriate symmetry for bonding with the π orbital of the C–C double bond. This back donation is responsible for a reduced charge on silicon, e.g. +0.059 is obtained for tetramethylsilacyclopropene compared with +0.108 for hexamethylsilacyclopropane. Thus, the remarkable stability of silacyclopropenes may be attributed to the pseudo-aromatic character of the ring and the reduced polarity of the bonds.

Charge-transfer spectra of silacyclopentenes and cyclopentenylsilanes have

been measured and interpreted on the basis of simple orbital diagrams obtained from CNDO/2 calculations [404]. It is not necessary to invoke 3*d* orbital interaction in order to explain the results, as hyperconjugative interaction of the Si–C or Si–X bonds with the π-orbital system can rationalise the spectra.

Frenking et al. [405] have discussed the higher reactivity of cyclic organosilanes compared to that of the cycloalkanes. In particular, the ring-size dependence of the cyclic organosilanes [$(CH_2)_{n-1}SiMeH$] for a substitution reaction is $n = 4 \gg 5 > 6$. In contrast, the reactivity of the cycloalkanes $(CH_2)_{n-1}CMeCl$ is in the order $n = 3 < 4 < 5 > 6$. CNDO/2 calculations on $(CH_2)_{n-1}SiMeH$ and $(CH_2)_{n-1}CMeH$ for $n = 3, 4, 5, 6$ were employed to give possible explanations of the experimental behaviour. The LUMOs and HOMOs of the cyclic compounds play a dominant role in the reactivity. The energy of the LUMOs, with the exception of the cyclosilane for $n = 6$, can be correlated directly to the reactivity. Moreover, a small reactivity can be predicted for the hypothetical cyclosilane with $n = 3$. The energy of the LUMOs for the cyclosilanes is less than the LUMOs of the corresponding cycloalkanes and may be the reason for the higher reactivity of the silicon compound. These trends and those of the electron distribution at the reaction centre give reasons for the different dependence of reactivity on ring size.

The structures and relative conformational energies for a variety of acyclic and cyclic catenated organopolysilanes have been evaluated [406] by the empirical force-field method.

The results of both ultraviolet and photoelectron spectroscopic investigations for linear and cyclic permethylated oligosilanes were interpreted by Nagy [407], using simplified LCVO–MO calculations [408]. The results indicate that the $(d$–$d)\pi$ effect can be neglected in the interpretation of chemical properties. The dominant interaction is the σ conjugation, which is much larger for silicon–silicon chains compared to carbon–carbon chains because the diffuse sp^3 hybrid orbitals of silicon represent a stronger geminal interaction which does not occur in the carbon oligomers. This results in a larger splitting of the ionisation energies and in a more considerable bathochromic shift in the ultraviolet absorption values.

Silabenzene, like silaethylene, has so far proved elusive to synthesis. One of the unsuccessful attempts to generate a substituted silabenzene was by rearrangement of the corresponding carbene [409], a process which works well for the carbon analogue. Calculations of the STO-3G quality have been performed [393] on silabenzene and the isomeric carbene silacyclohexadienylidene to throw light on the reasons for the non-success of the reaction.

The geometries of both the singlet and triplet states of the silabenzene and

the singlet state of the silacyclohexadienylidene were obtained by energy-optimisation routines. The most stable state is the singlet state of silabenzene, which lies 107 kcal mole^{-1} lower than the triplet state and 66 kcal mole^{-1} lower than the isomeric carbene. The energy of isomerisation between the silicon isomers is 31 kcal mole^{-1} less exothermic than the corresponding energy for the formation of benzene. This is due to a lower π bond strength of the C–Si bond (ΔE = ca. 20 kcal mole^{-1}) and a smaller resonance energy (ΔE = ca. 10 kcal mole^{-1}).

The geometrical parameters of silabenzene are not unlike those of benzene. A planar structure is found for both the singlet and triplet states. The singlet C–C bond lengths (1.381 Å and 1.395 Å) are essentially the same as in benzene and the Si–C bond length (1.72 Å) is intermediate between a single bond and a double bond. The π-electron distribution is reasonably uniform with 0.82 π electrons on the silicon and the consequent build-up of π electrons at the *ortho* (1.09) and *para* (1.09) positions. The σ framework shows a more distinct polarisation of the C–Si bond than the π electron system with a group charge on the SiH of +0.59. This suggests that the silabenzene may have considerable ylide character. The elusive nature of the silabenzene may thus be due to its high reactivity as opposed to a lack of aromaticity.

An FSGO method [410] has been used to investigate the electronic structure of silabenzene. The geometry-optimised structure of silabenzene yields the following bond lengths: $C_1-C_2(C_1-C_3) = 1.420$ Å, $C_2-C_4(C_3-C_5) = 1.409$ Å and $Si-C_4(Si-C_5) = 1.819$ Å. The alternation in C–C bond lengths is a common feature of heteroaromatic systems. The C–Si–C angle is 102° and is smaller than the tetrahedral angle. The electronic effect of silicon substitution in the benzene ring is to draw π electrons to the silicon atom, which, in turn, loses more σ electrons to the adjacent carbon atoms. The disposition of electron population indicates that the molecule is open to nucleophilic attack at the silicon centre and so strong nucleophiles should be excluded in the final steps of possible schemes to prepare silabenzene. However, the main obstacle to the formation of silabenzene is thought to be thermodynamic.

A double-zeta basis set has been used to calculate the electronic structure of 1-silacyclopentadiene [411]. The ordering of the five highest filled MOs is $1a_2(\pi)$, $2b_1(\pi)$, $4b_2$, $6a_1$ and $1b_1(\pi)$. The ordering is very similar to that of cyclopentadiene [411] except for the position of $1b_1$, which is much lower in energy by ca. 2 eV in the hydrocarbon and is the seventh MO. A many-body approach which includes the effect of electron correlation and reorganisation was used to evaluate the ionisation potentials of $C_4H_4SiH_2$. The revised order is $1a_2(\pi)$, $4b_2$, $2b_1(\pi)$, $6a_1$, $1b_1(\pi)$ and so the Hartree–Fock approximation is found to be incorrect with respect to the order of the $4b_2$ and

$2b_1(\pi)$ orbitals. The Mulliken population analysis of the SCF wavefunction indicates that the Si atom has lost about 0.5 electrons. This charge is found on the neighbouring C and H atoms. Several one-electron properties of the SCF wavefunction of $C_4H_4SiH_2$ have been computed.

The electronic distributions and energies of the various isomers of silylcyclopentadiene have been investigated by ab initio methods [412]. The total energies predict that the order of stability is 5-SiH_3 > 2-SiH_3 > 1-SiH_3. The electron distribution of 5-SiH_3 shows a +0.29 charge on the silane group, and donated electrons are mainly localised on the neighbouring carbon (5) atom. The four other C–H groups possess a small negative charge. The C–Si σ bond is represented entirely by a single MO in the 1-silyl and 2-silyl isomer but is heavily delocalised over the ring "π-system" in the 5-silyl compound. This appears to rationalise the NMR spectra of 5-silylcyclopentadiene at room temperature where all five ring protons become equivalent. In methylcyclopentadiene where fluxional behaviour is not observed, the methyl bonding involvement in the ring "π-system" is small. The photoelectron spectrum of the 5-silyl derivative is interpreted in terms of the orbital energies.

The transition states [413] and reaction paths [414] for an intramolecular rearrangement of the SiH_3 group in cyclopentadienylsilane have been calculated by CNDO techniques. There are three energetically favourable transition states and these are shown in Fig. 39. They are (2c) for the 1,2 shift of SiH_3 group, (3c) for the 1,3 shift, and (5c) for the 1,2 and 1,3 migration.

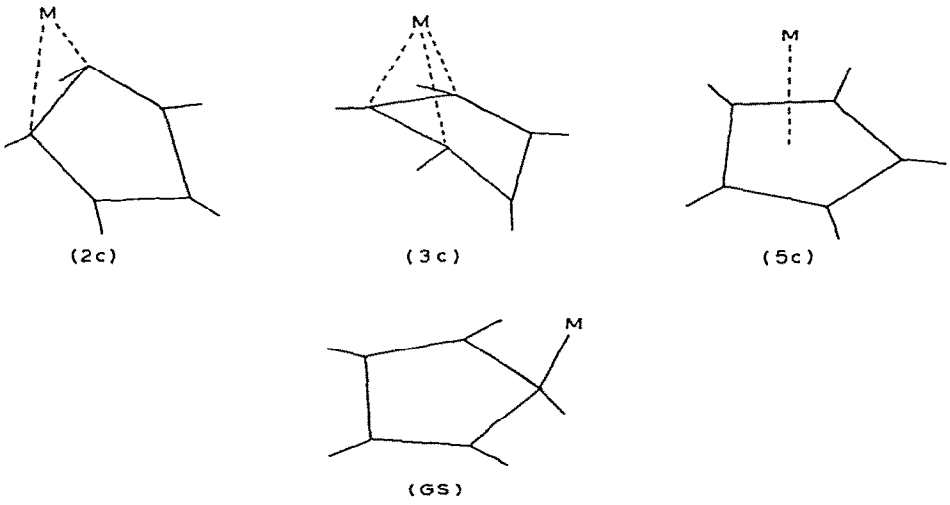

Fig. 39. The transition states for the intramolecular rearrangement of the SiH_3 group in cyclopentadienylsilane.

Geometry-optimisation techniques gave no energy minimum for (3c), while the energy of (2c) and (5c) are 6 kcal $mole^{-1}$ and 29 kcal $mole^{-1}$ higher than the ground state. Consequently, the 1,2 shift predominates, i.e. the rearrangement is a [1,5]-sigmatropic rearrangement in terms of the Woodward–Hoffmann [311] notation.

An early Pariser–Parr–Pople calculation [415] on *p*-disilylbenzene indicated that a silicon atom has little net effect on the π bonding orbitals of benzene but has a significant stabilising effect on the antibonding orbitals. Pitt showed in calculations [371] of silyl- and methylbenzenes that the methyl group acted as a donor and the silyl group as a π acceptor, in agreement with the conclusions from photoelectron spectroscopy [416].

Ramsey [417] has made a comprehensive study of the role of charge transfer, hyperconjugation, inductive and field interactions in substituted silyl substituent effects on benzene π vertical ionisation energies. He compares the first two vertical π energies obtained from photoelectron spectra with the results of modified CNDO calculations for $C_6H_5SiX_3$ where X = H, F, Cl and OCH_3. A satisfactory description of the SiH_3 group in $C_6H_5SiH_3$ is probably one of a nearly net zero inductive-field effect and a very small hyperconjugating ability. SiF_3 and $SiCl_3$ substituents also exhibit calculated opposing field and σ-inductive effects. The first vertical ionisation energy of $PhSiCl_3$ is assigned to ionisation from the a' π-orbital rather than the a'' orbital. Silicon–chlorine hyperconjugation is a suggested stabilising interaction in the $PhSiCl_3$ $^2A'$ cation. The $Si(OCH_3)_3$ group exerts a positive charge-stabilising effect on phenyl groups.

^{29}Si chemical shifts in a series of substituted phenyltrifluorosilanes and phenyltrimethylsilanes were found to be totally different for each series. Although each series exhibited high degrees of linearity with Hammett constants, the slopes of the regression lines were of opposite sign. CNDO calculations [418] of electron density at silicon for the silanes indicated no unusual reversal in the density trends to account for the observations. An additional although nonlinear relationship between $\delta^{29}Si$ and the summed electronegativities of the groups bound to silicon was found.

The photoelectron spectra of $(CH_3)_3SiC_6H_5$ and $(CH_3)_3SiCH_2C_6H_5$ have been interpreted by MINDO/3 and first-order perturbation theory [419]. $p\pi$–$d\pi$ bonding is important in the phenyl silane, whilst hyperconjugative and inductive effects are of comparable magnitude in the benzyl silane. Schweig et al. [372] show that the destabilisation of the π molecular orbitals in benzyl compounds of silicon can be quantitatively predicted on the basis of the hyperconjugative "Si–C with π" model.

Ponec and Chvalovsky [420] measured the charge-transfer spectra of a series of substituted phenyl and benzyl silanes. The results can be interpreted by the interaction of the low-lying σ^*(Si–X) or $\sigma^*(CH_2-Si)$ with the phenyl

π system. The participation of silicon $3d$ orbitals is not necessary for the rationalisation of the spectra. Charge-transfer spectra of a series of substituted silaacenaphthenes with tetracyanoethylene gave wavenumbers of ν_{CT} increasing in the sequence $Si(CH_3)_2 < SiH_2 < SiCl_2 < SiF_2$. Electron-accepting properties of the silyl substituents can be explained [421] in terms of interaction with low-lying antibonding orbitals of $\sigma^*(Si-X)$ bonds without considering $(p_\pi - d_\pi)$ bonding. A similar conclusion was reached for silafluorenes [422].

The σ dipole moments for some vinyl, phenyl, allyl and benzyl derivatives of silicon were calculated [423] using the Del Re [347] method. The π dipole moments of the compounds, assuming various interactions, were calculated by the Pariser–Parr–Pople method. The comparison between experimental dipole moments and the vectorial sum of σ and π dipole moments proved the distant interactions to be significant; the role of $3d$ orbitals of silicon cannot be neglected.

Ultraviolet spectra data of vinyl, phenyl, allyl and benzyl derivatives of silicon are compared with the transition energies calculated by the Pariser–Parr–Pople method [424]. The role of d orbitals was investigated. In the phenyl and vinyl derivatives, α-interaction was found to have a dominant effect; in the case of the allyl and benzyl, β- and γ-interactions can be effective.

The electronic structure of $PhSi(Me)_3$ was evaluated by the CNDO method [425]. The equilibrium Si–C (aromatic) bond distance appears to be 1.886 Å, from total energy considerations. There is a small electron flow into the ring of 0.03 electrons and this is found at carbons 1, 3 and 5.

Long-range spin–spin coupling constants between protons bonded to silicon and ring protons in $C_6H_5SiH_3$, $C_6H_5SiH_2Cl$, $C_6H_5SiH_2CH_3$, $C_6H_5SiHCl_2$ and $C_6H_5SiH(CH_3)_2$ are determined from proton magnetic resonance spectra of benzene solutions [426]. A hindered rotor treatment of the barrier to internal rotation about the C–Si bond allows the deduction of the low-energy conformations for $C_6H_5SiH(CH_3)_2$ and for $C_6H_5SiHCl_2$. Ab initio STO-3G MO calculations were performed on $C_6H_5SiH_3$, $C_6H_5SiH_2Cl$, and $C_6H_5SiHCl_2$. The calculations agree with the coupling-constant data as to the low- and high-energy forms of the chlorine derivatives. For $C_6H_5SiH_2Cl$ the low-energy conformation has the chlorine atom in a perpendicular position with respect to the phenyl ring and this is 0.39 kcal $mole^{-1}$ more stable than the high-energy conformation, which has the chlorine atom in the same plane as the phenyl ring. The low-energy form of $C_6H_5SiHCl_2$ has the hydrogen atom of the SiH_2Cl group in the same plane as the phenyl ring. The high-energy conformation, which is 0.5 kcal $mole^{-1}$ less stable, has the hydrogen atom in a perpendicular position.

CNDO calculations [427,428] on $4\text{-}(CH_3)_3SiCH_2$ and $4\text{-}(CH_3)_3Si$ sub-

stituted styrenes have been performed to help rationalise the NMR data. The calculation illustrated the electron-donating properties of the $(CH_3)_3SiCH_2$ group and indicates that σ–π hyperconjugation is present. The trimethylsilyl calculation showed that the $(CH_3)_3Si$ group is a π-electron acceptor, even when 3*d* orbitals are excluded.

Jones and co-workers have calculated the ground-state properties [429] and excited-state interactions [430] of *p*- and *m*-trimethylsilyl-*N*,*N*-dimethylaniline. The trimethylsilyl group is strongly electron-releasing to the σ system of these compounds. Despite this electron-releasing effect in the σ system, the net perturbation of the ground state produced by silicon substitution is electron withdrawal and stabilisation of the ground state compared to the t-butyl compound. This effect is even more pronounced in the excited states where the symmetric and antisymmetric π^* levels are affected by π interactions. The magnitude of the effects is proportional to the π density at the point of substitution. For the *para*-substituted compounds, the excited state, which has large density at the point of substitution, is stabilized to the greatest extent. In the *m*-substituted compound the antisymmetric excited state shows the greatest stabilisation. The ground-state charge densities correlate well with the changes in the chemical shifts of the carbon atoms [431].

Trimethylsilyl substituted naphthalenes [432] and their radical anions [433] have been studied by a simple molecular-orbital method. The electronic absorption, charge transfer, and ESR spectra have been interpreted by the calculations and it is shown that there is significant $d\pi$–$p\pi$ conjugation.

The photolysis of 1-disilanylnaphthalenes [434] in the presence or absence of a trapping agent afforded isomers, 1-hydrosilyl-2-silylnaphthalenes, via photochemical formation of the silicon–carbon double-bonded intermediate, followed by an intramolecular 1,3 hydrogen shift. In marked contrast, the photolysis of 2-disilanylnaphthalenes in the presence of a trapping agent yields addition products which could be formed from the reaction of the unsaturated silicon species with the trapping agent. In this photolysis, the silyl group migrates only to the C_3 atom (and not to the C_1 atom) of the naphthalene ring. Molecular orbital calculations based on the CNDO/2 approximation were carried out on 1- and 2-disilanylnaphthalenes and three types of intermediates (see Fig. 40).

The total energies of C′ and D′, possible intermediates in the photolysis of 2-disilanylnaphthalenes, indicate that C′ is less stable than D′. Chemical evidence, however, favours C′ and so the symmetry nature of the frontier orbitals may be important. A $\pi \rightarrow \sigma^*$ transition is thought to be brought about by the photoabsorption. The σ^* orbital is an antibonding orbital about the Si–Si bond and the subsequent orbital interaction occurs between the HOMO, i.e. π orbital of the naphthyl group and the terminal silyl group

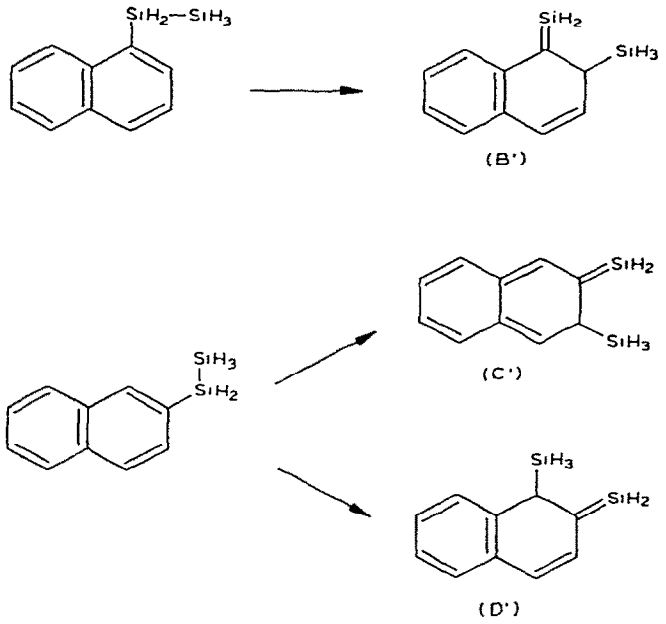

Fig. 40. Three intermediates which are possibly produced by photolysis of 1- and 2-disilanylnaphthalenes.

of σ^*. For intermediate C′ the phase relationship between the $2p_z$ atomic orbital C_3 atom of the HOMO and the $3p_z$ atomic orbital at Si_2 of the LUMO is favourable for forming a new C_3-Si_2 bond. In the formation of D′, however, the phase relationship between C_1 and Si_2 is antibonding and, hence, unfavourable for forming a C_1-Si_2 bond. In a similar manner, the 1,3-hydrogen shift in intermediate C′ from the C_3 atom to the Si_1 atom is unfavourable. The intermediate C′ thus undergoes addition reactions.

In the photolysis of 1-disilanylnaphthalenes a $\pi-\pi^*$ transition is thought to contribute to the reaction leading to intermediate B′. The phase between Si_2 and C_2 is bonding in the π^* orbital of B′ and so the through-space migration of the hydrogen occurs easily.

Empirical force field calculations [435] have been performed on the conformations of tetraarylsilanes. Tetraphenylsilane, in contrast to tetraphenylmethane, has a ground state symmetry S_4 rather than D_{2d} symmetry. Tetra *o*-tolylsilane also has a ground-state of S_4 symmetry with the substituents oriented *exo*. Further calculations [436] performed on an isomerisation pathway of tetra *o*-tolylsilane indicate a mechanism involving a six-fold energy potential for isomerisation. The mechanism which is the least motion pathway has a calculated activation energy for isomerisation of less than 19.6 kcal $mole^{-1}$.

X-ray fluorescence data [437] for triphenylsilane and tetraphenylsilane indicated that Si–C σ bonds were secured mainly by molecular orbitals formed by interaction of the $3p$ orbitals of silicon with the $2e_{2g}$ and $2e_{1u}$ orbitals of the phenyl group. A $p\pi$–$p\pi$ interaction was found which was weak in Ph_4Si and more intense in Ph_3SiH.

Nagy and co-workers have published [438–441] the charge distributions, dipole moments, transition energies and ionisation energies of various phenylsilanes calculated by the Del Re, Pariser–Parr–Pople or CNDO techniques. The photoelectron spectra of 2,4,6,8-tetrasila-bicyclo[3,3,0]oct-1(5)ene and its Si-methylated as well as its Si-fluorinated derivative were assigned via a CNDO calculation [442].

Bock et al. have reported [443] the photoelectron and UV spectra of Group IV azo compounds $R_3X–N{=}N–YR_3$ (X, Y = C, Si) and $H_5C_6–N{=}N–XR_3$ (X = C, Si, Ge). CNDO calculations were invoked to support the assignments. The first PE band is readily assigned to ionisation from the nitrogen electron pairs. This ionisation energy is considerably lowered by R_3Si and R_3Ge substituents due to substantial electron donation to, and destabilisation of, the nitrogen lone pair of electrons of the azo group.

Silylmethyl anion and silylethyl anion have been investigated by an ab initio technique [444]. Comparison between SiH_3 and CH_3 as substituents on CH_2^- indicates that they have the same geometry, while the energy of stabilisation differs by 50 kcal $mole^{-1}$ in favour of the silyl substituent. The proton affinity of $SiH_3CH_2^-$ is calculated to be 450 kcal $mole^{-1}$ and the approximate pK is 3.4, leading to the conclusion that CH_3SiH_3 is as strong an acid as Ph_2CH_2 and that SiH_3 has a stronger stabilising effect on CH_2^- than has a phenyl group.

The electronic structures of silyl-substituted alkanes, alkyl radicals and carbonium ions have been obtained by non-empirical techniques [445]. The carbonium ion is destabilised by an α-silyl group but stabilised by a β-silyl group relative to the corresponding methyl group. By contrast, replacement of α- or β-methyl by silyl has little effect on the stability of the radicals or alkanes. There is, therefore, a substantial change in the hyperconjugation energy of the carbonium ion when methyl is replaced by silyl and this is not the case for the radical. This is confirmed by the electron distribution. Replacement of methyl by silyl in the propyl radical increases the electron occupation of the $p\pi$ orbital by only 0.007 but, in the propyl cation, the increase in the orbital population is 0.07. In the α-series the destabilisation due to substitution could be attributed to a smaller hyperconjugative effect for silyl; however, the relative importance of the inductive effect of the CH_3 and SiH_3 groups is impossible to measure in this series.

The classical "open" and non-classical "bridged" structures of β-silylethyl cation have been investigated [445] by ab initio methods. The latter is more

stable by 0.4 eV. This contrasts with the more stable (by 0.1 eV) open structure of propyl cation.

The $CH_3SiH_2^+$ ion has been studied [446] by an ab initio technique using an STO-3G basis set. The following geometry-optimised parameters were obtained: Si–C = 1.845 Å, Si–H = 1.435 Å, C–H = 1.087 Å, H–Si–C = 121.5° and Si–C–H = 110.8°. The energy of the reaction

$$SiH_2CH_3^+ + SiH_4 \rightarrow SiH_3^+ + SiH_3CH_3$$

is 12.7 kcal mole^{-1} and is a measure of the stabilising power of the CH_3 substituent compared to H. In a similar manner, the energy of the reaction

$$SiH_2CH_3^+ + CH_3CH_3 \rightarrow CH_2CH_3^+ + SiH_3CH_3$$

gives a direct measure (55.3 kcal mole^{-1}) of the greater stability of the α-silyl cation compared to the α-methyl cation.

The effect of SiH_3 on the stability of the methyl cation has been evaluated [35] by an ab initio technique employing an STO-3G basis set. The optimised geometry of $SiH_3CH_2^+$, assuming local C_{3v} symmetry at Si has the following structural parameters: C–Si = 1.941 Å, C–H = 1.113 Å, Si–H = 1.425 Å, angles H–C–Si = 124° and C–Si–H = 102.4°. The total charge on the SiH_2 group is +0.567 and this arises from a σ-electron charge transfer of 0.535 and a π-electron charge transfer of 0.032. Comparison of the stabilising effects of the silyl and methyl groups is obtained from the following isodesmic reaction

$$H_3SiCH_2^+ + CH_3CH_3 \rightarrow CH_3CH_2^+ + CH_3SiH_3$$

Using energy optimised geometries; the energy of the reaction is +4.0 kcal mole^{-1}, indicating that silyl is more effective than methyl for stabilising the methyl cation. The addition of a single set of *d* orbitals to Si changes this energy only slightly to +2.2 kcal mole^{-1}. The comparison of SiH_3 and CH_3 in the stabilisation of a cationic centre indicates a stronger inductive effect but a weaker hyperconjugative effect of the SiH_3 group.

CNDO/2 calculations [447] on a series of free radicals of type $Me_xH_{3-x}Si$ (where $x = 0$–3) indicate that these radicals are not planar. The deviation from planarity decreases with increasing number of methyl groups. By contrast, the methyl and ethyl free radicals are calculated to be planar. The electron densities for $MeSiH_2$ radical are 0.93, 4.19, 3.73 and 1.16 for the H(C), C, Si and H(Si), respectively. On progressive replacement of the hydrogens by methyl groups, the electron density of Si, H(Si) and H(Me) increases and decreases at C. The spin density at the silicon atom increases with methyl substitution.

CNDO/2 calculations have been performed on pentamethyldisilane and tetramethyldisilane free radicals [448]. The change in the total energy of the

radicals was investigated as a function of Si–Si–C and Si–Si–H bond angles. According to the calculations, the Si–Si–C bond angle is about 114° for both radicals and the Si–Si–H bond angle has a value of about 99° in tetramethyldisilane radicals. The delocalisation of the unpaired electron is not significant in the radicals; the spin density is small in the $(CH_3)_3Si$ group.

United-atom theory has been applied to the radical and anion of $Si(CH_3)_3$ [449]. The radical can act as a π acid and a synergic ligand. For the anion the Lewis basicity is only slightly higher than the radical because the extra charge is moved onto the methyl groups.

Hase and Schweig [450] have examined the electronic structure of $H_3SiCH_2CH_2^+$ and $H_3SiCH_2CH_2^-$ by the CNDO technique. The perpendicular conformation is found to be more stable than the coplanar conformation for both the cation and anion. The structure is discussed in terms of (a) the inductive mechanism of the $2p_\pi$ atomic orbital of carbon, (b) the σ–π hyperconjugation between the σ orbitals of SiH_3 and the $2p_\pi$ orbital of carbon, and (c) the conjugation of $3d$ orbitals of Si and the $2p_\pi$ orbital of carbon. The $3d$ orbitals stabilise the coplanar configuration more than they do in the perpendicular rotamer. Hence, hyperconjugation effects which are favoured by the perpendicular conformation, and $3d$-orbital effects are opposing in nature, with the former playing a dominant role.

CNDO calculations [451] have been performed on β-SiH_3 and β-$SiMe_3$ substituted ethyl cations, radicals and anions. The optimised geometries of these species were obtained by energy-minimising techniques. The radicals and cations favour a three-centred cyclic form over open distorted forms, while the anions prefer an open structure where the optimised C–C–Si angle is 75°. The distortion towards a bridged structure may be considered to be due to 1,3 homoconjugative interactions between the carbon p_z orbital (lying in the CCSi plane and pointing towards the Si) and the silicon d_{yz} orbital. A separation of conjugative effects based upon conformation dependence of hyperconjugation suggests that both hyperconjugative and homoconjugative stabilisations are of major importance in stabilising the cation, whereas the latter appears more important in the radical and anion. The gross atomic populations of the silicon $3d$ orbitals are 0.65, 0.90 and 1.09 electrons for the cation, radical and anion, indicating the degree of participation of these atomic orbitals in bond formation in the species.

Solvation of the β-silyl cation by water molecules was simulated by calculations by including from one to three water molecules at optimal distances from silicon and carbon atoms in both the distorted bisected and cyclic geometries of the cation. The largest solvation energy is calculated when the silicon atom is solvated and the effect is similar for both the open and cyclic forms. As the number of water molecules increases, so the energy

of solvation increases, although the energy changes are small, e.g. the calculated energy of solvation is 72.7 kcal mole^{-1}, 81.1 kcal mole^{-1} and 84.5 kcal mole^{-1} for one, two and three molecules of water of solvation, respectively. By contrast, the most effective solvation of $Me_3SiCH_2CH_2^+$ occurs at the carbon atoms, as a large steric effect due to the methyl groups prevents effective solvation at the silicon atom.

The ω-technique and the McLachlan method were applied to the quantum-chemical interpretation of several organosilicon radical anions [452–454]. The ^{29}Si hyperfine coupling constant is closely related to the spin density on the carbon atom substituted by silicon.

The base-catalysed decomposition of the species $SiH_3CH_2CH_2O^-$ to SiH_3O^- and CH_2CH_2 is an example of the Peterson [455] olefination reaction which is becoming increasingly useful for the synthesis of heteroatom substituted olefins. A CNDO study [456] of the decomposition was undertaken to investigate possible reaction paths (displayed in Fig. 41).

The calculated potential surfaces about the four-centre transition state show that cleavage of the C–O bond is characterised by a steep rise to an energy maximum which is considered to be thermally inaccessible. The cleavage of the Si–C bond is much more favourable and cleavage of the C–O bond subsequent to Si–C bond cleavage is a process of low energy and is presumed to be rapid. The four-centre transition state is only 18–25 kcal mole^{-1} more stable than the initial anion and, given the bias inherent in the calculations towards condensed structures, this may mean that the dihydrooxasiletanide anion is by-passed as a true intermediate and may represent only an approximation of the transition state for conversion of

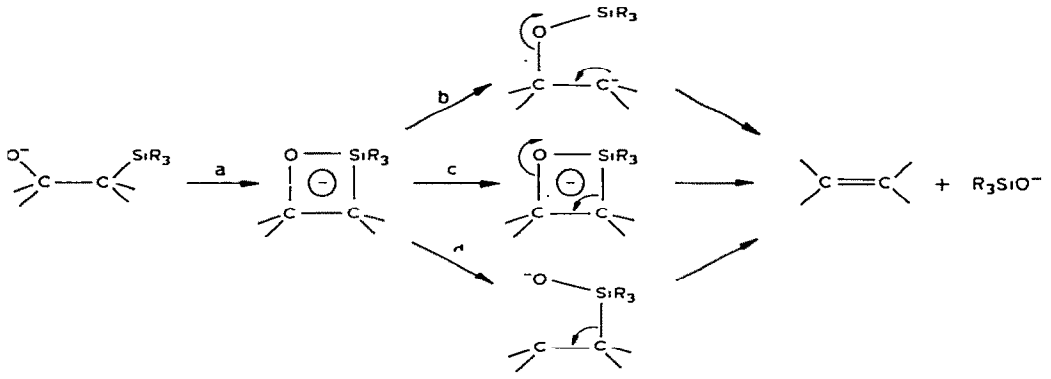

Fig. 41. Reaction paths in the decomposition of $SiH_3CH_2CH_2O^-$ to SiH_3O^- and C_2H_4: (a) initial formation of dihydrooxasiletanide anion; (b) nonconcerted decomposition of dihydrooxasiletanide anion via Si–C cleavage; (c) concerted decomposition of dihydrooxasiletanide; and (d) nonconcerted decomposition of dihydrooxasiletanide via C–O cleavage.

$H_3SiCH_2\dot{C}H_2O^-$ to $H_3SiOCH_2\dot{C}H_2^-$ by attack of silicon on the oxygen.

The methylphenylsilane anion radicals have been investigated by CNDO techniques [457]. There is a linear correlation between the coupling constants and the carbon π electron densities for both $PhSiMe_3^-$ and $PhSiHMe_2^-$ but there is no linear relationship for $PhSiH_3^-$. The spin density is highest at the *para* carbon atom and smallest at the *meta* carbon atom. The progressive replacement of the methyl groups on the silicon by hydrogen atoms causes a decrease in the Si–C(Ph) bond order and an increase in the residence of the unpaired electron at the silicon atom.

The ESR data of the radical anions of organosilyl-benzenes, -biphenyls and -naphthalenes are reproduced by empirical MO calculations [458]. The silicon–methyl proton ESR splittings are related to a combination of the π spin densities on silicon and on the aromatic carbon to which silicon is bonded. The ESR spectra of the anion radicals of the related organosilicon substituted toluenes, xylenes, mesitylenes and t-butylbenzenes have been similarly investigated [459]. The trimethylsilyl group dominates the ordering of the MO energy levels by accepting electron density more effectively than the alkyl substituents release it.

m-Trimethylsilyl- and *p*-trimethylsilyl-*N*,*N*-dimethylaniline radical cations have been investigated by CNDO calculations [460]. The relative stabilities of these compounds are in the same order as the amount of the π character of the Si–C bond in the cation (i.e. *meta* > *para*). This π character is due to both $(p-p)\pi$ and $(d-p)\pi$ interactions. The *para* substituted *N*,*N*-dimethylaniline radical anion has also been investigated by a CNDO calculational technique [461]. The dimethylamino group is more stable by 29 kcal $mole^{-1}$ in a tetrahedral configuration than in a planar trigonal environment. The total energy of the system is also lower when the Si–H bond of the silyl substituent is perpendicular to the ring. The calculations indicate that the primary interaction between silicon and aniline involves a σ^* level of the silyl group and the π system of aniline and this accounts for the trends observed in the aniline radical anions.

Five silyl substituted cyclopentadienyl radicals (XC_5H_4, where X = Ph_2MeSi, $PhMe_2Si$, Me_3Si, Me_5Si_2 and Me_7Si_3) were characterised by ESR and the results rationalised by simple MO calculations [462]. The substituents Ph_2MeSi, $PhMe_2Si$ and Me_3Si are electron-accepting due to the $d_\pi - p_\pi$ conjugation, while Me_7Si_3 and Me_5Si_2 groups are electron-donating due to $\sigma-\pi$ mixing.

Very comprehensive, lucidly written, and highly recommended annual reviews of the bonding in organosilicon compounds have been published by Jones [463–467].

(ii) Organogermanium compounds

The number of calculations performed on organogermanium compounds is somewhat small compared with the number of theoretical investigations on organosilicon compounds. This partly arises from the general absence of ab initio investigations on organogermanium compounds. An exception occurs for CH_3GeH_3 which was examined both by an STO-4G basis set and by a pseudopotential approach [327]. The calculated barriers to internal rotation amount to 1330 cal mole^{-1} and 1280 cal mole^{-1} for the pseudopotential and SCF approach, respectively, and are in reasonable agreement with the experimental value of 1239 cal mole^{-1} [468]. A second pseudopotential calculation [328] yielded 1220 cal mole^{-1} for the barrier height. The highest filled orbital for CH_3GeH_3 is of *a* symmetry rather than the *e* symmetry which is found for CH_3CH_3 and CH_3SiH_3 [328].

The force fields, frequencies, Coriolis constants and the centrifugal distortion constants for the series GeH_3CH_3, GeH_3CN and GeH_3CCH, as well as the corresponding GeD_3 series, have been evaluated [469]. The force constant of the Ge–H bond increases along the series $GeH_3CH_3 < GeH_3CCH < GeH_3CN$ and this may be explained on the basis of the inductive effect which increases the ionic character of the Ge–C bond when the CH_3 group is replaced by the more electronegative groups CN and CCH.

The photoelectron spectra of Me_3GeCl and Me_3GeBr have been recorded and CNDO calculations [352] performed to aid the assignment of the bands. The halogen lone pairs participate in bonding via the symmetrically related orbitals of the trimethylgermanium moiety. This interaction is much stronger in the chloride than in the bromide and it may occur through the 4*d* orbitals of the germanium.

The photoelectron spectra of the series $MeGeX_3$ [470] and Me_3GeX [471] (X = H, F, Cl) have been reported and assignments aided by CNDO calculations. For $MeGeH_3$, the highest filled orbital at −11.0 eV is essentially localised about the Ge–C bond. The next orbital is concentrated about the GeH_3 group and it is followed by an orbital based on the CH_3 group. The final orbital in the low-energy range of He(I) is centred about the GeH_3 moiety. The corresponding orbitals of the halogeno compounds $MeGeF_3$ and $MeGeCl_3$ are lower in energy. The HOMO of $MeGeF_3$ is an orbital based on the Ge–C–F framework and lies at −12.5 eV. Then follow three orbitals delocalised about the eight atoms, and an orbital with mainly GeF_3 character. The molecular orbitals of $MeGeCl_3$ have a similar composition to those of $MeGeF_3$.

The highest filled orbital of Me_3GeH lies at −10.9 eV and is delocalised over the H–Ge–C–H framework. The second orbital has mainly Ge–C character, while orbitals 3–5 are localised about the CH_3 portion. The sixth

and seventh levels are delocalised in composition. The two highest occupied orbitals of Me_3GeF have energies of -10.5 and 11.6 eV and are spread over all the atoms. These are followed by an orbital centred on the $2p$ orbitals of the fluorines. Orbitals 3–5 are composed mainly of methyl orbitals, while the final three orbitals with energy in the He(I) range are concentrated over the $Ge(CH_3)_3$ region.

The photoelectron spectrum of Me_4Ge has been examined [336,337] and the Ge $4d$ orbital participation in the bonding is considered to be negligible. Core-level binding energies for the series of compounds, Me_nGeCl_{4-n}, Me_nGeBr_{4-n}, Me_nGeI_{4-n} and Me_3GeX ($n = 0$–4, X = F, Cl, Br, I, CN, N_3 and NCS) have been reported [472, 473]. A simple MO approach using the electronegativity-equalisation procedure of Huheey [474] based on the Hinze-Jaffé method [475] gives charges on the atoms and these form a linear relationship with the core-level binding energies.

Jolly and co-workers [476,477] have also examined the core electron binding energies for some germanium compounds. The chemical shifts have been correlated by an electrostatic potential equation using charge distributions from EHT, CNDO, and an electronegativity equalisation method. The data can be rationalised without any consideration of $p\pi$–$d\pi$ bonding in the germanium compounds. Morgan and Van Wazer have reported [478] the binding energies of solid-state germanium compounds.

The charge distribution and dipole moments of fifteen organogermanium compounds have been calculated by Ramalingam and Soundararajan [479] using a procedure outlined by Eyring and co-workers [480]. The difference between the experimental and calculated moments in the case of alkylhalogermanes is explained in terms of the p_π–d_π back-bonding effect outweighing the electron-releasing effect. In unsaturated compounds, the differences are attributed to possible mesomeric effects involving the expansion of the germanium valence shell. The electron charge flow from germanium to a chlorine substituent is ca. 0.9 electrons, while on average the methyl group donates ca. 0.22 electrons to the germanium atom.

Trimethylgermanium isocyanate, $(CH_3)_3GeNCO$, has been studied by an Extended Hückel calculation [481]. Geometry-optimisation routines yield a linear Ge–N–C framework and C–Ge–C angles of 105°. The occupancy of the Ge–N bond is 0.429 and is lower than that of the corresponding Si–N bond (0.507), possibly indicating a less effective participation of the free electron pairs of nitrogen in bonding. The total $p\pi$ population of nitrogen is 3.355 electrons.

Gowenlock and Hunter have performed CNDO calculations [482] on H_2GeCH_2, H_2GeCF_2, F_2GeCH_2 and F_2GeCF_2. The calculated Ge=C optimum bond lengths are 1.68 Å, 1.71 Å, 1.70 Å and1.72 Å, respectively and indicate some slight lengthening of the Ge=C bond when the atoms attached

to carbon are changed from hydrogen to fluorine. With the exception of F_2GeCH_2, the electron density for the germanium atom is always greater than that found on the carbon atom, so that the polarity of the Ge=C bond is always in the sense $Ge^-=C^+$. In the case of F_2GeCH_2 the difference may be attributed to electron withdrawal from the germanium towards the fluorine atoms. The calculated dipole moments are 1.02 D, 1.22 D, 3.35 D and 3.43 D for H_2GeCH_2, H_2GeCF_2, F_2GeCH_2 and F_2GeCF_2, respectively and indicate that the fluorine attached to the germanium has the most significant effect. The germanium–carbon bond appears to consist of a relatively weak σ bond and a much stronger π bond. Both of these components involve significant use of germanium 4*d* orbitals. A localised molecular orbital study of the dipole moments of the germaethylenes has also been performed [386].

The reaction of germylenes with mono-olefins yields polymeric compounds, while with conjugated dienes the product is a 1,4 cycloaddition compound [483,484]. These reactions were examined by an Extended Hückel treatment [485] of the reaction of CCl_2, $SiCl_2$ and $GeCl_2$ with ethylene and butadiene. The orientation for maximum stability of the $GeCl_2 + C_2H_4$ system corresponds to the "attack" of the free *p* orbital of the $GeCl_2$ molecule on one of the *p* orbitals of a carbon atom in ethylene. The probability of the synchronous 1,4 cycloaddition of these species to butadiene increases in the order $CCl_2 < SiCl_2 < GeCl_2$.

A perturbation scheme [368] involving the lowest unoccupied orbitals of the dienophiles $R_3GeCH{=}CH_2$ and $R_3GeC \equiv CH$ and the highest occupied orbital of a diene was used to explain the stereochemistry of Diels–Alder reactions and the regioselectivity of the diene reaction with organometallic compounds.

Schweig et al. [372,486] examined allyl and benzyl trimethylgermanium by a hyperconjugative Ge–C π interaction model and the interaction is undoubtedly hyperconjugative in nature. Bach and Scherr [373] found that the conformation of allyl dimethylgermanium affords an energy minimum when the angle between the dimethylgermanium moiety and the unsaturated group is 110° and so σ–π conjugation is maximised.

The UV spectrum of *p*-trimethylgermyl-*N*,*N*-dimethylaniline has been reported and the electronic transitions are calculated by a simple MO model [430].

The photoelectron spectra of phenyl and benzyl derivatives of trimethylgermane have been interpreted by a hyperconjugative model [419]. The $p\pi$–$d\pi$ contribution to bonding in $PhGe(Me)_3$ is important.

An ESR study [487,488] of alkyl- and aryl-substituted germyl radicals was complemented by McLachlan-type [489] calculations which evaluated the spin populations of the radicals. The agreement between experiment and

calculation is excellent. The spin populations at germanium are of particular interest and amount to 0.82, 0.86 and 0.91 for Ph_3Ge, Ph_2GeMe and $PhGeMe_2$, respectively. These values are high compared with the case of Ph_3C (0.42) [489] and indicate the smaller delocalisation of the lone electron of the germanium radicals due to the more limited $4p-2p$ conjugation. The g factors of the germyl radicals are larger than those of the carbinyl and silyl radicals and reflect the large spin-orbit coupling constant of germanium. An excellent linear relation exists between the g factors and spin densities at germanium.

The electronic structures of $H_3GeCH_2CH_2^+$ have been investigated [450] by a CNDO technique. The perpendicular conformation is favoured for both the cation and anion. The hyperconjugative interactions play a dominant role in determining the geometry.

The ESR spectra of the anion radicals of trimethylgermyl-tert-butylbenzenes have been reported [459]. The spectra have been interpreted in terms of a simple MO theory. The ordering of the energy levels is dominated by the trimethylgermyl substituent, which accepts electron density more effectively than the alkyl substituent releases it.

A united-atom treatment of $Ge(CH_3)_3$ radical has been performed [449]. The Lewis basicity of this radical is predicted to be substantially less than that of $Si(CH_3)_3$. The geometry is probably a more open pyramidal structure than the analogous carbon or silicon derivative.

(iii) Organotin compounds

There have been several theoretical investigations on the organometallic compounds of tin; this is in striking contrast with other elements of the fourth row of the Periodic Table.

The photoelectron spectrum of $Sn(CH_3)_4$ has been recorded [336,337] and rationalised by means of a simple MO treatment. $5d$-Orbital participation in the bonding is said to be insignificant.

The barrier to internal rotation in CH_3SnH_3 has been calculated via a pseudo-potential method [327] to be 690 cal mole^{-1} and this is in good agreement with the experimental value of 630 cal mole^{-1} [490].

Extended Hückel calculations [491] have been performed on methylchlorostannanes and methyltin hydrides and the contact term contributions to direct ^1J(Sn–H) and long-range ^2J(Sn–H) coupling constants have been evaluated. The behaviour of calculated coupling constants with tin $5d$-orbital participation was examined and for tetramethylstannane, the coupling constants are unaffected by $5d$-orbital participation while for the mixed methyltin hydrides and methylchlorostannanes a dependence is found. A study of the dependence of calculated coupling constants on the geometrical parame-

ters shows that the computed quantities are sensitive to small changes in bond lengths and bond angles. This indicates that the choice of selected geometry is of utmost importance if higher levels of sophistication are introduced into the computational methods. The charges on the tin for CH_3SnH_3, $(CH_3)_4Sn$, $(CH_3)_3SnCl$ and CH_3SnCl_3 are +1.49, +1.73, +1.60 and +1.54, respectively,while the corresponding Sn–C overlap populations are 0.77, 0.56, 0.61 and 0.65, respectively.

The intramolecular force fields of tetramethyltin have been examined [492] using Orbital Valence, Urey–Bradley and approximate General Valence force field potential functions. The vibrational mean amplitudes for the bonded and non-bonded distances have been reported.

Gupta and Majee, in a series of papers [493–500], and Majee in a review [501], examined the electronic structure of organotin compounds by the Del Re method. The bond orders of the Sn–Cl and Sn–C bonds in $Me_{4-n}SnCl_n$ ($n = 1-4$) were evaluated [493]. The Sn–Cl bond order increases progressively from 0.922 in Me_3SnCl to 0.977 in $SnCl_4$ and correlates satisfactorily with the experimental Sn–Cl bond distances. The Sn–C bond order remains constant over the series. Similarly, the variations in the stretching frequencies of these bonds can be correlated with the bond polarity. They also reported [494] the calculated dipole moment of twenty organotin compounds containing methyl, ethyl, tert-butyl, n-butyl, phenyl and vinyl groups. The agreement with the experimental values is generally good. The Sn–C bond polarity in R_nSnCl_{4-n}-type compounds follows the order vinyl > phenyl > methyl > ethyl > n-butyl > tert-butyl. The calculated heats of atomisation of thirteen organotin compounds [495] show an excellent correlation with the experimental heats of atomisation. The NMR data of organotin compounds have been interpreted [496] by means of the Del Re method. The methyl proton chemical shifts have been correlated with the partial charge on the methyl hydrogen atoms. Similarly, the variation in the C–H and Sn–H coupling constants has been correlated with the calculated coulomb integral values. A reactivity index [497] was developed for organotin compounds. The tin–carbon bond cleavage reactions of organotin compounds in polar and non-polar compounds have been successfully explained by this index.

The reactivity index for the vinyl carbon atom bonded to the tin atom in R_3SnVi compounds [498] decreases in the order R = Me > Et > nBu > iPr, which is in essential agreement with the observed [502] reactivity sequence of tin–vinyl bond-cleavage reactions. The relative rates of tin–aryl bond cleavage in polar solvents can also be correlated with the reactivity index.

Gupta and Majee have examined the polarisability [499] of the tin–carbon bond and have defined a bond polarisability index. The observed reactivity sequences for the cleavage of the alkyl groups from alkyltin compounds, both in polar and non-polar solvents, have been interpreted and the relative

rates of these reactions can be correlated with this index. The relative rates of the exchange reactions between trialkylaluminium and trialkyltin hydrides have also been satisfactorily interpreted.

Core-level X-ray photoelectron spectra of fifteen compounds of tin have been measured in the gas phase [503]. The tin binding energies span a range of 4.4 eV and are well correlated by the transition-state point-charge potential model equation using atomic charges calculated by the electronegativity equalisation method [476].

The UV photoelectron spectra of, and theoretical study with CNDO computations on, two classes of compounds containing the $S-Sn(CH_3)_2-S$ group, i.e. dithiolanes and the related open-chain species, are reported [504]. The preferred conformation of the $(CH_3)_2Sn(SCH_3)_2$ species contains a planar $Sn(SCH_3)_2$ moiety. The spectrum can be rationalised by assuming that both hyperconjugative interactions and interaction with the tin 5*d* orbitals are negligible and that mainly the inductive effect operates.

Extended Hückel calculations [505] have been performed on methyltin chlorides, $(CH_3)_nSnCl_{4-n}$ for $n = 1-4$. The structures were assumed to be undistorted tetrahedra and the results were compared with IR and NMR spectral data. The correlation between the electron distribution and the experimental results is reasonable for all four molecules but is much better when Me_3SnCl is excluded and this indicates that the tetrahedral model is perhaps inappropriate for Me_3SnCl or perhaps the formulation $Me_3Sn^+Cl^-$.

Simple MO calculations [506] and NQR spectra of octahedral complexes $SnCl_4 \cdot 2D$ (where $D = Et_2O$, EtOH, $PhCH_2Cl$, $MeOCH_2Cl$) have shown a dependence of frequency splittings and shifts on *cis–trans* isomerism. The spectral splittings are maximum at lowest charge transfer and decrease with increasing charge transfer, finally giving a single intense line which indicates equal dative properties for D and Cl.

A theoretical interpretation [507] of the tin-119 NMR chemical shifts of compounds of the type $Me_{4-n}SnX_n$ (where $X = NMe_2$, Cl, SMe, OMe, H and $SnMe_3$, and $n = 1-3$) has been put forward. The chemical shifts of the central atom were interpreted qualitatively in terms of the local paramagnetic screening term. The dependences of the calculated reduced paramagnetic constants and of the experimentally determined shifts on *n* confirm this interpretation.

De Poorter [508] has examined the geminal tin–proton coupling constant in $R_3SnCH_2CH_2X$ and R_3SnCH_2X (where X = Br and Cl). The theory developed by Pople and Bothner-By [509] for ^2J(HH) has been extended to ^2J(SnH) and the following trends obtained:

(i) ^2J(SnH) becomes more negative as the hybridisation at carbon changes from sp^3 to sp^2.

(ii) An electronegative group bonded to CH_2 leads to a negative shift of ^2J(SnH).

(iii) A π electron system bonded to CH_2 induces a positive shift of ^2J(SnH).

(iv) An electronegative group in the β position makes ^2J(SnH) more positive.

The CNDO method has been used [510] to calculate the chemical shifts in the Mössbauer spectra of some tin (IV) compounds. Amongst the compounds examined were $SnMe_4$, $SnMe_3F$, $SnMe_3Cl$, $SnMe_3Br$, $SnMe_3I$, $SnMe_3H$, $SnMeH_3$, $SnMe_2Cl_2$ and $SnMe_2H_2$. The occupation number of the 5*s* orbital of tin in each compound is correlated with their known experimental chemical shifts and an approximately linear relationship is found. The 5*s* electron density at the tin nucleus calculated from the Fermi–Segrè equation [511] using a modified form of Burns' screening rules [512] also exhibits a linear relation with the observed shifts.

An analysis of the valence electron distribution of the above molecules has been presented [513]. The electron density on tin for $SnMe_4$, $SnMe_3H$, $SnMe_2H_2$ and $SnMeH_3$ is 4.08, 3.94, 3.87 and 3.81, respectively. There is a decrease in electron density on Sn as the methyl groups are replaced by hydrogen atoms. The small formal charge on tin accords well with the known non-polar nature of these compounds. There is only a small 5*d* orbital population on tin which decreases from 0.07 for $SnMe_4$ to 0.02 for $SnMeH_3$. Sn–C and Sn–H bond orders in these compounds remain unchanged throughout the four compounds.

The charges on tin for $SnMe_3F$, $SnMe_3Cl$, $SnMe_3Br$ and $SnMe_3I$ are +0.54, +0.38, +0.28 and +0.31, respectively, whilst the Sn 5*d* orbital populations are 0.07, 0.13, 0.23 and 0.28, respectively. The charges on the molecules reflect the differing electronegativities of the halogens. The 5*d* orbitals on tin assume greater importance when the nature of the ligand allows most of the original charge to remain on the tin. These trends are also displayed in the dihalogenodimethylstannanes.

The electron densities of twenty organotin compounds calculated from the Del Re calculations of Gupta and Majee [500] show a fair correlation with the experimental Mössbauer isomer shifts. Since the electrical field gradient is determined by the deviation from spherical symmetry, Gupta and Majee introduce a parameter, *A*, capable of expressing this deviation, defined as

$$A = \left[(n_p/3 - n_x)^2 + (n_p/3 - n_y)^2 + (n_p/3 - n_z)^2\right]^{1/2}$$

A correlation is found between the asymmetry parameter *A* and the experimental quadrupole splitting.

The electronic structure of $(CH_3)_3SnNCO$ has been calculated [481] by

the Extended Hückel method. A linear SnNC structure and a C–Sn–C angle of 105° gave the lowest energy. The occupancy of the Sn–N bond is 0.162, considerably lower than the corresponding Si–N (0.507) and Ge–N (0.629) bonds. The total p_π orbital population of nitrogen is 3.364.

The hyperconjugative interactions in tin compounds have been discussed by Pitt [371]. Schweig et al. [372,486] have shown that the destabilisation of the π MOs in allyl and benzyl compounds of tin can be quantitatively predicted on the basis of the hyperconjugative interaction model. The conformation of allyltrimethyltin has been evaluated [373] by an Extended Hückel calculation. The energy minimum occurs at $\alpha = 110°$, which favours σ–π conjugation. The photoelectron spectra [419] have been obtained for the compounds $(CH_3)_3SnPh$ and $(CH_3)_3SnCH_2Ph$. The results have been partitioned by first-order perturbation theory into hyperconjugation, induction and p_π–d_π bonding in phenyl derivatives.

The carbon-13 NMR spectra of the compounds $ArCH_2Sn(CH_3)_3$ (where Ar = phenyl, 1- and 2-naphthyl and 4-biphenyl) have been recorded [514,515]. Comparisons have been made with the appropriate neopentyl compounds and, at conjugated positions, substantial shielding is experienced. The substituent chemical shift, $\Delta\delta$, correlates well with the SCF π MO change in π charge density for the change $ArCH_3 \rightarrow ArCH_2^-$ as expected for a conjugative interaction.

Empirical Force Field calculations [516] have been performed on trimesitylstannane. The calculated energies for the idealised transition state point to the two-ring flip mechanism as the pathway of lowest energy over a wide range of structures. The three-ring flip is consistently higher in energy than the two-ring flip. The predicted activation energy is 5–7 kcal $mole^{-1}$.

A united-atom treatment of $Sn(CH_3)_3$ radical and anion has been carried out [449]. The Lewis basicity of the radical is predicted to be higher than that of $Ge(CH_3)_3$, while the Lewis basicity of the anion is higher than that of the radical.

Finally, there have been many empirical schemes whose aim is to rationalise and predict the NMR and Mössbauer experimental data. Two of these procedures are summarised here. An additive treatment of partial quadrupole splittings [517] has been used to interpret quadrupole splittings in Sn(IV) compounds. The acceptable agreement between predicted and observed quadrupole splittings are 0.4 ma s^{-1}. A simple MO scheme for an additive electric field gradient at the tin nucleus in organotin(IV) compounds has been formulated [518]. The partial field gradient associated with a given ligand is different for tetrahedral, trigonal, bipyramidal and octahedral positions. In particular, the partial field gradient for octahedral coordination is about 70% of that for the tetrahedral situation.

(iv) Organolead compounds

There have been a small number of calculations on the electronic structure of organolead compounds and these are generally part of a series incorporating all elements of Group IV.

The photoelectron spectrum of Me_4Pb has been obtained [336,337] and *d*-orbital participation by lead in the bonding is considered to be negligible. The most stable conformation of allyltrimethyllead, according to Extended Hückel calculations [373], occurs when $\alpha = 110°$ and so favours σ–π conjugation.

The carbon-13 NMR spectra of a series of compounds $ArPb(CH_3)_3$ (where Ar = phenyl, 1-, 2-naphthyl, 4-biphenyl and 9-anthryl) have been recorded [514]. The substituent chemical shifts at formally conjugated positions have been considered in terms of mesomeric electron withdrawal associated with π orbitals on Pb and the dominating electron-donating mechanism resulting from the aryl C–Pb bond polarisation. The Jahn–Teller effect has been invoked to rationalise the observed structure of $(C_5H_5)_2Pb$ [118].

A qualitative MO model of π-$C_6H_6Pb(AlCl_4)_2 \cdot C_6H_6$ has been presented [519] and this can account for many of the features of Pb(II) coordination. These include the relatively long Pb–Cl distance, the C_{6v} symmetry of the Pb–C_6H_6 interaction, and the relatively long Pb–C distances.

F. PERIODIC GROUP V

(i) Organoarsenic compounds

CNDO calculations [520] have been performed on a number of compounds which undergo pyramidal inversion at arsenic. The computed barriers are in satisfactory agreement with reported experimental results. The inversion barrier of trimethylarsine is 50.5 kcal $mole^{-1}$, which is considerably higher than earlier estimates [521,522] of 29 kcal $mole^{-1}$, based on valence force-field calculations. Replacement of the methyl groups by hydrogens increases the barrier to inversion, arsine having a value of 54.5 kcal $mole^{-1}$. Substitution of a methyl group by a phenyl group lowers the barrier to 43.8 kcal $mole^{-1}$, whilst halogen substitution raises the barrier. The barrier to pyramidal inversion of tetramethyldiarsine is 34.3 kcal $mole^{-1}$.

The ionisation potential and dipole moment of trimethylarsine have been calculated [523] by a CNDO method to be 11.38 eV and 2.10 D. These values are in fair agreement with the experimental values of 8.3 eV [524] and 0.86 D [525], respectively. The vibrational force fields and amplitude and zero-point average structure of $(CH_3)_3As$ have been determined [526]. The

zero-point average bond length of As–C is 1.979 Å.

EHMO calculations [527] with partial inclusion of spin-orbit coupling have been used to confirm assignments of the photoelectron spectra for Me_2AsX and $MeAsX_2$ where X = Cl, Br and I.

The lone-pair orbital ionisation potentials of the compounds Me_3N, Me_3P, Me_3As and Me_3Sb are found to be constant along the series [528]. This behaviour is in contrast to other atomic and molecular properties which vary characteristically and predictably from Me_3N to Me_3Sb. A qualitative MO model is used to discuss the interactions of the a_1 orbitals of Me_3X. The constancy of the lone-pair orbital energies of Me_3X can be explained by changes in hybridisation of the lone-pair orbitals on the central atom X. Schweig and co-workers have studied [529] the ground-state conformations of dimethylvinylarsine, dimethylphenylarsine, allyldimethylarsine and benzyldimethylarsine theoretically (CNDO calculations) and by UV photoelectron spectroscopy. For each compound the relative conformational energy is plotted against the dihedral angle α (i.e. the torsional angle around =C–As for the first two compounds or around the =C–CH_2– angle for the latter two compounds). The most stable configuration for dimethylvinylarsine occurs when $\alpha = 229°$, i.e. when the lone pair of arsenic is *cis* to the π fragment. This particular geometry is determined by conjugative and not by steric effects. The stable geometry of dimethylphenylarsine is, not surprisingly, favoured by steric and hyper-plus-n conjugative effects and occurs at $\alpha = 49°$. For allylarsine and benzylarsine compounds two locations of the lone pair were considered, i.e. either *cis* to the π fragment or *trans* to it. The n-*cis* conformer of allyldimethylarsine has $\alpha = 0°$, with the steric interactions determining the geometry. The n-*trans* isomer has $\alpha = 90°$ and is a compromise between As–C hyperconjugative and $p_\pi d_\pi$ conjugative forces on the one hand and steric forces on the other. The n-*cis* and n-*trans* conformations of benzyldimethylarsine have $\alpha = 0°$ and 90°, respectively, with steric effects dominating the choice of geometry.

Structures of the model ylides of phosphorus and arsenic, H_3PCH_2 and H_3AsCH_2, have been studied by ab initio calculations [530]. A full geometrical optimisation was performed for both species. The following parameters were obtained for H_3AsCH_2: angle H–As–H = 99.6°, angle H–C–H = 121.5°, H–As = 1.49 Å, H–C = 1.075 Å and As–C = 1.782 Å. The angle between the CH_2 plane and the As–C bond is between 0–5° where the total energy remains constant over this ring. The planarity at the ylide carbon atom is rationalised in terms of maximum arsenic–carbon π overlap. The barrier to rotation of the methylene group in H_3AsCH_2 is calculated to be 1×10^{-4} a.u.

The charge distribution in H_3AsCH_2 illustrates the anionic nature of the carbon atom with a −0.995 charge residing on this atom. The methylene

hydrogen atoms have a +0.165 charge, while the arsine hydrogen atoms possess a small negative charge. The arsenic atom carries a large positive charge (+0.831) which is much higher than the +0.474 charge associated with the P atom in H_3PCH_2. The higher zwitterionic character of H_3AsCH_2 explains why the trialkylmethylenearsoranes are more reactive than their phosphorane analogues [531].

The He(I) photoelectron spectra of the arsenic ylide $(CH_3)_3As{=}CH_2$ and its two trimethylsilyl derivatives $(CH_3)_3As{=}CHSi(CH_3)_3$ and $(CH_3)_3As{=}C(Si(CH_3)_3)_2$ have been discussed [532]. Using semiempirical (CNDO and EHMO) calculations, a model of the electronic structure has been obtained which permitted a rationalisation of the remarkable differences between the parent arsenic and phosphorus ylides and their mono- and bis-silyl derivatives. The ionisation potentials and the calculated total energies point to possible changes in the structure at the ylide methyl anion upon a phosphorus/arsenic substitution.

The photoelectron spectra of Ph_3M(M = N, P, As and Sb) have been recorded [533]. The deep mixing of the lone pair of the heteroatom with the π system of the benzene rings decreased from N to Sb. It was argued that *d*-orbital participation cannot explain the gross features of the spectra even if it cannot be ruled out. In particular, the *d* orbitals may be responsible for the decrease of the first ionisation potential going from $(CH_3)_3M$ to Ph_3M for M = P, As and Sb. Debies and Rabalais [534] have investigated the electronic structure of Ph_2MH where M = N, P and As, and Ph_3M where M = N, P, As and Sb, with the help of CNDO/2 calculations. The non-bonding electrons of M reside in the most loosely bound orbital for M = P, As and Sb but are more tightly bound for M = N. The stabilisation of the non-bonding orbitals and destabilisation of the π orbitals relative to the M = N molecules suggests the expansion of the valence shell of P, As and Sb includes *d* orbitals in the molecular bonding.

Schweig and coworkers have examined the electronic structure of some arsoles using a CNDO/2 calculational method [535]. They find that the out-of-plane angle (i.e. the angle between the ring plane and the As–H bond) for the parent arsole is 95°, whilst the corresponding angle for the phosphole compound is 92°. A pyramidal geometry is the most stable conformation for both the arsenic and phosphorus heterocycle. The calculated inversion barrier for arsole is 3 kcal $mole^{-1}$ greater than phosphole. The charge distribution of both heterocycles shows that the charge on P and As is +0.087 and +0.158, respectively, while all the ring positions in arsole are negative.

The inversion barrier of arsole has been calculated to be 33.9 kcal $mole^{-1}$ [520] and is 14.8 kcal $mole^{-1}$ higher than that in phosphole. The barrier is lower by ca. 10–15 kcal $mole^{-1}$ than that in the simple arsines. This latter

finding led to the conclusion that the electron pair on arsenic in arsoles is involved in cyclic $4p-2p$ π delocalisation, which is at a maximum in the planar transition state to inversion. The ground-state calculation yields an out-of-plane angle of 76° for arsole.

The photoelectron spectra of 2,5-dimethyl-1-phenylarsole as well as four phospholes have been recorded [536]. The results appear to show that there is no conjugative interaction between the 5- and 6-membered rings. Further, the lone pairs in the phospholes and arsoles take no part in a cyclic five-membered-ring conjugation. Hence, phospholes and arsoles in their ground-state conformations consist of localised diene systems and lone pairs of electrons of P and As, respectively. In this sense, arsoles and phospholes are said to be non-aromatic.

Epiotis and Cherry have investigated [537] the aromaticity of phospholes and arsoles. The photoelectron data of Schaeffer et al. have been examined with the aid of CNDO calculations. They find an interaction between the arsenic lone pair and the butadiene π system, leading to aromatic stabilisation of arsole in both the planar and pyramidal geometries. In 1-phenylarsole there is also a small interaction between the arsenic lone pair and the adjacent π system of the phenyl ring, due to twisting of the ring. Epiotis and Cherry present reasons for the non-planar structure of phosphole and arsole which contrasts with the planar pyrrole molecules. In addition to the aromaticity of the π system, there are also interactions present in the σ system which favour a pyramid at the heteroatom, i.e. a non-planar geometry. In pyrrole, these σ interactions are small and the geometry is determined by the aromaticity of the π system. However, in phosphole and arsole these σ interactions are larger and dictate a non-planar geometry. They disagree with Palmer [538], who suggests that a lack of aromaticity of the π system is the principal reason for non-planarity.

Ab initio calculations have been performed on arsabenzene [539] using an STO-3G basis set. The population analysis yields a -0.195 charge on the arsenic which can be partitioned into a $+0.265$ charge with regard to the σ-electron network and a -0.459 charge within the π-electron framework. The total electron populations on the *ortho, meta* and *para* carbon atoms are 6.061, 5.989 and 6.009, respectively. If the electron distribution of the carbon and its bonded hydrogen is jointly investigated, then the group charges are $+0.011$, $+0.056$ and $+0.045$, respectively. The π-bond overlap populations suggest that, compared with pyridine, increased bond localisation has occurred. The highest filled orbitals are $b_1\pi$ (7.41 eV), $a_2\pi$ (8.66 eV) and $b_2\sigma$ (11.21 eV) in agreement with the experimentally observed order [540]. The core orbital energies for the carbon atoms are also recorded.

The electronic structure of arsabenzene has been obtained by a CNDO/2 method [541] and compared with those of phosphabenzene and pyridine.

Arsabenzene has a π-orbital sequence which is the same as phosphabenzene but which is inverted compared to pyridine. The order is confirmed by photoelectron spectra and the calculated orbital energies correlate well with the experimental ionisation potentials. The charge distribution of the heterocycles shows that the arsenic possesses a positive charge, while the nitrogen has a negative charge. The *ortho* positions in the arsabenzene ring have a negative charge, while the *meta* positions carry a positive charge.

The He(II) photoelectron spectra of phosphabenzene and arsabenzene have been recorded [542]. The angular dependence of the bond intensities is in excellent agreement with the theoretical predictions of Cederbaum and co-workers [543].

(ii) Organoantimony and organobismuth compounds

Pentaphenylantimony is unusual, since its observed geometries, which are square pyramidal in one crystal form and trigonal bipyramidal in a second form, are thought to be influenced by crystal packing forces. Furthermore, of all pentaaryl Group V molecules, $(C_6H_5)_5Sb$ is alone in exhibiting a square pyramidal structure [544]. Attempts have been made to assess the magnitudes of any lattice effects and the calculation of the intramolecular strain energy and lattice energy for various geometries of pentaphenylantimony. The initial investigation [545] found that the square pyramid had a more favourable lattice energy (4.6 kJ mole^{-1}) but this was not large enough to offset the more dominant intramolecular interactions (30.5 kJ mole^{-1}). The second calculation [546] included potential functions with $1/r$ terms which predicted that the square pyramid would be more stable with a lattice-energy stabilisation of 15 kJ mole^{-1}.

There have been several empirical schemes which attempt to rationalise the Mössbauer experimental data in terms of the electron population on antimony. Bowen and Long [547] and Bowen and Hedges [548] have used an empirical relationship between the Mössbauer isomer shift and the quadrupole coupling constant to obtain the electron population in the hybrid bond-forming atomic orbitals of Sb(V). In phenylantimony compounds, the electron population along the Sb–C bond increases as the number of electronegative groups attached to antimony increases. The Sb 5*s* character of the apical bonds in R_3SbX_2 and Rb_4SbX compounds is appreciable but varies only slightly among a series of compounds. A related method has been developed for Sb(III) compounds [549]. Here a linear relationship between the isomer shift δ and the antimony *s* electron population is inadequate for Sb(III) compounds and so an empirical quadratic equation has been developed. Sams and his co-workers [550–552] have shown that the quadrupole splitting data from ^{121}Sb Mössbauer spectra can be interpreted in terms of

an additive model. They have reported a number of ligand partial field gradients for R and X ligands in trigonal bipyramidal and octahedral geometries.

There have been no significant investigations into the electronic nature of organobismuth compounds.

G. PERIODIC GROUP VI

(i) Organoselenium compounds

Ab initio calculations have been performed [553] on $CH_3SeCH_2^-$ and $HSeCH_2^-$ and the corresponding protonated species CH_3SeCH_3 and $HSeCH_3$. The α-selenocarbanions are found to be more stable than the corresponding α-thiacarbanions by about 3 kcal mole^{-1}. The stabilisation is related to the greater polarisation of Se compared with the S atom.

The carbanions stabilised by a selenium α-heteroatom are conformation-dependent. The equatorial forms illustrated in Fig. 42 (a and c) are always more stable by ca. 6.3 kcal mole^{-1} than the axial position (b and d). The proton affinity of $CH_3SeCH_2^-$ and $HSeCH_2^-$ is 422.5 and 421.3 kcal mole^{-1}, respectively. The charge of the anions is, as expected, distributed over the $SeCH_2^-$ portion whilst the electronic charge of Se is -0.28 and

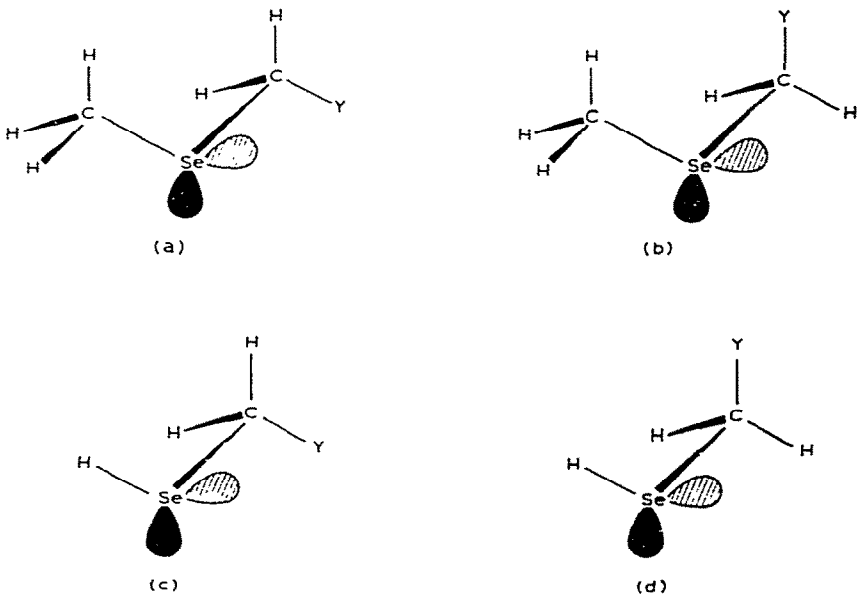

Fig. 42. The structures of CH_3SeCH_2Y and $HSeCH_2Y$ for Y = − and H.

-0.46 for $CH_3SeCH_2^-$ and $HSeCH_2^-$, respectively. The corresponding charges on Se for CH_3SeCH_3 and $HSeCH_3$ are -0.07 and -0.23. The *d* orbitals of Se are mainly core orbitals without any specific effect on the α-selenocarbanion stability.

Hase and Schweig [523] have calculated by a CNDO method the ionisation potential and dipole moment of dimethylselenide to be 11.33 eV and 1.050 D, respectively. These values are in fair agreement with the experimental values of 8.2 eV [554] and 1.32 D [555]. The energy levels of $Se(CH_3)_2$ have been evaluated by CNDO [556] and compared with experiment [557]. There is substantial agreement between the photoelectron data and the calculated values when a 90% scaling factor is applied.

The photoelectron spectrum of dimethyldiselenide has been recorded [558] and the assignment of the bands has been helped by EHMO calculations which included spin-orbit coupling. The two lowest ionisation potentials arise from the selenium lone-pair orbitals and they differ by 0.23 eV.

The dipole moments of some diaryldiselenides were calculated [559] using the Del Re and Pariser–Parr–Pople methods for the σ and π electron networks respectively. The agreement with the observed values is good. The selenium atoms have π donor properties towards the aromatic ring and this produces a negative charge at the *ortho* and *para* carbon atoms.

The electronic structure of diphenylselenide, as well as the corresponding sulphide and oxide, has been obtained by an EHMO method [560]. The "butterfly" conformation where the phenyl groups are rotated (by 38°) about the C–Se bonds out of coplanarity with the CSeC triangle is calculated to be the most stable conformation. In this geometry there is a balance between the relief of steric hindrance due to the *ortho* hydrogen atoms and a decrease in resonance energy resulting from non-planarity. Small energy barriers are predicted for the conversion of this butterfly conformation into other possible structures which have, (i) both rings planar, (ii) both rings perpendicular, and (iii) one ring planar and the other ring perpendicular. This supports the hypothesis of a non-rigid structure for these compounds. The charge on selenium is -0.265 and this stems from the bonded carbon atoms which are positively charged ($+0.232$). The remaining carbon atoms carry a small negative charge lying between -0.021 and -0.065, while all the hydrogen atoms are positively charged ($+0.02$).

The ESR of seven selenium containing aromatic radicals are reported [561]. Simple Hückel and McLachan MO calculations are used to rationalise the observed hyperfine splittings.

Findlay has performed ab initio minimal basis set calculations [562] of the electronic structure of selenophen. Reasonable agreement is obtained between the computed and experimental values of one-electron properties especially when selenium 4*d* functions are included. The direction of the

dipole moment has the negative end towards the selenium. The first two ionisation potentials are predicted to be 8.85 eV and 9.35 eV. Both orbitals are π in character with the order being $b_1 > a_2$ which is the reverse of that found for thiophen [563]. Open shell RHF calculations confirm this order. Photoelectron spectroscopy [563] reveals that the two occupied MOs reverse their sequence from thiophen [$\pi(1a_2) > \pi(2b_1)$] through selenophen to tellurophen [$\pi(2b_1) > \pi(1a_2)$].

CNDO and INDO calculations [564–566] have been performed in the chalcogen 5-membered heterocycles and their benzo derivatives to provide an insight into the relative importance of the σ and π contributions to the nuclear spin coupling constants. The INDO results, in general, gave better agreement with experimental findings and the difference between the two calculational findings can be regarded as an index of the π contribution to J. The most important contribution to the vicinal couplings J_{23} and J_{34} in the five-membered ring is due to a σ-electron mechanism. An interesting finding from this investigation is the different nature of the two long-range couplings J_{24} and J_{25}. The former is predicted to be transmitted through the σ system while the latter is dominated by the π mechanism and since this coupling is transmitted through a pathway involving selenium its particular nature can be ascribed to the role played by the diffuse lone pair of the p orbital of selenium. The coupling constants for the benzo derivative show that the vicinal couplings are dominated by the σ-electron contribution. The inter-ring couplings are transmitted via a σ-electron mechanism. The couplings in the phenyl ring are of two types; the *meta* coupling has a σ mechanism while the *para* coupling arises from a π mechanism.

The stereochemistries of 2,2′-, 2,3′- and 3,3′-biselenophenes have been investigated [567] using the EHMO method. These systems can have the following geometries, planar *syn*, planar *anti*, or a conformation where the rings are twisted by some angle around the central bond. For all three compounds the calculated energy difference between the *syn* and *anti* conformers is small. The planar *syn* conformation is predicted to be more stable than the *anti* for the 2,2′- isomer while the 2,3′- and 3,3′-biselenophenes are less stable in the planar *syn* conformation. The tendency to assume a non planar conformation at equilibrium is shown by 2,3′- and 3,3′-biselenophen. For all three molecules there is very little charge polarisation.

Pariser–Parr–Pople calculations have been performed on benzoselenazolium systems [568], on selenium heterocycles [569,570], on symmetric dyes based on selenine [571] and on selenium-substituted carbocyanine [572].

(ii) Organotellurium compounds

A CNDO study [573] of the *cis*-influence in substituted octahedral TeF_5X compounds has been carried out. The calculations confirm the experimental observations that the fluorine atoms positioned *cis* to ligand X are more labile and hence, more susceptible to replacement. The order of increasing *cis* influence for a series of ligands, X, is calculated to be $H < OH < NH_2 < Cl < CH_3 < Br < SH \sim PH_2 < SiH_3$. For CH_3TeF_5 the following charges are obtained CH_3 (+0.05), Te (+2.39), *cis* F (−0.50) and *trans* F (−0.44) while the bond indices are 0.63, 0.66 and 0.99 for *cis* Te–F, *trans* Te–F and Te–C bonds respectively.

The photoelectron spectrum of PhTeMe has been rationalised with the help of EHMO calculations [574]. Depending on the dihedral angle between the plane of the phenyl ring and the tellurium lone pair, the π conjugation amounts to between 0.1 eV and 0.3 eV, respectively. These limits are larger than those found with the analogous PhSeMe and PhSMe compounds.

The electronic structure of a series of aryltrichlorotellurium compounds has been calculated by an EHMO method [575]. The most stable conformation for $PhTeCl_3$ has a phenyl group in the equatorial position rather than an axial conformation. This arrangement is also calculated for CH_3TeCl_3. The π system of the phenyl ring is only slightly affected by the $TeCl_3$ group. The charge on the tellurium is +1.81 while the chlorine atoms have a negative charge −0.53 (apical) and −0.36 (equatorial). The population of the Te $d\pi$ orbital is 0.15 while the Te $p\pi$ is 0.57 and there is an absence of any conjugation effects of the $TeCl_3$ group with the aryl group. The strong descreening effect at the *ortho* and *meta* protons observed in PMR experiments must be due to the large charge on the tellurium in the $TeCl_3$ group.

REFERENCES

1 U. Lamanna and M. Maestro, Theor. Chim. Acta, 36 (1974) 103.
2 N.C. Baird, R.F. Barr and R.K. Datta, J. Organomet. Chem., 59 (1973) 65.
3 N.J. Fitzpatrick, Inorg. Nucl. Chem. Lett., 10 (1974) 263.
4 A. Streitweiser, Jr., J.E. Williams, S. Alexandratos and J.M. McKelvey, J. Am. Chem. Soc., 98 (1976) 4778.
5 J.D. Dill, P.v.R. Schleyer, J.S. Binkley and J.A. Pople, J. Am. Chem. Soc., 99 (1977) 6159.
6 M.F.Guest, I.H. Hillier and V.R. Saunders, J. Organomet. Chem., 44 (1972) 59.
7 G.R. Peyton and W.H. Glaze, Theor. Chim. Acta, 13 (1969) 259.
8 A.H. Cowley and W.D. White, J. Am. Chem. Soc., 91 (1969) 34.
9 A. Hinchliffe and E. Saunders, J. Mol. Struct., 31 (1976) 283.
10 P.O. Löwdin, J. Chem. Phys., 21 (1953) 374; R. Daudel, A. Laforgue and C. Vroelant, J. Chem. Phys., 49 (1952) 545.

11 N.K. Ray, S.P. Mehandru and S. Bhargava, Int. J. Quantum Chem., 13 (1978) 529.
12 M. Witanowski and J.D. Roberts, J. Am. Chem. Soc., 88 (1966) 737.
13 G. Fraenkel, W.E. Beckenbaugh and P.P. Yang, J. Am. Chem. Soc., 98 (1976) 6878.
14 J.B. Collins, J.D. Dill, E.D. Jemmis, Y. Apeloig, P.v.R. Schleyer, R. Seeger and J.A. Pople, J. Am. Chem. Soc., 98 (1976) 5419.
15 T. Clark, P.v.R. Schleyer and J.A. Pople, J.Chem. Soc., Chem. Commun., (1978) 137.
16 A. Streitweiser, Jr., J. Organomet. Chem., 156 (1978) 1.
17 E. Weiss and G. Hencken, J. Organomet. Chem., 21 (1970) 265.
18 J.B. Smart, R. Hogan, P.A. Scherr, L. Ferrier and J.P. Oliver, J. Am. Chem. Soc., 94 (1972) 8371.
19 W. McLean, L.G. Pedersen and R.C. Jarnagin, J. Chem. Phys., 65 (1976) 2491.
20 Z. Latajka, H. Ratajczak, K. Romanowska and Z. Tomczak, J. Organomet. Chem., 131 (1977) 347.
21 Yu. Ye. Eizner, B.L. Erussalimsky and E.B. Milovskaya, Polym., J., 5 (1973) 1.
22 J.D. Dill, P.v.R. Schleyer and J.A. Pople, J. Am. Chem. Soc., 98 (1976) 1663.
23 T.A. Albright and E.E. Schweizer, J. Org. Chem., 41 (1976) 1168.
24 M.T. Reetz and W. Stephan, Tetrahedron Lett., (1977) 2693.
25 L. Radom, P.J. Stiles and M.A. Vincent, Nouv. J. Chim., 2 (1978) 115.
26 A. Hinchliffe, J. Mol. Struct., 37 (1977) 289.
27 J. Kriz, J. Polym. Sci. Part A-2, 10 (1972) 615.
28 Y. Apeloig, P.v.R. Schleyer, J.S. Binkley and J.A. Pople, J. Am. Chem. Soc., 98 (1976) 4332.
29 S. Nagase and K. Morokuma, J. Am. Chem. Soc., 100 (1978) 1661.
30 A. Hinchliffe, J. Mol. Struct., 37 (1977) 145.
31 A. Veillard, J. Chem. Phys., 48 (1968) 2012.
32 J.B. Moffat, J. Mol. Struct., 42 (1977) 251.
33 Y. Apeloig, P.v.R. Schleyer, J.S. Binkley, J.A. Pople and W.L. Jorgensen, Tetrahedron Lett., (1976) 3923.
34 G. Rauscher, T. Clark, D. Poppinger and P.v.R. Schleyer, Angew. Chem. Int. Ed. Engl., 17 (1978) 276.
35 Y. Apeloig, P.v.R. Schleyer and J.A. Pople, J. Am. Chem. Soc., 99 (1977) 1291.
36 Y. Apeloig, P.v.R. Schleyer and J.A. Pople, J. Am. Chem. Soc., 99 (1977) 5901.
37 E.W. Nilssen and A. Skancke, J. Organomet. Chem., 116 (1976) 251.
38 W.D. Laidig and H.F. Schaefer III, J. Am. Chem. Soc., 100 (1978) 5972.
39 E.D. Jemmis, P.v.R. Schleyer and J.A. Pople, J. Organomet. Chem., 154 (1978) 327.
40 J.M. Lehn and G. Wipff, J. Am. Chem. Soc., 98 (1976) 7498.
41 A. Borgini, G. Cainelli, G. Cardillo, P. Palmieri and A. Umani-ronchi, J. Organomet. Chem., 110 (1976) 1.
42 E.R. Tidwell and B.R. Russell, J. Organomet. Chem., 80 (1974) 175.
43 T. Clark, E.D. Jemmis, P.v.R. Schleyer, J.S. Binkley and J.A. Pople, J. Organomet. Chem., 150 (1978) 1.
44 J.F. Sebastian, J.R. Grunwell and B. Hsu, J. Organomet. Chem., 78 (1974) C1.
45 M.M. Szcześniak and H. Ratajczak, J. Chem. Phys., 67 (1977) 5400.
46 A. Borgini, G. Cainelli, G. Cardillo, P. Palmieri and A. Umani-ronchi, J. Organomet. Chem., 92 (1975) C1.
47 J.F. Sebastien, B. Hsu and J.R. Grunwell, J. Organomet. Chem., 105 (1976) 1.
48 R.J. Bushby and A.S. Patterson, J. Organomet. Chem., 132 (1977) 163.
49 Y. Apeloig and R. Schreiber, Tetrahedron Lett., (1978) 4555.
50 E.D. Jemmis, J. Chandrasekhar and P.v.R. Schleyer, J. Am. Chem. Soc., 101 (1979) 2848.

51 E.D. Jemmis, D. Poppinger, P.v.R. Schleyer and J.A. Pople, J. Am. Chem. Soc., 99 (1977) 5796.
52 J.Y. Becker, A.Y. Meyer and J. Klein, Theor. Chim. Acta, 29 (1973) 313.
53 A. Skancke and J.E. Boggs, J. Mol. Struct., 50 (1978) 173.
54 S. Alexandratos, A. Streitweiser, Jr. and H.F. Schaefer III, J. Am. Chem. Soc., 98 (1976) 7959.
55 I.A. Abronin, Ya.A. Shteinshneider, G.M. Zhidomirov and F.M. Stoyanovich, Izv. Akad. Nauk SSSR, Ser. Khim., 28 (1979) 307.
56 J.D. Dill, P.v.R. Schleyer and J.A. Pople, J. Am. Chem. Soc., 99 (1977) 1.
57 S.P. Patterman, I.L. Karle and G.D. Stucky, J. Am. Chem. Soc., 92 (1970) 1150.
58 J.J. Brooks and G.D. Stucky, J. Am. Chem. Soc., 94 (1972) 7333.
59 J.J. Brooks, W.E. Rhine and G.D. Stucky, J. Am. Chem. Soc., 94 (1972) 7339.
60 J.J. Brooks, W.E. Rhine and G.D. Stucky, J. Am. Chem. Soc., 94 (1972) 7346.
61 W.E. Rhine and G.D. Stucky, J. Am. Chem. Soc., 97 (1975) 737.
62 M. Walczak and G.D. Stucky, J. Organomet. Chem., 97 (1975) 313.
63 W.E. Rhine, J. Davis and G.D. Stucky, J. Am. Chem. Soc., 97 (1975) 2079.
64 M. Walczak and G.D. Stucky, J. Am. Chem. Soc., 98 (1976) 5531.
65 W.E. Rhine and G.D. Stucky, J. Organomet. Chem., 134 (1977) 139.
66 G.D. Stucky, Adv. Chem. Seri., 130 (1974) 56.
67 J. Klein, A. Medick and A.Y. Meyer, Tetrahedron, 32 (1976) 51.
68 F.M. Stoyanovich, Ya.L. Goldfarb, I.A. Abrouin and G.M. Zhidomirov, Tetrahedron Lett., (1973) 1761.
69 T.A. Claxton and D. McWilliams, Trans. Faraday Soc., 65 (1969) 3129.
70 S. Miertus and O. Kysel, Chem. Phys. Lett., 35 (1975) 531.
71 A. Hinchliffe, J.C. Cobb and A.J. Duke, Theor. Chim. Acta, 32 (1974) 341.
72 P. Cremaschi, A. Gamba, G. Morosi, C. Oliva and M. Simonetta, J. Chem. Soc., Faraday Trans. 2, 71 (1975) 1829.
73 F. Bernardi and G.F. Pedulli, J. Chem. Soc., Perkin Trans. 2, (1975) 194.
74 A. Pullman and P. Schuster, Chem. Phys. Lett., 24 (1974) 472.
75 P. Schuster, W. Marius, A. Pullman and H. Berthod, Theor. Chim. Acta, 40 (1975) 323.
76 S.G. Gagarin and I.A. Lygina, Zh. Strukt. Khim., 16 (1975) 675.
77 E.E. Dil'mukhambetov and V.I. Lygin, Zh. Fiz. Khim., 48 (1974) 1245.
78 E.E. Dil'mukhambetov, A.V. Kiselev and V.I. Lygin, Zh. Fiz. Khim., 49 (1975) 2984.
79 E.E. Dil'mukhambetov and V.I. Lygin, Zh. Strukt. Khim., 17 (1976) 357.
80 P. Kollman and S. Rothenberg, J. Am. Chem. Soc., 99 (1977) 1333.
81 A. Pullman and P. Brochen, Chem. Phys. Lett., 34 (1975) 7.
82 J.F. Hinton, A. Beeler, D. Harpool, R.W. Briggs and A. Pullman, Chem. Phys. Lett., 47 (1977) 411.
83 A. Pullman, C. Giessner-Prettre and Y.V. Kruglyak, Chem. Phys. Lett., 35 (1975) 156.
84 B.M. Rode and H. Preuss, Theor. Chim. Acta, 35 (1974) 369.
85 B.M. Rode and R. Fussenegger, J. Chem. Soc., Faraday Trans. 2, 71 (1975) 1958.
86 R. Fussenegger and B.M. Rode, Chem. Phys. Lett., 44 (1976) 95.
87 B.M. Rode and R. Ahlrichs, Z. Naturforsch. Teil A, 30 (1975) 1792.
88 B.M. Rode, H. Preuss and P. Schuster, Chem. Phys. Lett., 32 (1975) 34.
89 F. Bernardi, G. Pedulli, M. Guerra and H.B. Schlegel, Gazz. Chim. Ital., 105 (1975) 711.
90 M. Brustolon, L. Pasimeni and C. Corvaja, J. Chem. Soc., Faraday Trans. 2, 71 (1975) 193.
91 L. Pasimeni, M. Brustolon and C. Corvaja, J. Chem. Soc., Faraday Trans. 2, 70 (1974) 734.

92 P.V. Kostetsky, V.T. Ivanov, Yu.A. Ovchinnikov and G. Shchembelov, FEBS Lett., 30 (1973) 205.
93 M. Perricaudet and A. Pullman, FEBS Lett., 34 (1973) 222.
94 A. Pullman, Int. J. Quantum Chem. Quantum Biol. Symp., 1 (1974) 33.
95 D. Perahia, A. Pullman and B. Pullman, Theor. Chim. Acta, 43 (1977) 207.
96 D. Michel, Surf. Sci., 42 (1974) 453.
97 W.D. Hoffmann, Z. Phys. Chem., Leipsig, 257 (1976) 315.
98 M. Iwaizumi, M. Suzuki, T. Isobe and H. Azumi, Bull. Chem. Soc. Jpn., 41 (1968) 732.
99 B.J. McClelland, Chem. Rev., 64 (1964) 301.
100 I.B. Goldberg and J.R. Bolton, J. Phys. Chem., 74 (1970) 1965.
101 G.W. Canters, C. Corvaja and E. de Boer, J. Chem. Phys., 54 (1971) 3026.
102 C.V. Borczyskowski and K. Möbius, Chem. Phys., 12 (1976) 281.
103 A.D. McLachlan, Mol. Phys., 3 (1960) 233.
104 V.W. Vos, C. MacLean and N.H. Velthorst, J. Chem. Soc., Faraday Trans. 2, 72 (1976) 63.
105 M.T. Jones and T.C. Kuechler, J. Phys. Chem., 81 (1977) 360.
106 K. Gustav, Z. Chem., 8 (1968) 193.
107 A. Pullman, Int. J. Quantum Chem. Quantum Biol. Symp., 1 (1974) 33.
108 B. Pullman, N. Gresh, H. Berthod and A. Pullman, Theor. Chim. Acta, 44 (1977) 151.
109 D.S. Marynick and H.F. Schaefer III, Proc. Natl. Acad. Sci. U.S.A., 72 (1975) 3794.
110 K. Ohkubo, H. Shimada and M. Okado, Bull. Chem. Soc. Jpn., 44 (1971) 2025.
111 J.S. Binkley, R. Seeger, J.A. Pople, J.D. Dill and P.v.R. Schleyer, Theor. Chim. Acta, 45 (1977) 69.
112 M.J.S. Dewar and H.S. Rezpa, J. Am. Chem. Soc., 100 (1978) 777.
113 C.P. Baskin, C.F. Bender, R.R. Lucchese, G.W. Bauschlicher, Jr. and H.F. Schaefer III, J. Mol. Struct., 32 (1976) 125.
114 P.G. Mezey, F. Bernardi, I.G. Csizmadia and O.P. Strausz, Chem. Phys. Lett., 59 (1978) 117.
115 W.C. Swope and H.F. Schaefer III, J. Am. Chem. Soc., 98 (1976) 7962.
116 A. Almenningen, O. Bastiansen and A. Haaland, J. Chem. Phys., 40 (1964) 3434.
117 O.Y. Lopatko, N.M. Klimenko and M.E. Dyatkina, Zh. Strukt. Khim., 13 (1972) 1045.
118 C. Glidewell, J. Organomet. Chem., 102 (1975) 339
119 C.H. Wong, T.Y. Lee, K.J. Chao and S. Lee, Acta Crystallogr., Sect. B, 28 (1972) 1662.
120 C.S. Liu, J. Chin. Chem. Soc., 24 (1977) 79.
121 D.S. Marynick, J. Am. Chem. Soc., 99 (1977) 1436.
122 J.B. Collins and P.v.R. Schleyer, Inorg. Chem., 16 (1977) 152.
123 E.D. Jemmis, S. Alexandratos, P.v.R. Schleyer, A. Streitweiser Jr. and H.F. Schaefer III, J. Am. Chem. Soc., 100 (1978) 5695.
124 J. Demuynck and M.M. Rohmer, Chem. Phys. Lett., 54 (1978) 567.
125 N.S. Chiu and L. Schäfer, J. Am. Chem. Soc., 100 (1978) 2604.
126 A. Almenningen, A. Haaland and J. Lusztyk, J. Organomet. Chem., 170 (1979) 271.
127 R. Gleiter, M.C. Böhm, A. Haaland, R. Johansen and J. Lusztyk, J. Organomet. Chem., 170 (1979) 285.
128 J. Lusztyk and K.B. Starowieyski, J. Organomet. Chem., 170 (1979) 293.
129 O.P. Charkin, 13Vses. Chugaev. Soveshch. Po. Khimii Kompleks Soedin, (1978) 435.
130 O.P. Charkin, A. Veillard, J. Demuynck and M. Rohre, Koord. Khim., 5 (1979) 501.
131 M.J.S. Dewar and H.S. Rzepa, Inorg. Chem., 18 (1979) 602.
132 J. Bicerano and W.N. Lipscomb, Inorg. Chem., 18 (1979) 1565.
133 A. Streitweiser Jr. and J.E. Williams, J. Organomet. Chem., 156 (1978) 33.

134 Z. Latajka, H. Ratajczak, K. Romanowska and Z. Tomczak, J. Organomet. Chem., 139 (1977) 129.
135 C. Chavant, J.C. Daron, Y. Jeannin, G. Kaufmann and J. MacCordick, Inorg. Chim. Acta, 14 (1975) 281.
136 M. Astier and P. Millie, J. Organomet. Chem., 31 (1971) 139.
137 M. Astier and P. Millie, J. Organomet. Chem., 47 (1973) 311.
138 H. Kato and S. Tsuruya, Bull. Chem. Soc. Jpn., 46 (1973) 1001.
139 K. Ohkubo and F. Watanabe, Bull. Chem. Soc. Jpn., 44 (1971) 2867.
140 M.A. Ratner, J.W. Moskowitz and S. Topiol, J. Am. Chem. Soc., 100 (1978) 2329.
141 O.P. Charkin, Zh. Strukt. Khim., 15 (1974) 320.
142 K. Ohkubo, H. Shimada and M. Okada, Bull. Chem. Soc. Jpn., 44 (1971) 2025.
143 J. Haber, M. Sochacka, B. Grzybowska and A. Golebiewski, J. Mol. Catal., 1 (1975) 35.
144 A. Haaland, J. Lusztyk, J. Brunvoll and K.B. Starowieyski, J. Organomet. Chem., 85 (1975) 279.
145 W. Bünder and E. Weiss, J. Organomet. Chem., 92 (1975) 1.
146 S. Evans, M.L.H. Green, B. Jewitt, A.F. Orchard and C.F. Pygall, J. Chem. Soc., Faraday Trans. 2, 68 (1972) 1847.
147 B. Pullman, N. Gresh and H. Berthod, Theor. Chim. Acta, 40 (1975) 71.
148 R.K. Nanda and G. Govil, Theor. Chim. Acta, 38 (1975) 71.
149 D. Perahia, A. Pullman and B. Pullman, Theor. Chim. Acta, 42 (1976) 23.
150 R.K. Nanda and G. Govil, Indian J. Biochem. Biophys., 11 (1974) 336.
151 A.M. Schaffer, M. Gouterman and E.R. Davidson, Theor. Chim. Acta, 30 (1973) 9.
152 M. Zerner and M. Gouterman, Theor. Chim. Acta, 8 (1967) 26.
153 T. Oie, G.M. Maggiora and R.E. Christoffersen, Int. J. Quantum Chem. Quantum Biol. Symp., 3 (1976) 119.
154 J.D. Dill, P.v.R. Schleyer and J.A. Pople, J. Am. Chem. Soc., 97 (1975) 3402.
155 D. Cremer, J.S. Binkley, J.A. Pople and W.J. Hehre, J. Am. Chem. Soc., 96 (1974) 6900.
156 C. Trindle and L.C. Weiss, J. Phys. Chem., 79 (1975) 2435.
157 C. Trindle and J.K. George, Theor. Chim. Acta, 40 (1975) 119.
158 E. Flood, P. Pulay and J.E. Bloggs, J. Am. Chem. Soc., 99 (1977) 5570.
159 R.S. Mulliken, Chem. Rev., 41 (1947) 207.
160 K.A. Levison and P.G. Perkins, Theor. Chim. Acta, 17 (1970) 1.
161 K. Ziegler, Conf. Coordination Chem., Chem. Soc. Special Publication No. 13, The Chemical Society, London, 1959.
162 N.J. Fitzpatrick and N.J. Mathews, J. Organomet. Chem., 94 (1975) 1.
163 G.K. Barker, M.F. Lappert, J.B. Pedley, G.J. Sharp and N.P.C. Westwood, J. Chem. Soc., Dalton Trans., (1975) 1765.
164 H.O. Berger, J. Kroner and H. Nöth, Chem. Ber., 109 (1976) 2266.
165 O. Gropen and A. Haaland, Acta Chem. Scand., 27 (1973) 521.
166 M.J.S. Dewar and M.L. McKee, J. Am. Chem. Soc., 99 (1977) 5231.
167 T. Clark and P.v.R. Schleyer, J. Organomet. Chem., 156 (1978) 191.
168 M.J.S. Dewar and M.L. McKee, Inorg. Chem., 17 (1978) 1075.
169 M.J.S. Dewar and M.L. McKee, J. Am. Chem. Soc., 100 (1978) 7499.
170 M.J.S. Dewar, E.A.C. Lucken and M.A. Whitehead, J. Chem. Soc., (1960) 2423.
171 S. Dasgupta, M.K. Datta and R. Datta, Tetrahedron Lett., (1978) 1309.
172 K.R. Sundberg, G.D. Graham and W.N. Lipscomb, J. Am. Chem. Soc., 101 (1979) 2863.
173 N.J. Fitzpatrick and M.O. Fanning, J. Mol. Struct., 50 (1978) 127.
174 N.N. Vyshinskii, V.N. Kokorev, I.A. Abronin, Yu.A. Aleksandrov, G.M. Zhidomirov and V.P. Maslennikov, Dokl. Akad. Nauk SSSR, 236 (1977) 883.

175 R. Hoffmann, L. Radom, J.A. Pople, P.v.R. Schleyer, W.J. Hehre and L. Salem, J. Am. Chem. Soc., 94 (1972) 6221.
176 N.L. Summers and J. Tyrrell, J. Am. Chem. Soc., 99 (1977) 3960.
177 D.R. Armstrong and P.G. Perkins, J. Chem. Soc. A, (1969) 1044.
178 H. Basch, Chem. Phys. Lett., 12 (1971) 110.
179 P.-O. Löwdin, J. Chem. Phys., 18 (1950) 365.
180 B.C. Carlson and J.M. Keller, Phys. Rev., 105 (1957) 102.
181 E.R. Davidson, J. Chem. Phys., 46 (1967) 3320.
182 R.E. Christoffersen and K.A. Baker, Chem. Phys. Lett., 8 (1971) 4.
183 R.S. Mulliken, J. Chim. Phys., 46 (1949) 497.
184 G.R. Runtz and R.F.W. Bader, Mol. Phys., 30 (1975) 129.
185 R.F.W. Bader and G.R. Runtz, Mol. Phys., 30 (1975) 117.
186 L.C. Snyder, J. Chem. Phys., 61 (1974) 747.
187 M.W.P. Strandberg, C.S. Persall and M.T. Weiss, J. Chem. Phys., 17 (1949) 429.
188 W.C. Ermler and C.W. Kern, J. Chem. Phys., 61 (1974) 3860.
189 W.C. Ermler, F.D. Glasser and C.W. Kern, J. Am. Chem. Soc., 98 (1976) 3799.
190 S. Kato, H. Fujimoto, S. Yamabe and K. Fukui, J. Am. Chem. Soc., 96 (1974) 2024.
191 H. Umeyama and K. Morokuma, J. Am. Chem. Soc., 98 (1976) 7208.
192 T.K. Ha, J. Mol. Struct., 30 (1976) 103.
193 L.T. Redmon, G.D. Purvis III and R.J. Bartlett, J. Am. Chem. Soc., 101 (1979) 2856.
194 K.F. Purcell and R.L. Martin, Theor. Chim. Acta, 35 (1974) 141.
195 J.F. Labarre and C. Leibovici, J. Chim. Phys. Physicochim. Biol., 69 (1972) 404.
196 R. Datta, M.K. Datta and D.C. Ghosh, Indian J. Chem. A, 15 (1977) 259.
197 D.R. Armstrong, Inorg. Chim. Acta, 18 (1976) 13.
198 L.D. Brown and W.N. Lipscomb, Inorg. Chem., 16 (1977) 1.
199 R. Dorschner and G. Kauffman, Inorg. Chim. Acta, 23 (1977) 97.
200 C.D. Good and D.M. Ritter, J. Am. Chem. Soc., 84 (1962) 1162.
201 V.J. Hammond and W.C. Price, Trans. Faraday Soc., 51 (1955) 605.
202 T.D. Coyle, S.L. Stafford and F.G.A. Stone, J. Chem. Soc., (1961) 3103.
203 D.R. Armstrong and P.G. Perkins, Theor. Chim. Acta, 4 (1966) 352.
204 D.R. Armstrong and P.G. Perkins, Theor. Chim. Acta, 5 (1966) 11.
205 D.R. Armstrong and P.G. Perkins, Theor. Chim. Acta, 5 (1966) 215.
206 D.R. Armstrong and P.G. Perkins, Theor. Chim. Acta, 5 (1966) 222.
207 D.R. Armstrong and P.G. Perkins, Theor. Chim. Acta, 8 (1967) 138.
208 G. Kuehnlenz and H.H. Jaffé, J. Chem. Phys., 58 (1973) 2238.
209 D.R. Armstrong and P.G. Perkins, Theor. Chim. Acta, 9 (1967) 412.
210 N.L. Allinger and J.H. Siefert, J. Am. Chem. Soc., 97 (1975) 752.
211 J.E. Williams, Jr. and A. Streitweiser, Jr., Tetrahedron. Lett., (1973) 5041.
212 H.M. Seip and H.H. Jensen, Chem. Phys. Lett., 25 (1974) 209.
213 V. Bonacic-Koutecký, J. Koutecký and L. Salem, J. Am. Chem. Soc., 99 (1977) 842.
214 J.H. Van 't Hoff, La Chimie dans L'Espace, Bazendijk, Rotterdam, 1875.
215 K. Krogh-Jespersen, D. Cremer, D. Poppinger, J.A. Pople, P.v.R. Schleyer and J. Chandrasekhar, J. Am. Chem. Soc., 101 (1979) 4843.
216 A.K. Uriarte and K.G. Hancock, Inorg. Chem., 12 (1973) 1428.
217 K.G. Hancock and A.K. Uriarte, J. Am. Chem. Soc., 92 (1970) 6374.
218 P.G. Perkins and D.H. Wall, J. Chem. Soc. A, (1966) 235.
219 M.F. Guest, I.H. Hillier and I.C. Shenton, Tetrahedron, 31 (1975) 1943.
220 D.R. Lloyd and N. Lynaugh, J. Chem. Soc., Chem. Commun., (1971) 125.
221 J. Kroner, D. Proch, W. Fuss and H. Bock, Tetrahedron, 28 (1972) 1585.

222 F. Grein and K. Weiss, J. Chem. Soc., Chem. Commun., 34 (1974) 315.
223 T.H. Hseu, J. Mol. Struct., 53 (1979) 121.
224 H.B. Klevens and J.R. Platt, J. Chem. Phys., 17 (1949) 470.
225 D.R. Armstrong and P.G. Perkins, J. Chem. Soc. A, (1966) 1026.
226 D.R. Armstrong and P.G. Perkins, J. Chem. Soc. A, (1967) 123.
227 D.R. Armstrong and P.G. Perkins, J. Chem. Soc. A, (1967) 790.
228 B.G. Ramsey and S.J. O'Neill, J. Organomet. Chem., 141 (1977) 257.
229 J.F. Blount, P. Finocchiaro, D. Gust and K. Mislow, J. Am. Chem. Soc., 95 (1973) 7019.
230 P. Finocchiaro, D. Gust and K. Mislow, J. Am. Chem. Soc., 95 (1973) 7029.
231 C.U. Pittman, Jr., A. Kress, T.B. Patterson, P. Walton and L.D. Kispert, J. Org. Chem., 39 (1974) 373.
232 M.N. Paddon-Row, L. Radom and A.R. Gregory, J. Chem. Soc., Chem. Commun., (1976) 427.
233 A.R. Gregory, M.N. Paddon-Row, L. Radom and W.D. Stohrer, Aust. J. Chem., 30 (1977) 473.
234 J. Kroner and B. Wrackmeyer, J. Chem. Soc., Faraday Trans. 2, 72 (1976) 2283.
235 M. Jallali-Heravi and G.A. Webb, J. Mol. Struct., 55 (1979) 113.
236 C. Edmiston and K. Ruedenberg, Rev. Mod. Phys., 35 (1963) 457.
237 S.F. Boys, Rev. Mod. Phys., 32 (1960) 296.
238 J.M. Foster and S.F. Boys, Rev. Mod. Phys., 32 (1960) 300.
239 S.F. Boys, in P.O. Löwdin (Ed.), Quantum Theory of Atoms, Molecules and Solid State, Academic Press, New York, 1966, p. 253.
240 M.F. Guest and I.H. Hillier, Mol. Phys., 26 (1973) 435.
241 D.R. Armstrong, Rev. Roum. Chim., 20 (1975) 883.
242 N.J. Fitzpatrick and M.O. Fanning, J. Mol. Struct., 40 (1977) 271.
243 D.A. Dixon, D.A. Kleier, T.A. Halgren, J.H. Hall and W.N. Lipscomb, J. Am. Chem. Soc., 99 (1977) 6226.
244 C.-C.S. Cheung, R.E. Beudet and G.A. Segal, J. Am. Chem. Soc., 92 (1970) 4158.
245 T.F. Koetzle and W.N. Lipscomb, Inorg. Chem., 9 (1970) 2743.
246 R. Hoffmann and W.N. Lipscomb, Inorg. Chem., 2 (1963) 231.
247 B.J. Meneghelli and R.W. Rudolph, Inorg. Chem., 14 (1975) 1429.
248 I.R. Epstein, T.F. Koetzle, R.M. Stevens and W.N. Lipscomb, J. Am. Chem. Soc., 9 (1970) 7019.
249 I.R. Epstein, D.S. Marynick and W.N. Lipscomb, J. Am. Chem. Soc., 95 (1973) 1760.
250 D.A. Kleier, T.A. Halgren, J.H. Hall, Jr. and W.N. Lipscomb, J. Chem. Phys., 61 (1974) 3905.
251 D.S. Marynick and W.N. Lipscomb, J. Am. Chem. Soc., 94 (1972) 1748.
252 H.J.T. Preston, J.J. Kaufman and W.S. Koski, Int. J. Quantum Chem. Symp., 9 (1975) 137.
253 T.A. Halgren, I.M. Pepperberg and W.N. Lipscomb, J. Am. Chem. Soc., 97 (1975) 1248.
254 D.S. Marynick and W.N. Lipscomb, J. Am. Chem. Soc., 94 (1972) 8699.
255 J.P. Chester and N.J. Fitzpatrick, J. Mol. Struct., 56 (1979) 117.
256 R.N. Camp, D.S. Marynick, G.D. Graham and W.N. Lipscomb, J. Am. Chem. Soc., 100 (1978) 6781.
257 J.A. Ulman and T.P. Fehlner, J. Am. Chem. Soc., 98 (1976) 1119.
258 G.L. McKown, B.P. Don, R.A. Beaudet, P.J. Vergamini and L.H. Jones, J. Chem. Soc., Chem. Commun., (1974) 765.
259 S.K. Lambiris, D.S. Marynick and W.N. Lipscomb, Inorg. Chem., 17 (1978) 3706.
260 E. Groszek, J.B. Leach, G.T.F. Wong, C. Ungermann and T. Onak, Inorg. Chem., 10 (1971) 2770.

261 D.S. Marynick and W.N. Lipscomb, J. Am. Chem. Soc., 94 (1972) 8692.
262 J.H. Hall, Jr., D.A.Dixon, D.A. Kleier, T.A. Halgren, L.D. Brown and W.N. Lipscomb, J. Am. Chem. Soc., 97 (1975) 4202.
263 D.R. Armstrong and R.H. Findlay, Inorg. Chim. Acta, 21 (1977) 55.
264 P.A. Wegner, Inorg. Chem., 14 (1975) 212.
265 C. Glidewell, J. Organomet. Chem., 128 (1977) 13.
266 H.M. Colquhoun, T.J. Greenough and M.G.H. Wallbridge, J. Chem. Soc., Chem. Commun., (1976) 1019.
267 D.M.P. Mingos, M.I. Forsyth and A.J. Welch, J. Chem. Soc., Chem. Commun., (1977) 605.
268 D.M.P. Mingos, J. Chem. Soc., Dalton Trans., (1977) 602.
269 D.M.P. Mingos, M.I. Forsyth and A.J. Welch, J. Chem. Soc., Dalton Trans., (1979) 1363.
270 D.M.P. Mingos and M.I. Forsyth, J. Organomet. Chem., 146 (1978) C37.
271 H.M. Colquhoun, T.J. Greenhough and M.G.H. Wallbridge, J. Chem. Soc., Chem. Commun., (1977) 737.
272 K. Wade, J. Chem. Soc., Chem. Commun., (1971) 792.
273 D.A. Brown, M.O. Fanning and N.J. Fitzpatrick, Inorg. Chem., 17 (1978) 1620.
274 M.F. Hawthorne and R.L. Pilling, J. Am. Chem. Soc., 87 (1965) 3987.
275 K. Wade, Adv. Inorg. Chem. Radiochem., 18 (1975) 1.
276 M. Elian, M.M.L. Chen, D.M.P. Mingos and R. Hoffmann, Inorg. Chem., 15 (1976) 1148.
277 M. Elian and R. Hoffmann, Inorg. Chem., 14 (1975) 1058.
278 D.M.P. Mingos, Adv. Organomet. Chem., 15 (1977) 1.
279 R.B. King and D.H. Rouvray, J. Am. Chem. Soc., 99 (1977) 7834.
280 E.K. Nishimura, J. Chem. Soc., Chem. Commun., (1978) 858.
281 R.E. Glick and A. Zwickel, J. Inorg. Nucl. Chem., 16 (1961) 149.
282 G.E. Coates and K. Wade, Organometallic Compounds, Vol. 1, Methuen, London, 1967, Chap. 3.
283 P.H. Lewis and R.E. Rundle, J. Chem. Phys., 21 (1953) 986.
284 K.A. Levison and P.G. Perkins, Theor. Chim. Acta, 17 (1970) 15.
285 M. Pelissier, J.-F. Laberre, L.V. Vilkov, A.V. Golubinsky and V.S. Mastryukov, Phys. Physicochim. Biol., 71 (1974) 702.
286 G.K. Barker, M.F. Lappert, J.B. Pedley, G.J. Sharp and N.P.C. Westwood, J. Chem. Soc., Dalton Trans., (1975) 1765.
287 M.F. Lappert, J.B. Pedley, G.J. Sharp and N.P.C. Westwood, J. Electron Spectrosc. Relat. Phenom., 3 (1974) 237.
288 M.F. Lappert, J.B. Pedley, G.J. Sharp and M.F. Guest, J. Chem. Soc., Faraday Trans. 2, 72 (1976) 539.
289 D.A. Sanders, P.A. Scherr and J.P. Oliver, Inorg. Chem., 15 (1976) 861.
290 V.A. Bolotin, V.B. Zurba and A.B. Bolotin, Liet. Fiz. Rinkinys, 15 (1975) 35.
291 B.M. Bulychev, O.E. Grikina, N.F. Stepanov, V.A. Bolotin and V.B. Zurba, Zh. Obshch. Khim., 46 (1976) 378.
292 D.F. Shriver and A. Alick, Inorg. Chem., 11 (1972) 2984.
293 D.A. Drew and A. Haaland, Acta. Chem. Scand., 27 (1973) 3735.
294 O. Gropen and A. Haaland, J. Organomet. Chem., 92 (1975) 157.
295 M.J.S. Dewar and D.B. Patterson, J. Chem. Soc., Chem. Commun., (1970) 544.
296 M.J.S. Dewar, D.B. Patterson and W.I. Simpson, J. Am. Chem. Soc., 93 (1971) 1030.
297 M.J.S. Dewar, D.B. Patterson and W.I. Simpson, J. Chem. Soc., Dalton Trans., (1973) 2381.

298 C.H. Townes and B.P. Dailey, J. Chem. Phys., 17 (1949) 782.
299 P.H. Kasai and D. McLeod, Jr., J. Am. Chem. Soc., 97 (1975) 5609.
300 P.H. Kasai, D. McLeod, Jr. and T. Watanabe, J. Am. Chem. Soc., 99 (1977) 3521.
301 M. Trenary, M.E. Casida, B.R. Brooks and H.F. Schaefer III, J. Am. Chem. Soc., 101 (1979) 1638.
302 S.G. Gargarin, Teor. Eksp. Khivor., 11 (1975) 375.
303 K. Ziegler, E. Holzkamp, H. Breil and H. Martin, Angew. Chem., 67 (1955) 541.
304 G. Natta, Makromol. Chem., 16 (1955) 213.
305 P. Cossee, J. Catal., 3 (1964) 80.
306 D.R. Armstrong, P.G. Perkins and J.J.P. Stewart, J. Chem. Soc., Dalton Trans., (1972) 1972.
307 O. Novaro, S. Chow and P. Magrouat, J. Catal., 41 (1976) 91.
308 G. Giunchi, E. Clementi, M.E. Ruiz-Vizcaya and O. Novaro, Chem. Phys. Lett., 49 (1977) 8.
309 O. Novaro, E. Blaisten-Barojas, E. Clementi, G. Giunchi and M.E. Ruiz-Vizcaya, J. Chem. Phys., 68 (1978) 2337.
310 Yu.A. Sangalov, O.A. Ponomarev, Yu.Ya. Nel'kenbaum, V.G. Romanko, V.D. Petrovka and K.S. Minskei, Vysokomol. Soedin. Ser A, 20 (1978) 1331.
311 R.B. Woodward and R. Hoffmann, J. Am. Chem. Soc., 87 (1965) 395.
312 K. Yamaguchi, T. Fueno and H. Fukutome, Chem. Phys. Lett., 22 (1973) 466.
313 K. Tatsumi, K. Yamaguchi and T. Fueno, Tetrahedron, 31 (1975) 2899.
314 K. Tatsumi, K. Yamaguchi and T. Fueno, J. Mol. Catal., 2 (1977) 437.
315 C.S. Ewig, R. Osman and J.R. Van Wazer, J. Am. Chem. Soc., 100 (1978) 5017.
316 A. Veillard, Chem. Phys. Lett., 3 (1969) 128.
317 D.R. Herschbach, J. Chem. Phys., 31 (1959) 91.
318 C.S. Ewig, W.E. Palke and B. Kintman, J. Chem. Phys., 60 (1979) 2749.
319 D.H. Liskow and H.F. Schaefer III, J. Am. Chem. Soc., 94 (1972) 6641.
320 J.S. Muenter and V.W. Laurie, J. Chem. Phys., 45 (1966) 855.
321 R.L. Shoemaker and W.L. Flygare, J. Am. Chem. Soc., 94 (1972) 684.
322 J.M. Bellama, R.S. Evans and J.E. Huheey, J. Am. Chem. Soc., 95 (1973) 7242.
323 P. Blustin, J. Organomet. Chem., 105 (1976) 161.
324 D. Quane, J. Phys. Chem., 75 (1971) 2480.
325 D.B. Adams, J. Chem. Soc., Faraday Trans. 2, 73 (1977) 991.
326 J.B. Collins, P.v.R. Schleyer, J.S. Binkley and J.A. Pople, J. Chem. Phys., 64 (1976) 5142.
327 C.S. Ewig and J.R. Van Wazer, J. Chem. Phys., 65 (1976) 2035.
328 G. Nicolas, J.C. Barthelat and Ph. Durand, J. Am. Chem. Soc., 98 (1976) 1346.
329 M.S. Gordon and L. Neubauer, J. Am. Chem. Soc., 96 (1974) 5690.
330 M. Corosine, F. Crasnier, M.-C. Labarre, J.-F. Labarre and C. Leibovici, Chem. Phys. Lett., 20 (1973) 111.
331 G. Robinet, C. Leibovici and J.-F. Labarre, Chem. Phys. Lett., 15 (1972) 90.
332 C. Leibovici, J. Mol. Struct., 18 (1973) 303.
333 J.R. Durig, Y.S. Li and C.C. Tong, J Mol. Struct., 14 (1972) 255.
334 A.E. Jonas, G.K. Schweitzer, F.A. Grimm and T.A. Carlson, J. Electron Spectrosc. Relat. Phenom., 1 (1972/3) 29.
335 W.B. Perry and W.L. Jolly, J. Electron Spectrosc. Relat. Phenom., 4 (1974) 219.
336 R. Boschi, M.F. Lappert, J.B. Pedley, W. Schmidt and B.T. Wilkins, J. Organomet. Chem., 50 (1973) 69.
337 S. Evans, J.C. Green, P.J. Joachim, A.F. Orchard, D.W. Turner and J.P. Maier, J. Chem. Soc., Faraday Trans. 2, 68 (1972) 905.

338 L. Szepes, G. Naray-Szabo, F.P. Colonna and G. Distefano, J. Organomet. Chem., 117 (1976) 141.
339 G. Distefano, A. Ricci, F.P. Colonna, D. Pietropaolo and S. Pignataro, J. Organomet. Chem., 78 (1974) 93.
340 K.D. Summerhays and D.A. Deprez, J. Organomet. Chem., 118 (1976) 19.
341 M.J.S. Dewar, D.H. Lo and C.A. Ramsden, J. Am. Chem. Soc., 97 (1975) 1311.
342 R.R. Gupta, J. Chem. Phys., 67 (1977) 3298.
343 K. Kovačević and Z.B. Maksić, J. Mol. Struct., 17 (1977) 203.
344 K. Kovačević, K. Krmpotic and Z.B. Maksić, Inorg. Chem., 16 (1977) 1421.
345 J. Nagy and J. Reffy, J. Organomet. Chem., 22 (1970) 565.
346 M.T. Vandorffy, T.N. Marchenko and A.E. Lutskii, Teor. Eksp. Khim., 11 (1975) 530.
347 G. Del Re, J. Chem. Soc., (1958) 4031.
348 E. Bolygo, J. Borossay, L. Szepes and G. Innorta, Magy. Kem. Foly., 82 (1976) 593.
349 C. Sierio and J.I. Fernandez-Alonso, An. Quim., 71 (1975) 548.
350 C. Sierio, J.I. Fernandez-Alonso and P. Gonzalez-Diaz, An. Quim., 71 (1975) 462.
351 M.C. Green, M.F. Lappert, J.B. Pedley, W. Schmidt and B.T. Wilkins, J. Organomet. Chem., 31 (1977) C55.
352 A. Flamini, E. Semprini, F. Stefani, S. Sorriso and G. Cardaci, J. Chem. Soc., Dalton Trans., (1976) 731.
353 V.I. Baranovskii, M.S. Nakhmanson and Yu.M. Zaitsev, Zh. Strukt. Khim., 13 (1972) 848.
354 R. Wolff and R. Radeglia, Org. Magn. Reson., 9 (1977) 64.
355 R. Wolff and R. Radeglia, Z. Phys. Chem., 258 (1977) 145.
356 F.F. Roelandt, D.F. Van De Vondel and E.V. Van Den Berghe, J. Organomet. Chem., 94 (1975) 377.
357 R. Ponec, L. Dejmek and V. Chvalovsky, Collect. Czech. Chem. Commun., 42 (1977) 1859.
358 A.G. Brooks, M.A. Quigley, G.J.D. Peddle, N.V. Schwartz and C.M. Warner, J. Am. Chem. Soc., 82 (1960) 5102.
359 B.G. Ramsey, A.G. Brooks, A.R. Bassindale and H. Bock, J. Organomet. Chem., 74 (1974) C41.
360 D.R. Armstrong and P.G. Perkins, Theor. Chim. Acta, 5 (1966) 69.
361 J. Nagy and M.T. Vandorffy, J. Organomet. Chem., 31 (1971) 205.
362 J. Nagy and M.T. Vandorffy, J. Organomet. Chem., 31 (1971) 217.
363 U. Weidner and A. Schweig, J. Organomet. Chem., 39 (1972) 261.
364 U. Weidner and A. Schweig, Angew. Chem., 84 (1972) 167.
365 P.D. Mollère, H. Bock, G. Becker and G. Fritz, J. Organomet. Chem., 46 (1972) 89.
366 W. Ensslin, H.H. Schmidtke and T.H. Kuehn, Inorg. Chim. Acta, 24 (1977) 159.
367 E. Heilbronner, Pure Appl. Chem., 40 (1974) 549.
368 C. Minot, A. Laporterie and J. Dubac, Tetrahedron, 32 (1976) 1523.
369 M. Horn and J.N. Murrell, J. Organomet. Chem., 70 (1974) 51.
370 E. Zeeck, Theor. Chim. Acta, 35 (1974) 301.
371 C.G. Pitt, J. Organomet. Chem., 61 (1973) 49.
372 A. Schweig, U. Weidner and G. Manuel, J. Organomet. Chem., 67 (1974) C4.
373 R.D. Bach and P.A. Scherr, Tetrahedron Lett., (1973) 1099.
374 R. Ponec and V. Chvalovsky, Collect. Czech. Chem. Commun., 38 (1973) 3845.
375 K.A.O. Starzewski, H.T. Dieck and H. Bock, J. Organomet. Chem., 64 (1974) 311.
376 H. Bock and H. Seidl, J. Chem. Soc. B, (1968) 1158.
377 C.G. Pitt, J. Chem. Soc. D, (1971) 816.

378 G. Bieri, F. Brogli, E. Heilbronner and E. Kloster-Jensen, J. Electron Spectrosc. Relat. Phenom., 1 (1972) 67.
379 W. Ensslin, H. Bock and G. Becker, J. Am. Chem. Soc., 96 (1974) 2757.
380 G. Stehlik and V. Hoffmann, Z. Naturforsch. Teil A, 27 (1972) 1764.
381 P.A. Kollman, C.F. Bender and J. McKelvey, Chem. Phys. Lett., 28 (1974) 407.
382 H. Oberhammer and M. Dakkouri, J. Mol. Struct., 22 (1974) 369.
383 W. Kosmus and E. Nachbaur, J. Mol. Struct., 23 (1974) 113.
384 M.D. Curtis, J. Organomet. Chem., 60 (1973) 63.
385 R. Damrauer and D.R. Williams, J. Organomet. Chem., 66 (1974) 241.
386 B.G. Gowenlock and J.A. Hunter, J. Organomet. Chem., 140 (1977) 265.
387 H.B. Schlegel, S. Wolfe and K. Mislow, J. Chem. Soc., Chem. Commun., (1975) 246.
388 O.P. Strausz, L. Gammie, G. Theodorakopoulos, P.G. Mezey and I.G. Csizmadia, J. Am. Chem. Soc., 98 (1976) 1622.
389 O.P. Strausz, M.A. Robb, G. Theodorakopoulos, P.G. Mezey and I.G. Csizmadia, Chem. Phys. Lett., 48 (1977) 162.
390 R. Ahlrichs and R. Heinzmann, J. Am. Chem. Soc., 99 (1977) 7452.
391 D.M. Hood and H.F. Schaefer III, J. Chem. Phys., 68 (1978) 2985.
392 M.S. Gordon, Chem. Phys. Lett., 54 (1978) 9.
393 H.B. Schlegel, B. Coleman and M. Jones, Jr., J. Am. Chem. Soc., 100 (1978) 6499.
394 R. Noyori, M. Yamakawa and W. Ando, Bull. Chem. Soc. Jpn., 51 (1978) 811.
395 J.N. Murrell, H.W. Kroto and M.F. Guest, J. Chem. Soc., Chem. Commun., (1977) 619.
396 J.-C. Barthelat, G. Trinquier and G. Bertrand, J. Am. Chem. Soc., 101 (1979) 3758.
397 G. Bertrand, G. Manuel and P. Mazerolles, Tetrahedron, 34 (1978) 1951.
398 Y.A. Ustynyuk, P.I. Zakharov, A.A. Azizov, G.A. Shchembelov and I'P. Glomozov, J. Organomet. Chem., 96 (1975) 195.
399 G.L. Decker, Y. Wang, G.D. Stucky, R.L. Lambert, Jr., C.K. Haas and D. Seyferth, J. Am. Chem. Soc., 98 (1976) 1779.
400 R.L. Lambert, Jr. and D. Seyferth, J. Am. Chem. Soc., 94 (1972) 9246.
401 D. Seyferth and D.C. Annarelli, J. Am. Chem. Soc., 97 (1975) 2273.
402 P.D. Mollère and R. Hoffmann, J. Am. Chem. Soc., 97 (1975) 3680.
403 P.R. Jones and D.D. White, J. Organomet. Chem., 154 (1978) C33.
404 R. Ponec, V. Chvalovsky, E.A. Chernyshev, N.G. Komarenkova and S.A. Baskirova, Collect. Czech. Chem. Commun., 39 (1974) 1177.
405 G. Frenking, H. Kato and K. Fukui, Bull. Chem. Soc. Jpn., 49 (1976) 2095.
406 J.P. Hummel, J. Stackhouse and K. Mislow, Tetrahedron, 33 (1977) 1925.
407 J. Nagy, Period. Polytech. Chem. Eng., 21 (1977) 211.
408 J. Nagy, Period. Polytech. Chem. Eng., 21 (1977) 247.
409 B. Coleman and M. Jones, Jr., J. Organomet. Chem., 168 (1979) 393.
410 P.H. Blustin, J. Organomet. Chem., 166 (1979) 21.
411 W.V. Niessen, W.P. Kraemer and L.S. Cederbaum, Chem. Phys., 11 (1975) 385.
412 S. Cradock, R.H. Findlay and M.H. Palmer, J. Chem. Soc., Dalton Trans., (1974) 1650.
413 G.A. Shchembelov and Yu.A. Ustynyuk, J. Organomet. Chem., 70 (1974) 343.
414 G.A. Shchembelov and Yu.A. Ustynyuk, J. Am. Chem. Soc., 96 (1974) 4189.
415 P.G. Perkins, Theor. Chim. Acta, 12 (1969) 427.
416 R.A.N. McLean, Can. J. Chem., 51 (1973) 2089.
417 B.G. Ramsey, J. Organomet. Chem., 135 (1977) 307.
418 C.R. Ernst, L. Spialter, G.R. Buell and D.L. Wilhite, J. Am. Chem. Soc., 96 (1974) 5375.
419 P.K. Bischof, M.J.S. Dewar, D.W. Goodman and T.B. Jones, J. Organomet. Chem., 82 (1974) 89.

420 R. Ponec and V. Chvalovsky, Collect. Czech. Chem. Commun., 39 (1974) 1185.
421 R. Ponec, E.A. Chernyshev, N.G. Tolstikova and V. Chvalovsky, Collect. Czech. Chem. Commun., 41 (1976) 2714.
422 R. Ponec, V. Chvalovsky, E.A. Chernyshev, S.A. Scepinov and T.L. Krasnova, Collect. Czech. Chem. Commun., 39 (1974) 1313.
423 J. Reffy, T. Veszpremi, G. Csonka and J. Nagy, Period. Polytech. Chem. Eng., 21 (1977) 259.
424 J. Reffy, T. Veszpremi and J. Nagy, Period. Polytech. Chem. Eng., 20 (1976) 223.
425 J. Reffy, P. Hencsei and J. Nagy, Period. Polytech. Chem. Eng., 20 (1976) 279.
426 W.J.E. Parr and T. Schaeffer, Can. J. Chem., 55 (1977) 557.
427 G.K. Hamer, I.R. Peat and W.F. Reynolds, Can. J. Chem., 51 (1973) 897.
428 W.F. Reynolds, G.K. Hamer and A.R. Bassindale, J. Chem. Soc., Perkin Trans. 2, (1977) 971.
429 M.J. Drews, P.S. Wong and P.R. Jones, J. Am. Chem. Soc., 94 (1972) 9122.
430 M.J. Drews and P.R. Jones, J. Organomet. Chem., 82 (1974) 57.
431 C.D. Schaeffer, Jr., J.J. Zuckerman and C.H. Yoder, J. Organomet. Chem., 80 (1974) 29.
432 A.G. Evans, B. Jerome and N.H. Rees, J. Chem. Soc., Perkin Trans. 2, (1973) 447.
433 A.G. Evans, B. Jerome and N.H. Rees, J. Chem. Soc., Perkin Trans. 2, (1973) 2091.
434 M. Ishikawa, M. Oda, N. Miyoshi, L. Fabry, M. Kumada, T. Yamabe, K. Akagi and K. Fukui, J. Am. Chem. Soc., 101 (1979) 4612.
435 M.G. Hutchings, J.D. Androse and K. Mislow, J. Am. Chem. Soc., 97 (1975) 4553.
436 M.G. Hutchings, J.D. Androse and K. Mislow, J. Am. Chem. Soc., 97 (1975) 4562.
437 M.M. Tatevosyan, A.T. Shuvaev, A.P. Zemlyanov, Yu.V. Kalodyazhhyi, O.A. Osipov and T.M. Krasnova, Zh. Strukt. Khim., 18 (1977) 684.
438 J. Reffy, T. Veszpremi, P. Hencsei and J. Nagy, Acta Chim. (Budapest), 93 (1977) 107.
439 J. Reffy, T. Veszpremi, P. Hencsei and J. Nagy, Acta Chim. (Budapest), 96 (1978) 95.
440 P. Hencsei, O. Mestyanck, J. Reffy, T. Veszpremi and J. Nagy, Kem. Kozlem., 46 (1976) 414.
441 T. Veszpremi, J. Reffy and J. Nagy, Kem. Kozlem., 46 (1976) 418.
442 V.G. Fritz, E. Matern, H. Bock and G. Braehler, Z. Anorg. Allg. Chem., 439 (1978) 173.
443 H. Bock, K. Wittel, M. Veith and N. Wiberg, J. Am. Chem. Soc., 98 (1976) 109.
444 S. Durmaz, J. Organomet. Chem., 96 (1975) 331.
445 C. Eaborn, F. Feichtmayr, M. Horn and J.N. Murrell, J. Organomet. Chem., 77 (1974) 39.
446 Y. Apeloig and P.v.R. Schleyer, Tetrahedron Lett., (1977) 4647.
447 J. Reffy, J. Organomet. Chem., 97 (1975) 151.
448 J. Reffy and J. Nagy, Period. Polytech. Chem. Eng., 22 (1978) 349.
449 B.R. Hollebone, J. Chem. Soc., Dalton Trans., (1974) 1889.
450 H.L. Hase and A. Schweig, Tetrahedron, 29 (1973) 1759.
451 M. Heaton, P.Z. Rogers and D.D. Davis, Bull. Soc. Chim. Belg., 85 (1976) 407.
452 J. Reffy, J. Karger-Kocsis and J. Nagy, Period. Polytech. Chem. Eng., 20 (1976) 77.
453 J. Karger-Kocsis, Magy. Kem. Lapja, 31 (1976) 276.
454 J. Reffy, J. Karger-Kocsis and J. Nagy, Kem. Kozlem., 46 (1976) 407.
455 D.J. Peterson, J. Org. Chem., 33 (1968) 780.
456 C. Trindle, J.-T. Hwang and F.A. Carey, J. Org. Chem., 38 (1973) 2664.
457 J. Reffy, J. Organomet. Chem., 96 (1975) 187.
458 H.J. Sipe and R. West, J. Organomet. Chem., 70 (1975) 353.
459 H.J. Sipe and R. West, J. Organomet. Chem., 70 (1975) 367.
460 M.J. Drews and P.R. Jones, J. Organomet. Chem., 44 (1972) 253.

461 I.N. Jung and P.R. Jones, J. Organomet. Chem., 101 (1975) 35.
462 J. Reffy and J. Karger-Kocsis, Magy. Kem. Foly., 83 (1977) 410.
463 P.R. Jones, J. Organomet. Chem., 83 (1974) 213.
464 P.R. Jones, J. Organomet. Chem., 109 (1976) 113.
465 P.R. Jones, J. Organometallic Chemistry Library, Vol. 4, Organometallic Chemistry Reviews; Annual Surveys: Silicon-Tin-Lead (1977).
466 P.R. Jones, J. Organometallic Chemistry Library, Vol. 6, Organometallic Chemistry Reviews; Annual Surveys: Silicon-Germanium-Tin-Lead (1978).
467 P.R. Jones, J. Organometallic Chemistry Library, Vol. 8, Organometallic Chemistry Reviews; Annual Surveys: Silicon-Germanium-Tin-Lead (1979).
468 V.W. Laurie, J. Chem. Phys., 30 (1959) 1210.
469 V.N. Yarandina and L.M. Sverdlov, Russ. J. Chem., 47 (1973) 153.
470 J.E. Drake, B.M. Glavinčevski and K. Gorzelska, J. Electron Spectrosc. Relat. Phenom., 17 (1979) 73.
471 J.E. Drake, B.M. Glavinčevski and K. Gorzelska, J. Electron Spectrosc. Relat. Phenom., 16 (1979) 331.
472 J.E. Drake, C. Riddle and L. Coatsworth, Can. J. Chem., 53 (1975) 3602.
473 J.E. Drake, C. Riddle, H.E. Henderson and B.M. Glavinčevski, Can. J. Chem., 54 (1976) 3876.
474 J.E. Huheey, J. Phys. Chem., 69 (1965) 3284.
475 J. Hinze and H.H. Jaffé, J. Am. Chem. Soc., 84 (1962) 540.
476 W.B. Perry and W.L. Jolly, Inorg. Chem., 13 (1974) 1211.
477 W.L. Jolly and A.A. Bakke, J. Am. Chem. Soc., 98 (1976) 6500.
478 W.E. Morgan and J.R. Van Wazer, J. Phys. Chem., 77 (1973) 964.
479 S.K. Ramalingam and S. Sundararajan, J. Organomet. Chem., 72 (1974) 59.
480 R.P. Smith, T. Ree, J.L. Magee and H. Eyring, J. Am. Chem. Soc., 73 (1951) 2263.
481 V.I. Ganina, M.A. Antonets and L.M. Ternian, Zh. Strukt. Khim., 16 (1975) 276.
482 B.G. Gowenlock and J.A. Hunter, J. Organomet. Chem., 111 (1976) 171.
483 O.M. Nefedov and S.P. Kolesnikov, Vysokomol. Soedin., 7 (1965) 1857.
484 W.H. Atwell and D.R. Weyenberg, Usp. Khim., 39 (1970) 1244.
485 A.I. Ioffe, L.I. Korzhenevich, S.P. Kolesnikov and O.M. Nefedov, Izv. Akad. Nauk SSSR, Ser. Khim., 2 (1976) 343.
486 A. Schweig, U. Weidner and G. Manuel, J. Organomet. Chem., 54 (1973) 145.
487 H. Sakurai, K. Mochida and M. Kira, J. Am. Chem. Soc., 97 (1975) 929.
488 H. Sakurai, K. Mochida and M. Kira, J. Organomet. Chem., 124 (1977) 235.
489 A.D. McLachlan, Mol. Phys., 2 (1960) 271.
490 P. Cahill and S. Butcher, J. Chem. Phys., 35 (1961) 2255.
491 G. Barbieri, R. Bonassi and F. Taddei, J. Organomet. Chem., 129 (1977) 27.
492 N.K. Sanyal, D.N. Verma and L. Dixit, Spectrosc. Lett., 9 (1976) 697.
493 R. Gupta and B. Majee, J. Organomet. Chem., 36 (1972) 71.
494 R. Gupta and B. Majee, J. Organomet. Chem., 33 (1971) 169.
495 R. Gupta and B. Majee, J. Organomet. Chem., 29 (1971) 419.
496 R. Gupta and B. Majee, J. Organomet. Chem., 40 (1972) 97.
497 R. Gupta and B. Majee, J. Organomet. Chem., 40 (1972) 107.
498 R. Gupta and B. Majee, J. Organomet. Chem., 49 (1973) 191.
499 R. Gupta and B. Majee, J. Organomet. Chem., 49 (1973) 197.
500 R. Gupta and B. Majee, J. Organomet. Chem., 49 (1973) 203.
501 B. Majee, Rev. Silicon, Germanium, Tin and Lead Compd., 2 (1975) 5.
502 P. Baekelmans, M. Gielen, P. Melfroid and J. Nasielski, Bull. Soc. Chim. Belg., 77 (1968) 85.

503 S.C. Avanzino and W.L. Jolly, J. Electron Spectrosc. Relat. Phenom., 8 (1976) 15.
504 F. Bernardi, G. Stefano, A. Modelli, D. Pietropaolo and A. Ricci, J. Organomet. Chem., 128 (1977) 331.
505 M.E. Krasnyanskii, Yu.A. Lysenko, A.O. Litinskii and E.I. Shifrovich, Zh. Strukt. Khim., 15 (1974) 711.
506 Yu.K. Maksyutin, E.N. Guryanoa, E.A. Kravchenko and G.K. Semin, J. Chem. Soc., Chem. Commun., (1973) 429.
507 R. Radeglia and G. Engelhardt, Z. Chem., 14 (1974) 319.
508 B. De Poorter, J. Organomet. Chem., 128 (1977) 361.
509 J.A. Pople and A.A. Bothner-By, J. Chem. Phys., 42 (1965) 1339.
510 N.N. Greenwood, P.G. Perkins and D.H. Wall, Symp. Faraday Soc., 1 (1967) 51.
511 E. Fermi and E. Segré, Z. Phys., 82 (1933) 729.
512 G. Burns, J. Chem. Phys., 41 (1964) 1521.
513 P.G. Perkins and D.H. Wall, J. Chem. Soc. A, (1971) 3620.
514 M. Bullpitt, W. Kitching, W. Adcock and D. Doddrell, J. Organomet. Chem., 116 (1976) 187.
515 M. Bullpitt, W. Kitching, W. Adcock and D. Doddrell, J. Organomet. Chem., 116 (1976) 161.
516 M.R. Kates, J.D. Andose, P. Finocchiaro, D. Gust and K. Mislow, J. Am. Chem. Soc., 97 (1975) 1772.
517 G.M. Bancroft and K.D. Butler, Inorg. Chim. Acta, 15 (1975) 57.
518 M.G. Clark, A.G. Maddock and R.H. Platt, J. Chem. Soc., Dalton Trans., (1972) 281.
519 A.G. Gash, P.F. Rodesiler and E.L. Amma, Inorg. Chem., 13 (1974) 2429.
520 J.D. Andose, A. Rauk and K. Mislow, J. Am. Chem. Soc., 96 (1974) 6904.
521 R.E. Weston, Jr., J. Am. Chem. Soc., 76 (1954) 2645.
522 G.W. Koeppl, D.S. Sagatys, G.S. Krishnamurthy and S.I. Miller, J. Am. Chem. Soc., 89 (1967) 3396.
523 H.L. Hase and A. Schweig, Theor. Chim. Acta, 31 (1973) 215.
524 W.R. Cullen and D.C. Frost, Can. J. Chem., 40 (1962) 390.
525 D.R. Lide, Spectrochim. Acta, 15 (1959) 473.
526 B. Beagley and A.R. Medwid, J. Mol. Struct., 38 (1977) 229.
527 S. Elbel and H.T. Dieck, Z. Naturforsch. Teil B, 31 (1976) 178.
528 S. Elbel, H. Bergmann and W. Ensslin, J. Chem. Soc., Faraday Trans. 2, 70 (1974) 555.
529 H. Schmidt, A. Schweig and H. Vermeer, J. Mol. Struct., 37 (1977) 93.
530 R. Strich, Nouv. J. Chim., 3 (1979) 105.
531 H. Schmidbaur, Adv. Organomet. Chem., 14 (1976) 205.
532 K.A.O. Starzewski, W. Richter and H. Schmidbaur, Chem. Ber., 109 (1976) 473.
533 G. Distefano, S. Pignataro, L. Szepes and J. Borossay, J. Organomet. Chem., 102 (1975) 313.
534 T.P. Debies and J.W. Rabalais, Inorg. Chem., 13 (1974) 308.
535 H.L. Hase, A. Schweig, H. Hahn and J. Radloff, Tetrahedron, 29 (1973) 469.
536 W. Schäfer, A. Schweig, G. Markl, H. Hauptmann and F. Mathey, Angew. Chem. Int. Ed. Engl., 12 (1973) 145.
537 N.D. Epiotis and W. Cherry, J. Am. Chem. Soc., 98 (1976) 4365.
538 M.H. Palmer, J. Chem. Soc., Perkin Trans. 2, (1975) 974.
539 D.T. Clark and I.W. Scanlan, J. Chem. Soc., Faraday Trans. 2, 70 (1974) 1227.
540 C. Batich, E. Heilbronner, V. Hornung, A.J. Ash, III, D.T. Clark, U.T. Cobley, D. Kilcast and I.W. Scanlan, J. Am. Chem. Soc., 95 (1973) 928.
541 H.L. Hase, A. Schweig, H. Hahn and J. Radloff, Tetrahedron, 29 (1973) 475.

542 A.J. Ash, III, F. Burger, M.Y. El-Sheik, E. Heilbronner, J.P. Maier and J.-F. Muller, Helv. Chim. Acta, 59 (1976) 1944.
543 W. v. Niessen, G.H.F. Diercksen and L.S. Cederbaum, Chem. Phys., 10 (1975) 345.
544 C.P. Brock and D.F. Webster, Acta Crystallogr., Sect. B, 32 (1976) 2089.
545 C.P. Brock and J.A. Ibers, Acta Crystallogr., Sect. A, 32 (1976) 38.
546 C.P. Brock, Acta Crystallogr., Sect. A, 33 (1977) 193.
547 L.H. Bowen and G.G. Long, Inorg. Chem., 15 (1976) 1039.
548 L.H. Bowen and S.W. Hedges, Inorg. Nucl. Chem. Lett., 13 (1977) 621.
549 S.W. Hedges and L.H. Bowen, J. Chem. Phys., 67 (1977) 4706.
550 J.N.R. Ruddick, J.R. Sams and J.C. Scott, Inorg. Chem., 13 (1974) 1503.
551 R.G. Goel, J.N.R. Ruddick and J.R. Sams, J. Chem. Soc., Dalton Trans., (1975) 67.
552 J.N.R. Ruddick and J.R. Sams, Inorg. Nucl. Chem. Lett., 11 (1975) 229.
553 J.M. Lehn, G. Wipff and J. Demuynck, Helv. Chim. Acta, 60 (1977) 1239.
554 A. Mangini, A. Tombetti and C. Zauli, J. Chem. Soc. B, (1967) 153.
555 L. Chierici, H. Lumbroso and R. Passerini, Compt. Rend., 237 (1953) 611.
556 M. Bossa, F. Maraschini, A. Flamini and E. Semprini, J. Chem. Soc., Dalton Trans., (1975) 596.
557 S. Cradock and R.A. Whiteford, J. Chem. Soc., Faraday Trans. 2, (1972) 281.
558 G. Tschmutowa and H. Bock, Z. Naturforsch., Teil B, 31 (1976) 1616.
559 L.A. Sorokina, N.S. Podkovyrina and L.M. Kataeva, Russ. J. Phys. Chem., 48 (1974) 1020.
560 V. Galasso, G. DeAlti and A. Bigotto, Tetrahedron, 27 (1971) 6151.
561 M.F. Chiu and B.C. Gilbert, J. Chem. Soc., Perkin Trans. 2, (1973) 258.
562 R.H. Findlay, J. Chem. Soc., Faraday Trans. 2, 71 (1975) 1397.
563 M.H. Palmer and R.H. Findlay, Tetrahedron Lett., (1972) 4166.
564 W. Schäffer, A. Schweig, S. Gronowitz, A. Taticchi and F. Fringuelli, J. Chem. Soc., Chem. Commun., (1973) 541.
565 V. Galasso, Chem. Phys. Lett., 32 (1975) 108.
566 V. Galasso and A. Bigotta, Org. Magn. Reson., 6 (1974) 475.
567 V. Galasso and N. Trinajstic, Tetrahedron, 28 (1972) 4417.
568 Y. Ferrè, E.-J. Vincent, H. Larivè and J. Metzger, Bull. Soc. Chim. Fr., (1972) 3862.
569 J. Fabian, A. Mehlhorn and R. Zahradnik, Theor. Chim. Acta, 12 (1968) 247.
570 J. Fabian, Z. Phys. Chem., 260 (1979) 81.
571 R.A.M.C. De Groote, An. Acad. Bras. Cienc., 44 (1972) 366.
572 V.E. Kleinpeter, R. Borsdorf, G. Bach and J. V. Grossman, J. Prakt. Chem., 315 (1973) 587.
573 D.R. Armstrong, G.W. Fraser and G.D. Meikle, Inorg. Chim. Acta, 15 (1975) 39.
574 G. Tschmutowa and H. Bock, Z. Naturforsch., Teil B, 31 (1976) 1611.
575 V.I. Minkin, I.D. Sadekov, L.M. Sayapina and R.M. Minyaev, Zh. Obsch. Khim., 43 (1973) 809.